

# **Role of cytokeratins 8 and 18 in differentiation and transformation of epithelial cells**

**By**

**SAPNA V. IYER  
LIFE09200604003**

**Tata Memorial Centre  
Mumbai**

**A thesis submitted to the  
Board of Studies in Life Sciences**

**In partial fulfilment of requirements  
For the Degree of**

**DOCTOR OF PHILOSOPHY**

**Of**

**HOMI BHABHA NATIONAL INSTITUTE**



**June, 2013**

# Homi Bhabha National Institute

## Recommendations of the Viva Voce Board

As members of the Viva Voce Board, we certify that we have read the dissertation prepared by Ms. Sapna V. Iyer entitled “Role of cytokeratins 8 and 18 in differentiation and transformation of epithelial cells” and recommend that it may be accepted as fulfilling the dissertation requirement for the Degree of Doctor of Philosophy.

\_\_\_\_\_  
Chairman – Dr. S.M. Zingde **Date:**

\_\_\_\_\_  
Guide / Convener – Dr. M. Vaidya **Date:**

\_\_\_\_\_  
Member 1 – Dr. S.N. Dalal **Date:**

\_\_\_\_\_  
Member 2 – Dr. T. Teni **Date:**

\_\_\_\_\_  
Member 3 - Dr. M. Narsimha **Date:**

\_\_\_\_\_  
External examiner- Prof. Dulal Panda **Date:**

Final approval and acceptance of this dissertation is contingent upon the candidate's submission of the final copies of the dissertation to HBNI.

I hereby certify that I have read this dissertation prepared under my direction and recommend that it may be accepted as fulfilling the dissertation requirement.

**Date:**

**Place:**

## **STATEMENT BY AUTHOR**

This dissertation has been submitted in partial fulfilment of requirements for an advanced degree at Homi Bhabha National Institute (HBNI) and is deposited in the Library to be made available to borrowers under rules of the HBNI.

Brief quotations from this dissertation are allowable without special permission, provided that accurate acknowledgement of source is made. Requests for permission for extended quotation from or reproduction of this manuscript in whole or in part may be granted by the Competent Authority of HBNI when in his or her judgment the proposed use of the material is in the interests of scholarship. In all other instances, however, permission must be obtained from the author.

Sapna V. Iyer

## **DECLARATION**

I, hereby declare that the investigation presented in the thesis has been carried out by me. The work is original and has not been submitted earlier as a whole or in part for a degree / diploma at this or any other Institution / University.

Navi Mumbai

Sapna V. Iyer

June 2013

## **CERTIFICATE**

I certify that the thesis titled “Role of cytokeratins 8 and 18 in differentiation and transformation of epithelial cells” submitted for the degree of Doctor of Philosophy by Ms. Sapna V. Iyer is a record of the research carried out by her during the period 2006 to 2013 under my supervision. This work has not formed the basis for the award of any degree, diploma, associateship or fellowship at this or any other institute or university.

Navi Mumbai,

June 2013

Milind M. Vaidya

**Dedicated to**

**Mumma for her innumerable  
blessings and perseverance!!!**

# Acknowledgments

Acknowledgement I believe is the most important page in a thesis. This page signifies my accomplishments which would have otherwise been almost impossible, if not for the support and the contributions from those mentioned below. I am elated to pen down my regards and appreciation to one and all during the course of my journey of PhD.

So first and foremost, I wish to thank Dr. Vaidya for believing in me and for his constant support. I couldn't have imagined myself coming this far. He indeed paved my path, giving me all that liberty to work & think, and also helped develop the person in me to face the world.

I am extremely thankful to Dr. Rajiv Sarin, Director of ACTREC, and Dr. Surekha Zingde, Deputy Director of ACTREC, for giving me the opportunity to work in this institute.

I have been most fortunate to have eminent DC members on my panel: Firstly, I wish to thank Dr. Zingde, the Chairperson of the committee, for all her efforts towards motivating me and. I also thank her for expert comments. I am also grateful to Dr. Teni for her relentless support throughout the tenure of my PhD and for the constant impetus for achieving my goal. I am thankful for all her suggestions during the assessment of my work. I am highly indebted to Dr. Sorab Dalal, for the pains he took to help me understand and analyse data. His comments were invaluable and had a major impact in shaping up my project as well as my paper. And I am grateful to Dr. Maithreyi for her critical analysis of my data and her helpful suggestions.

I also thank Dr. Arvind Ingle for carrying out all the strenuous animal surgeries during the course of my PhD work. I wish to profusely thank Dr. Neelam Shirsat for helping me in finding out meaningful information off the enormous microarray data. I also want to thank both Dr. Asawari Patil for all her efforts towards pulling out blocks for IHC studies and also unwearingly analysing my slides, and Dr. Anita Borges for analysing and interpreting all the tumor and metastasis slides.

Lab and lab members: Firstly, Vaishali, my "mom" in our lab. I cannot thank her enough for all the efforts she put in to teaching me and for being my pillar through thick and thin. I am entirely indebted to her for teaching me tissue culture. Again, without her guidance, I would not have made it this far. And I am thankful to Sharada Sawant or Vinita ma'am as I call her, for her suggestions on my project. I thank her for sharing her expertise on IHC and also for analysing my IHC slides.

Deepak my first senior- a rockstar!! He is one amazing personality who would just lighten up any dull moment through his pranks. I am also indebted to him for teaching me protein chemistry, critically analyse my data and also boosting my morale when things did not look so great. I also want to thank Alam for designing the plasmids that were used in my PhD research. I am thankful to him for his critical analysis. I am also appreciative of Soni, for his suggestions and also for his continuous support packaged with a very warm smile that helped me keep my cool. I wish to thank my lab members Crismita and Richa for constantly buzzing around with their non-stop chatter in the lab while at the same time pitching in with wonderful ideas, and also providing their support and assurance during my project. I am thankful to Prateik or Pattu "the little one" - he is like the apple of one's eye! It is

amazing to think how he could bring out the humour out of nowhere while at the same time he is equally good at his work.

I am also immensely thankful to Madhura for her help in IHC project and also for being such a wonderful colleague and friend. And Jyoti Bobade is another amazing friend I have had during my PhD tenure. I also want to thank Archana for the all her help and for being a good friend. I am grateful to Rajesh and Shridhar for their help and technical support and for their timely support in vital phases during my experiments. And special thanks to Prema ma'am and Yashwant. My trainees Chinmoyee or Chinu, and Swapnil have been amazing trainees. I am thankful to Chinmoyee for always being so vibrant and cheerful, and for all her hardwork in IHC though she believed that IHC just stood for "I Hate Chinmoyee". Swapnil Oak, my second only and last trainee is also close to my heart. His dedication towards work is commendable. I wish to thank Prakash Gangadharan, who is more of a younger brother to me, for all his support and assistance. I want to thank all the other trainees -Kruti, Neha, Shruti, Shreyas, Sid, Siddhesh, Sai, Nishikant, Satya, Ashok, Sima and Amruta etc.

A special thanks to my other seniors: Firstly, Samrat for his constant help, and also to Sanchita, Aditi, Elphine, Nitya, Amol, SrikanthB, Asha, Cheryl. Big thanks to Shreyas for teaching me real time analysis and also to Ratika, Kedar Gaurava and Ajit for all their help.

I am most thankful to my batchmates: I would not have been able to get all the way here without my best friend Amit Fulzele. Amit has been a major source of inspiration to me. He believed in me more than I did myself. I am indebted to him for having always been there, and I found a wonderful person and friend in him for life. I am most thankful to my friend Atul Pranay, whose wit and intelligence shooed away my tensions and helped me balance out things in life. I am also thankful to all my other batchmates, namely, Amit Singh, Amit Ranjan, Ajit Chande, Manoj Ramteke, Lalit Sehgal, Poulami Das, Tabish Hussain, Palavi Goel, Amit Verma, and Manoj Bhosale for helping me learn and making ACTREC such a joyful place.

Common Facility staff: I extend my gratitude to Vaishali Kailaje, Tanuja Jairaj and Mansi from Imaging Facility for helping me acquire all the microscopic images, and I appreciate their enthusiastic approach towards their work. I am thankful to Mr. Uday Dandekar for his efforts towards maintaining the Common Instrument Facility. I wish to thank Mr. Sawant and specially Shyam for their help and support. Animal House staff: I am extremely thankful to Shashi, Mahesh and Sada for helping me with animal handling, and I also thank Chavhan sir and Sakpal sir for providing me with sections and H&E slides.

I also am also grateful to CRI for my fellowship and also DBT for funding my project.

And last but not the least, My Family! They say when everything goes wrong, there is a family. And how there really IS one!!! Right from Mumma, Papa, Bhai, Preity, Sriram, and my new parents, these folks have been a pillar of tremendous support. I cannot thank God enough for giving me such an understanding family, and especially Sriram, my husband, for encouraging me in all my endeavours. I thank him for sharing all my worries and happiness, for being my source of strength, and for helping me in taking big decisions with ease.

Finally I thank God for all the opportunities and blessings that I have been endowed with. I am highly indebted to Him for everything that He has given me!



# INDEX

	Page No.
SYNOPSIS	11-30
LIST OF ABBREVIATIONS	31-32
LIST OF FIGURES	33-36
LIST OF TABLES	37
1. INTRODUCTION	39-41
2. AIMS AND OBJECTIVES	42
3. REVIEW OF LITERATURE	44-65
4. MATERIALS AND METHODS	67-85
5. RESULTS	87-136
I) Characterization of cell lines	87-92
II) Generation of K8 over-expressed MDA MB 435 clones	93-105
III) a) Generation of K8 down-regulated MDA MB 468 clones	106-116
b) Generation of K8 down-regulated MCF10A clone	117-125
IV) IHC analysis of K8, K18 and vimentin in primary tumors of breast cancer	126-128
V) Microarray analysis of K8 over-expressed MDAMB 435 & K8 down-regulated MDA MB 468 clones	129-136
6. DISCUSSION	138-149
7. SUMMARY AND CONCLUSION	151
8. REFERENCES	153-165
9. APPENDIX	166
10. REPRINT OF PUBLISHED ARTICLE	167

# *Synopsis*



## **Homi Bhabha National Institute**

### **Ph. D. PROGRAMME**

- 1. Name of the Student:** Sapna V. Iyer
- 2. Name of the Constituent Institution:** Tata Memorial Centre, Advanced Centre for Treatment Research and Education in Cancer
- 3. Enrolment No. :** LIFE09200604003 (28/08/2006)
- 4. Title of the Thesis:** Role of cytokeratins 8 and 18 in differentiation and transformation of epithelial cells.
- 5. Board of Studies:** Life sciences

### **SYNOPSIS**

## **Introduction:**

Breast cancer is the most prevalent form of cancer in women worldwide accounting for 23% of the total cancer cases and ranks second overall (10.9% of all cancers). It is the second most common cancer affecting women in India [1,2]. Breast cancers have been classified into many sub-types based on their receptor status [3]. The two major epithelial cell types found in the breast tissue are basal and luminal epithelial cells [4]. In the bilaminar breast epithelium, the basal or myoepithelial compartment represents the proliferating compartment, while the luminal compartment consists of differentiating cells [5]. The basal and luminal cell types can be distinguished based on their cytokeratin or keratin (K) profile.

Keratins, the largest family of intermediate filament proteins and are epithelia predominant in their expression [6,7]. The filaments are formed by non-covalent coiled coil interaction between one type I acidic (K9-K28) and one type II basic (K1-K8 and K971-K74) keratins which are obligatory heteropolymers [8]. They form cytoplasmic scaffold that emanates from the plasma membrane and spreads throughout the cytoplasm to provide shape and rigidity to the cells [9]. Apart from their structural role, they also provide a platform for various signaling events and form a complex with multiple proteins involved in signaling networks that regulate functions like cell cycle progression, apoptosis, cellular response to stress, cell size, protein synthesis and membrane trafficking [10].

An important feature of keratins is that their expression is regulated by tissue type and also during differentiation [10]. Stratified epithelia express different keratin pairs in different compartments. The cells of the basal compartment express the keratin pair of K5 and K14. As the basal cells differentiate they express K4/13 in the internal

epithelium and K1/10 in the cornified epithelium [6,11]. In breast epithelium the basal/myoepithelial cells (proliferation compartment) express K5 and K14, while the luminal cells (differentiation compartment) express K8 and K18 [5,6]. The strictly regulated tissue and differentiation specific pattern of expression is suggestive of the fact that the keratins may have tissue specific functions.

The keratin pair of K8 and K18 is the first pair to be expressed in embryogenesis and this pair is known to execute various regulatory functions, which include modulation of protein localization, protein targeting/trafficking and apoptosis [12]. The expression of this pair is restricted later to simple (e.g. liver, pancreas, kidney etc.) [6,13] and mixed (e.g. breast, lungs etc.) epithelia [6,14,15]. Further, over-expression of K8/18 is observed in adenocarcinomas [6,16]. Aberrant expression of this pair is found in squamous cell carcinomas (SCC) irrespective of their site of origin [17,18]. Previous studies in our laboratory and others have shown aberrant expression of K8/18 contributes to malignant transformation of stratified epithelial cells [19,20]. Recent studies from our laboratory have shown that K8/18 pair mediates neoplastic progression via  $\alpha 6\beta 4$  integrin mediated signaling in oral cancer derived cell line [21] and that K8 is required for the transformation induced by loss of plakophilin3 (PKP3) in simple epithelia [22].

There are differing reports about the role of K8/18 pair in breast cancer progression. K8/18 when expressed along with vimentin have been associated with drug resistance, invasion and metastasis in breast cell carcinomas and melanomas [23,24]. Other reports have suggested that the elevation of K18 expression in breast cancer patients correlates with favourable prognosis [25] and that the loss of K8 in conjunction with aberrant expression of vimentin correlates with early metastasis and poor prognosis [26,27]. Over-expression of K18 in MDA MB 231 breast carcinoma

cells, which are invasive and highly metastatic, produced differentiated phenotype [5]. Thus, the role of K8/18 in breast cancer progression is not yet clear.

A systematic study by over expression in highly invasive transformed breast epithelial cells and down regulation in non-transformed and transformed, but less invasive breast epithelial cells and have helped us to understand the role of this keratin pair in cell transformation and/or differentiation. Comparison of the RNA transcripts between the vector control and K8 gene or shRNA transfected clones using microarray have given us some leads about the underlying regulatory mechanism by which this keratin pair brings about these changes.

The objectives of the study were as follows:

### **Objectives:**

1. To transfect K8 in MDA MB 435 cells (invasive) to assess if it results in more differentiated phenotype.
2. To knockdown K8 in MCF -10A (non- transformed) and MDA MB 468 (transformed) cells to understand the role of K8 in transformation of these cells.
3. To study molecular changes as a result of either knockdown or introduction of K8 gene using microarray analysis.

### **Materials and methods:**

**1. Cell culture and transfection:** The MDA MB 435 breast cancer cell line was cultured in Dulbecco's Modified Eagle's Medium (DMEM; Gibco): Ham's F12 Gibco (1:1), with 10% fetal bovine serum (FBS, Hyclone) and standard antibiotic mixture. The MDA MB 468 breast cancer cell line was cultured in DMEM with 10% FBS and standard antibiotic mixture. MCF10A cell line was cultured in DMEM :

Ham's F12 (1:1), 10% FBS, Supplement cocktail (10 µg/ml Insulin, 0.5 µg/ml Hydrocortisone, 20ng/ml EGF, all from Sigma-Aldrich) and standard antibiotic mixture. All cell lines were cultured at 37°C and 5% CO<sub>2</sub> atmosphere.

**2. Plasmids and constructs:** K8 gene cloned in pCDNA3 (Invitrogen) was used for over-expression of K8. The shRNA to K8 gene - shRNA 8.2 designed previously was used for down-regulation of K8 [21].

**3. Transfections:** K8 over-expressing MDA MB 435 cells were generated by transfecting vector 2µg of either pCDNA3 alone or K8 expression vector pCDNA3-K8 with lipofectamine plus transfection reagent. The stable clones were selected in neomycin containing medium. To generate stable knock down clones in MDA MB 468 and MCF10A cells, 2µg of shRNA constructs and empty vector were transfected using Superfect (Qiagen) and ICAfectin 441(Eurogenetic). The selection of the K8 knockdown clones was done using puromycin containing medium.

**4. Keratin extraction and Western blotting:** The keratins were extracted in high salt extraction buffer and processed as described previously [28]. Whole-cell lysates were prepared in SDS lysis buffer (2% SDS, 50 mMTris-HCl, pH 6.8, 0.1% BME (β-Mercaptoethanol), and 10% glycerol. A protease inhibitor cocktail (Calbiochem, San Diego, CA) was added to lysis buffer. Equal amount of protein was loaded and resolved on SDS-PAGE gels followed by Western blotting.

**5. RNA isolation and Reverse Transcriptase –PCR:** RNA was isolated by TRI reagent (Sigma) and RT-PCR was conducted on the cells using RevertAid First Strand cDNA synthesis Kit (Fermentas) for cDNA preparation.

**6. Real-time PCR:** A total of 2µg of RNA was reverse transcribed using pdN<sub>6</sub> random primers. Real time PCR analysis was performed on 10ng of cDNA using gene specific primers using SYBR green-based real-time quantitative PCR analysis

on the ABI 7900HT Fast Real Time PCR System (Applied Biosystems, Foster, CA, USA). The relative gene expression was quantified by comparative Ct method using *GAPDH* as house keeping control.

**7. Mass spectrometry analysis:** Keratins extracted using high salt buffer were run on SDS-PAGE. The bands from Coomassie stained gels were excised for the mass spectrometry analysis. The gel pieces were washed with destainer (acetonitrile) further reduced and alkylated with Dithiothreitol and Iodoacetamide respectively. The processed gel pieces were digested with trypsin (10ng/μl) and subjected for mass spectrometry analysis.

**8. Immunofluorescence and laser confocal microscopy:** For immunofluorescence, cells were grown on coverslips for 48 hours and permeabilized with triton X-100 and fixed with chilled methanol (-20°C). The fixed cells were incubated with respective primary antibody and secondary antibody. The cells were further analyzed under LSM 510 Carl Zeiss Confocal system.

**9. F-actin staining:** To analyze changes in actin filamentous organization, the cells were fixed with paraformaldehyde and stained with FITC labelled Phalloidin (Sigma Aldrich, P5282) antibody and observed under LSM 510 Carl Zeiss Confocal system.

**10. Lipid droplets (Nile red staining):** Cells were stained with Nile red dye to determine the levels of lipid droplets (differentiation marker). The cells were incubated with Nile red (1 mg/ml in acetone) diluted in PBS, rinsed with PBS and observed for the presence of lipid droplets by confocal microscopy under LSM 510 Carl Zeiss Confocal system.

**11. Cell proliferation assay:** Cells (5000) were seeded, in triplicate in a 96-well microtiter plate in 100μl complete medium. Proliferation was studied every 24 hours up to a period of 4 days using MTT assay as described previously [29]. A growth



curve was prepared from three independent experiments by plotting O.D. at 540 nm (on y-axis) against time (on x-axis).

**12. Soft Agar colony forming Assay:** The cells were tested for anchorage-independent growth using soft agar colony-forming assay as described previously [19].

**13. Cell Motility:** For motility by scratch wound assay the cells were grown to 95% confluency and incubated with the medium containing 10 $\mu$ g/ml mitomycin-C for 3 hours to inhibit proliferation. A wound was scratched and wound closure was monitored under time lapse microscope for 20 hours. Motility by transwell assay was assessed by using Boyden chamber. For the assay, 2 x 10<sup>5</sup> cells in 0.1% BSA were seeded in the upper chamber while 10% FBS was added to the medium in the lower chamber. The migration of the cells to this chemoattractant on the underside of the membrane was determined by H & E staining. The number of migrated cells was counted microscopically.

**14. *In-vitro* invasion assay:** For invasion assay the Boyden chamber was coated with 40  $\mu$ g of Matrigel and processed further as described previously for motility by transwell assay.

**15. *In-vivo* Tumorigenicity assay:** To determine tumorigenic potential 1x 10<sup>6</sup> cells were injected in the mammary fat pad of five SCID mice. Tumor volume (mm<sup>3</sup>) was calculated by the formula (1/2  $\times$  width  $\times$  width  $\times$  length) as previously reported [30]. After 7 weeks the tumors were excised and wound was surgically sealed. The animals were sacrificed after 4 weeks post-surgery and the vital organs were collected for histological examination.

**16. Expression Profiling by Microarray analysis:** The K8 over-expressed and vector control transfected MDA MB 435 clones and K8 down-regulated and vector

control transfected MDA MB 468 clones were assessed for changes in gene expression as result of K8 modulation by microarray analysis. The stably transfected clones were analyzed by services offered by Genotypic (Bangalore) using Human whole genome 8 x 60 K format Agilent platform microarray by Cy3 labelled single color hybridization. The data normalization and analysis was done using Gene spring 11.2 software. The differential expression of a select set of genes was further validated by real time RT-PCR analysis.

**17. Statistical analysis:** Two groups of data were compared by performing a *t*-test statistical analysis  $p < 0.05$  was considered significant.

## **Results:**

### **Characterization of cell lines:**

**I) K8/18 and vimentin expression in non-transformed MCF10A, transformed less invasive MDA MB 468 and transformed and highly invasive MDA MB 435 cell lines:** K8/18 levels were found to decrease and vimentin level was found to increase from the non-transformed MCF10A cell line to highly invasive MDA MB 435 cell line.

**II) Lipid droplet levels:** To understand whether K8/18 levels can alter the differentiation status of breast epithelial cells, the levels of lipid droplets were determined. A differentiated mammary gland exhibits a specific secretory function of producing milk. Milk constitutes of triglycerides which are neutral lipids and can be stained by Nile red dye. The levels of lipid droplets were found to sequentially decrease from the MCF10A to MDA MB 435 cell lines.

**III) Soft agar colony forming assay:** The number and size of the colonies was found to increase from MCF10A to MDA MB 435 cell lines.

In summary K8/18 levels reflected the degree of differentiation of the cell lines.

## **I) Overexpression of K8 in an invasive cell line:**

### **1) Expression of K8/18 and vimentin in K8 over-expressed MDA MB 435**

**clones:** Keratin 8 transfected clones showed up-regulation of K18, immunofluorescence analysis showed formation of filaments on K8 over-expression. No change in vimentin expression was seen. K7 is known to pair with K18 and hence K7 expression was analyzed in the cells by western blot analysis, which remained undetected in vector control transfected and K8 over-expressed clones.

**2) Lipid droplets:** The over-expression of K8 did not result in any significant change in the lipid droplet levels.

**3) Soft agar colony forming assay:** No significant difference in the size or number of soft agar colonies was observed.

**4) Growth curve:** The K8 over-expressed clones showed significant decrease in cell proliferation as compared to the vector control cells as assessed by MTT assay ( $p < 0.05$ ).

**5) F-Actin organization:** K8 over-expressed clones showed no obvious difference in actin filament organization as compared to vector control clone.

**6) Motility:** The K8 over-expressed clones showed marginal reduction in motility in scratch wound assay, whereas in transwell assay significant decrease in motility was seen in K8 over-expressed clones as compared to vector control clone ( $p < 0.05$ ).

**7) Invasion *in-vitro*:** The K8 transfected MDA MB 435 clones demonstrated significant decrease in invasion as compared to the vector control clone ( $p < 0.05$ ) by matrigel invasion assay.

**8) Tumorigenicity assay:** The K8 transfected clones demonstrated delay in the onset of the tumor development as compared to the vector control cells when injected in mammary fat pad of SCID mice. Significant decrease in the tumor volume was seen in K8 transfected clones as compared to animals injected with vector control clone ( $p < 0.05$ ). Metastatic lesions were observed all over the lungs in all the animals injected with vector control transfected clone whereas only two out of five animals injected with K8 transfected clone showed metastasis which was drastically reduced to few islands as compared to vector control. Thus the K8 transfected cells demonstrated decrease in invasion as well as metastasis.

**9) E-cadherin expression and localization:** E-cadherin expression is known to change during malignant transformation. Thus change in E-cadherin levels and localization was assessed in K8 over-expressed MDA MB 435 clones. E-cadherin remained undetected even after K8 over-expression.

**10)  $\beta 4$  integrin expression:** To understand whether  $\beta 4$  integrin mediated signaling has any role in transformation /progression of breast cancer derived cell lines, its expression levels were analyzed.  $\beta 4$  integrin was not detected in either K8 over-expressed or vector control clones.

In summary, the over-expression of K8 in an invasive MDA MB 435 cell line resulted in the significant decrease in proliferation, *in-vitro* motility, *in-vitro* invasion, tumor volume and metastasis *in-vivo*. Keratin 7, E-cadherin and  $\beta 4$  integrin were not detected in vector control or K8 over-expressed clones.

**IIA) Down-regulation of K8 in a transformed less invasive MDA MB 468 cell line:**

**1) K8/18 and vimentin expression in K8 down-regulated MDA MB 468 cells:** K8 expression was undetectable in the shRNA transfected clones while no change in K18 levels or filament formation was seen on K8 down-regulation. No change in vimentin expression was seen. The western blot analysis showed up-regulation of K7 in K8 down-regulated MDA MB 468 clones as compared to vector control clone.

**2) Keratin Extraction:** High salt extraction showed the presence of K7, K18 along with K19 in both K8 down regulated and vector control clones and K8 only in the vector control clone indicating specificity of K8 shRNA.

**3) Lipid droplet staining:** The down-regulation of K8 did not result in any significant change in the lipid droplet levels.

**4) Soft agar colony forming assay:** K8 knockdown clones demonstrated significant increase in number and volume of soft agar colonies as compared to vector control transfected clones ( $p < 0.05$ ).

**5) Growth curve:** The K8 down-regulated clones showed no significant change in cell proliferation as compared to the vector control clone as assessed by MTT assay.

**6) Actin organization:** K8 down-regulated clones showed increased lamellipodia formation as compared to vector control clone.

**7) Motility:** K8 down-regulated clones demonstrated significant increase in motility as compared to vector control clone ( $p < 0.05$ ) both by scratch wound and transwell assay.

**8) *In-vitro* Invasion assay:** K8 knockdown clones demonstrated significant increase in invasion as compared to vector control clone ( $p < 0.05$ ) by matrigel invasion assay.

**9) E-cadherin expression and localization:** There was no change in E-cadherin protein levels on K8 down-regulation, but change in its localization was seen in these cells. Vector control clone showed membrane localization of E-cadherin, while it was localized in the cytoplasm in the K8 down-regulated clones.

**10)  $\beta 4$  integrin expression:** The analysis of  $\beta 4$  integrin levels indicated no change in  $\beta 4$  integrin protein levels in K8 down-regulated clones as compared to vector control clone.

In summary down-regulation of K8 in MDA MB 468 cells resulted in up-regulation of K7, significant increase in soft agar colony formation, *in-vitro* motility and invasion. K8 down regulation also resulted in change in E-cadherin localization to cytoplasm without change in its protein levels, while there was no change in  $\beta 4$  integrin levels.

#### **IIB) Down regulation of K8 in MCF10A (non-transformed cell line):**

**1) K8/18 and vimentin expression in K8 down-regulated cells:** Western blot analysis showed 80% down-regulation of K8 and 60-70% down-regulation of K18 expression levels in K8 knock down clones as compared to vector control clone. The immunofluorescence analysis showed diffused staining of K8 and K18 filaments in the K8 down-regulated clones. No change in vimentin expression was seen. K7 was undetected in the K8 down-regulated and vector control clones. MCF10A K8 down-regulated and vector control clones did not show any significant change in the lipid droplets levels, growth pattern, soft agar colony forming potential, actin

organization, *in-vitro* motility and invasion. *In-vivo* tumorigenicity assay did not show any tumor formation in K8 down-regulated clones and vector control transfected clone. There was no change in protein expression levels or localization of E-cadherin.

In summary K8 down-regulation in MCF10A did not result in any phenotypic alterations.

### **III) To understand the molecular changes on K8 up-/down-regulation, Microarray analysis was carried out:**

The differentially expressed genes on K8 up-/down-regulation were selected based on the fold change and Gi processed signal values. MCF10A cells were not analyzed because they did not show any significant phenotypic changes on K8 down-regulation. The genes associated with change in transformation, motility and invasive phenotype were selected. The list of genes showing up-regulation on K8 over-expression were TUBB6, RASSF4, THBS2 while the genes that showed down-regulation were CSPG4, PRKACB and LEF1. The analysis of differentially expressed genes on Keratin 8 down-regulation in MDA MB 468 cells showed up-regulation of FABP6, CAPG, BMP7 and down-regulation of FGFR1 and PTPRM.

**Validation of differentially expressed genes using Real time PCR:** The real time PCR data demonstrated significant increased expression of THBS2 and TUBB6 in K8 over-expressed MDA MB 435 clones. LEF-1 transcription factor was found to be significantly down-regulated in K8 over-expressed clones. CAPG, an actin binding protein was significantly over-expressed in K8 down-regulated MDA MB 468 clones.

## **Discussion:**

The available literature related to K8/18 expression in breast cancer progression is inconsistent. Some of the previous reports on tumor samples and cell lines suggested that the expression of K8/18 was associated with invasion and poor prognosis [4,24]. Other reports from breast tumor samples suggested that loss of K8/18 expression was associated with poor prognosis [25-27] which correlated with the results of our present study and with data previously reported for K18 expression *in-vitro* [5].

K8 over-expressed MDA MB 435 clones showed decreased tumor volume, motility, invasion and inhibition in metastasis. This was accompanied with up-regulation in K18, thus the K8/18 filaments now formed, might have imparted rigidity to the cells and hence these cells were less invasive [5]. While K8 down-regulation in MDA MB 468 resulted in no change in K18 level or filament formation, which indicates possible compensatory pairing of K18 with some other type II keratin like K7 [31]. Western blot analysis showed up-regulation of K7 in these clones, although these filaments (K7 and K18) may not have the same function as that of K8/18 filaments. We did not detect K7 in MDA MB 435 and MCF10A clones and we observe the concomitant up-/down-regulation of K18 in response to K8 up-/down-regulation, indicating that there was no compensation by K7 in these cells. In summary, these findings together underline the importance of K8/18 filaments in maintaining the non-transformed phenotype in breast cancer derived cell lines.

Previous reports have shown the role of vimentin in breast cancer progression [4,5,24]. Though vimentin is widely studied in breast cancer, present study shows that change in motility or invasion were independent of vimentin expression. This



indicates that K8/18 and vimentin may regulate invasion and motility via independent pathways in different cell types.

The expression of E-cadherin (cell adhesion molecule) is known to decrease in tumor progression [32]. Change in localization from membrane to cytoplasm without change in the protein levels was observed on K8 down-regulation in MDA MB 468 clones. There is no direct link between keratins and E-cadherin but keratins form cellular meshwork by binding at the desmosomal junction and Plakoglobin (PG) is an important component of both desmosomal plaque and adherens junction [33]. Thus the loss of K8 might have caused an indirect effect on its interaction with PG and thus E-cadherin localization. No induction in expression of E-cadherin after K8 over-expression in MDA MB 435 clones indicates that the changes seen in this cell line are independent of E-cadherin expression. To summarize, modulation of K8 expression and its effect on K8/18 filament formation does not induce/ repress the levels of E-cadherin but results in re-localization of this protein. Re-localization could be the result of altered interaction of E-cadherin with other junctional complex proteins.

Previous work from our laboratory has shown that the keratin pair of K8/18 plays a positive role in tumor progression in an oral SCC derived cell line via  $\beta 4$  integrin mediated signaling [21]. There are no alterations in the levels of  $\beta 4$  integrin on K8 up-/down- regulation in the cell lines used in this study. Thus the present study indicates that the changes in motility or invasion in these breast cancer derived cell lines may not be regulated by  $\beta 4$  integrin mediated pathway. Integrins  $\beta 1$  and  $\beta 3$  are the most common type of integrins that have been shown to mediate tumor progression in breast cancer. K8/18 have shown to mediate  $\beta 1$  integrin mediated cell adhesion in hepatomas [34]. Most of the previous studies show role of  $\alpha 3 \beta 1$  integrin

in promoting tumor progression and metastasis in breast cancer [35]. In several malignancies up-regulation of  $\alpha v\beta 3$  integrin correlated with tumor progression for e.g. in melanoma, glioma, ovarian cancer and breast cancer [36]. It will be interesting to see if the change in invasive property of the cell lines used in our study is brought about by any of these integrin pairs or by some other signaling pathways.

In breast epithelium K8/18 are normally expressed in the luminal/differentiation compartment and our results show that loss of same keratin pair in breast cancer derived cell lines resulted in an invasive phenotype. These findings suggest the possibility that the same keratin pair may have dissimilar role in neoplastic progression of different epithelia. Hence it will be important to analyze breast tumor samples for K8/18 expression to understand their clinical significance. Our results of K8 down-regulation in MCF10A suggest that K8 may not be involved in changing the motility or invasive potential of a non-transformed cell lines.

The exact mechanism by which these changes are brought about is still not understood. To understand the underlying mechanism, further detailed analysis of changes at the molecular and proteomic level in response to modulation of K8/18 level is required. As a first step in this direction microarray analysis was undertaken on the K8 over-expressed MDA MB 435 and MDA MB 468 K8 knock down clones in comparison to their respective vector controls to understand the molecular changes caused due to modulation of K8 in these cell lines.

Some of the changes associated with the decrease in the transformation and invasive potential in MDA MB 435 cell line on over-expression of K8 were up-regulation in TUBB6 and THBS2 and down-regulation in LEF1. TUBB6, beta tubulin 6 is also known to be largely reduced in most tumors [37]. THBS2, an inhibitor of metastasis might be contributing to the decreased or no metastasis seen in these cells [38]. We

found down regulation of LEF1 in K8 overexpressed MDA MB 435 clones. LEF1, transcription factor is the nuclear mediator of Wnt signaling pathway [39]. Since we did not find alterations in other mediators of Wnt signaling pathway it is not possible for us to hypothesize whether Wnt signaling pathway is altered based on our microarray data. On down-regulation of K8 in MDA MB 468 cell line there was increase in transformation potential motility and invasion. One of the major molecular changes observed in these clones was up regulation of CAPG. CAPG is Gelsolin-related actin-binding protein, is expressed at higher levels in breast cancer, previous data have shown that the product of this gene is responsible for increased motility and invasion in breast cancer [40].

We did not see commonalities in gene expression profiles in K8 up/down-regulated clones. It is possible that the changes observed are cell line specific and downstream effectors in case of K8 up/down-regulated clones may not be similar. The other possibility is that the alterations might have occurred at protein level and proteomic analysis may throw light on this aspect. Possible alterations like some PTMs which have already been reported in literature might have led to the change transformation potential of the cells [22,41]. Thus the molecular changes as result of K8 modulation need to be further substantiated with proteomic analysis.

### **Summary and Conclusion:**

Overexpression of K8 in MDA MB 435 resulted in a less invasive phenotype, while the knockdown of the K8 in MDA MB 468 resulted in increase in neoplastic potential and increased invasion *in-vitro*. The down-regulation of K8 in MCF10A did not result in any phenotypic alterations. These results are indicative of the role of K8/18 in modulating invasion in the breast cancer, the presence indicating less invasive phenotype while absence indicates highly invasive dedifferentiated

phenotype. Our microarray data has given us some leads regarding molecular changes occurring as a result of K8 up/down-regulation further validation at protein level may help us understand the down-stream effectors and interacting proteins.

K8/18 expression has been shown to correlate with poor prognosis in SCC of oral cavity and loss of same keratin pair in breast cancer derived cell lines resulted in an invasive phenotype. These findings suggest the possibility that the same keratin pair may have dissimilar role in neoplastic progression of different cancers.

## References :

1. Jemal A, Bray F, Center MM, Ferlay J, Ward E, et al. (2011) Global cancer statistics. *CA Cancer J Clin* 61: 69-90.
2. Hines MC, Dickerson K, Klein P, Mayer M, Noss K, et al. (2007) Shaping the future of biomarker research in breast cancer to ensure clinical relevance. *Nat Rev Cancer*. 2007/03/27 ed. pp. 309-315.
3. Reis-Filho JS, Pusztai L (2011) Gene expression profiling in breast cancer: classification, prognostication, and prediction. *Lancet* 378: 1812-1823.
4. Taylor-Papadimitriou J, Stampfer M, Bartek J, Lewis A, Boshell M, et al. (1989) Keratin expression in human mammary epithelial cells cultured from normal and malignant tissue: relation to in vivo phenotypes and influence of medium. *J Cell Sci* 94 ( Pt 3): 403-413.
5. Buhler H, Schaller G (2005) Transfection of keratin 18 gene in human breast cancer cells causes induction of adhesion proteins and dramatic regression of malignancy in vitro and in vivo. *Mol Cancer Res* 3: 365-371.
6. Moll R, Franke WW, Schiller DL, Geiger B, Krepler R (1982) The catalog of human cytokeratins: patterns of expression in normal epithelia, tumors and cultured cells. *Cell* 31: 11-24.
7. Moll R, Divo M, Langbein L (2008) The human keratins: biology and pathology. *Histochem Cell Biol* 129: 705-733.
8. Schweizer J, Bowden PE, Coulombe PA, Langbein L, Lane EB, et al. (2006) New consensus nomenclature for mammalian keratins. *J Cell Biol* 174: 169-174.
9. Fuchs E, Cleveland DW (1998) A structural scaffolding of intermediate filaments in health and disease. *Science* 279: 514-519.
10. Coulombe PA, Omary MB (2002) 'Hard' and 'soft' principles defining the structure, function and regulation of keratin intermediate filaments. *Curr Opin Cell Biol* 14: 110-122.
11. Sawaf MH, Ouhayoun JP, Forest N (1991) Cytokeratin profiles in oral epithelial: a review and a new classification. *J Biol Buccale* 19: 187-198.
12. Paramio JM, Jorcano JL (2002) Beyond structure: do intermediate filaments modulate cell signalling? *Bioessays* 24: 836-844.
13. Owens DW, Lane EB (2003) The quest for the function of simple epithelial keratins. *Bioessays* 25: 748-758.

14. Blobel GA, Moll, R., Franke, W. W. and Vogt-Moykopf, (1984) Cytokeratins in normal lung and lung carcinomas. I. Adenocarcinomas, squamous cell carcinomas and cultured cell lines. *Virchows Arch Cell Pathol Annu*: 407-429.
15. Franke WW, Schiller DL, Moll R, Winter S, Schmid E, et al. (1981) Diversity of cytokeratins. Differentiation specific expression of cytokeratin polypeptides in epithelial cells and tissues. *J Mol Biol* 153: 933-959.
16. Oshima RG, Baribault H, Caulin C (1996) Oncogenic regulation and function of keratins 8 and 18. *Cancer Metastasis Rev* 15: 445-471.
17. Vaidya MM, Borges AM, Pradhan SA, Rajpal RM, Bhisey AN (1989) Altered keratin expression in buccal mucosal squamous cell carcinoma. *J Oral Pathol Med* 18: 282-286.
18. Fillies T, Werkmeister R, Packeisen J, Brandt B, Morin P, et al. (2006) Cytokeratin 8/18 expression indicates a poor prognosis in squamous cell carcinomas of the oral cavity. *BMC Cancer* 6: 10.
19. Raul U, Sawant S, Dange P, Kalraiya R, Ingle A, et al. (2004) Implications of cytokeratin 8/18 filament formation in stratified epithelial cells: induction of transformed phenotype. *Int J Cancer* 111: 662-668.
20. Casanova L, Bravo A, Were F, Ramirez A, Jorcano JJ, et al. (1995) Tissue-specific and efficient expression of the human simple epithelial keratin 8 gene in transgenic mice. *J Cell Sci* 108 ( Pt 2): 811-820.
21. Alam H, Kundu ST, Dalal SN, Vaidya MM (2011) Loss of keratins 8 and 18 leads to alterations in alpha6beta4-integrin-mediated signalling and decreased neoplastic progression in an oral-tumour-derived cell line. *J Cell Sci* 124: 2096-2106.
22. Khapare N, Kundu ST, Sehgal L, Sawant M, Priya R, et al. (2012) Plakophilin3 Loss Leads to an Increase in PRL3 Levels Promoting K8 Dephosphorylation, Which Is Required for Transformation and Metastasis. *PLoS One* 7: e38561.
23. Bauman PA, Dalton WS, Anderson JM, Cress AE (1994) Expression of cytokeratin confers multiple drug resistance. *Proc Natl Acad Sci U S A* 91: 5311-5314.
24. Hendrix MJ, Seftor EA, Chu YW, Trevor KT, Seftor RE (1996) Role of intermediate filaments in migration, invasion and metastasis. *Cancer Metastasis Rev* 15: 507-525.
25. Schaller G, Fuchs I, Pritze W, Ebert A, Herbst H, et al. (1996) Elevated keratin 18 protein expression indicates a favorable prognosis in patients with breast cancer. *Clin Cancer Res* 2: 1879-1885.
26. Schaller G, Fuchs I, Ebert A, Gstettenbauer M, Herbst H, et al. (1999) [The clinical importance of keratin 18 in breast cancer]. *Zentralbl Gynakol* 121: 126-130.
27. Woelfle U, Sauter G, Santjer S, Brakenhoff R, Pantel K (2004) Down-regulated expression of cytokeratin 18 promotes progression of human breast cancer. *Clin Cancer Res* 10: 2670-2674.
28. Achtstaetter T, Hatzfeld M, Quinlan RA, Parmelee DC, Franke WW (1986) Separation of cytokeratin polypeptides by gel electrophoretic and chromatographic techniques and their identification by immunoblotting. *Methods Enzymol* 134: 355-371.
29. Alam H, Sehgal L, Kundu ST, Dalal SN, Vaidya MM (2011) Novel function of keratins 5 and 14 in proliferation and differentiation of stratified epithelial cells. *Mol Biol Cell* 22: 4068-4078.
30. Xiang R, Davalos AR, Hensel CH, Zhou XJ, Tse C, et al. (2002) Semaphorin 3F gene from human 3p21.3 suppresses tumor formation in nude mice. *Cancer Res* 62: 2637-2643.

31. Magin TM (1998) Lessons from keratin transgenic and knockout mice. *Subcell Biochem* 31: 141-172.
32. Berx G, Van Roy F (2001) The E-cadherin/catenin complex: an important gatekeeper in breast cancer tumorigenesis and malignant progression. *Breast Cancer Res* 3: 289-293.
33. Gosavi P, Kundu ST, Khapare N, Sehgal L, Karkhanis MS, et al. (2011) E-cadherin and plakoglobin recruit plakophilin3 to the cell border to initiate desmosome assembly. *Cell Mol Life Sci* 68: 1439-1454.
34. Bordeleau F, Galarneau L, Gilbert S, Loranger A, Marceau N (2010) Keratin 8/18 modulation of protein kinase C-mediated integrin-dependent adhesion and migration of liver epithelial cells. *Mol Biol Cell* 21: 1698-1713.
35. Morini M, Mottotese M, Ferrari N, Ghiorzo F, Buglioni S, et al. (2000) The alpha 3 beta 1 integrin is associated with mammary carcinoma cell metastasis, invasion, and gelatinase B (MMP-9) activity. *Int J Cancer* 87: 336-342.
36. Felding-Habermann B, O'Toole TE, Smith JW, Fransvea E, Ruggeri ZM, et al. (2001) Integrin activation controls metastasis in human breast cancer. *Proc Natl Acad Sci U S A* 98: 1853-1858.
37. Leandro-Garcia LJ, Leskela S, Landa I, Montero-Conde C, Lopez-Jimenez E, et al. (2010) Tumoral and tissue-specific expression of the major human beta-tubulin isotypes. *Cytoskeleton (Hoboken)* 67: 214-223.
38. Streit M, Riccardi L, Velasco P, Brown LF, Hawighorst T, et al. (1999) Thrombospondin-2: a potent endogenous inhibitor of tumor growth and angiogenesis. *Proc Natl Acad Sci U S A* 96: 14888-14893.
39. Behrens J, von Kries JP, Kuhl M, Bruhn L, Wedlich D, et al. (1996) Functional interaction of beta-catenin with the transcription factor LEF-1. *Nature* 382: 638-642.
40. Van den Abbeele A, De Corte V, Van Impe K, Bruyneel E, Boucherie C, et al. (2007) Downregulation of gelsolin family proteins counteracts cancer cell invasion in vitro. *Cancer Lett* 255: 57-70.
41. Alam H, Gangadaran P, Bhate AV, Chaukar DA, Sawant SS, et al. (2011) Loss of keratin 8 phosphorylation leads to increased tumor progression and correlates with clinico-pathological parameters of OSCC patients. *PLoS One* 6: e27767.

## **Publications:**

1. **Accepted:** Iyer SV, Dange PP, Alam H, Sawant SS, Ingle AD, et al. (2013) **Understanding the Role of Keratins 8 and 18 in Neoplastic Potential of Breast Cancer Derived Cell Lines.** *PLoS ONE* 8(1): e53532. doi:10.1371/journal.pone.0053532.

## ABBREVIATIONS

µg:	microgram
µl:	microliter
bp:	Base pairs
cAMP:	Cyclic AMP
CHCA:	Cyano Hydroxy Cinnamic acid
CRC:	Colorectal cancer
DAPI:	4, 6-diamidino-2-phenylindole
DNA:	Deoxyribonucleic acid
DP:	Desmoplakin
DSG:	Desmoglein
DTT:	Dithiothreitol
EB:	Ethidium bromide
ECL:	Enhanced chemiluminescence
ECM:	Extracellular matrix
EDTA:	Ethylenediaminetetraacetic acid
EGF:	Epidermal growth factor
EGTA:	Ethylene glycol tetra acetic acid
EMT:	Epithelial mesenchymal transition
ER:	Estrogen receptor
ERK:	Extracellular signal-regulated kinase
FITC:	Fluorescein isothiocyanate
GAPDH:	Glyceraldehyde 3-phosphate dehydrogenase
GFP:	Green fluorescent protein
H & E:	Haematoxylin and eosin
HEPES:	(N-(2-Hydroxyethyl) piperazine-N'-(2-ethanesulfonicacid)) sodium salt
Her2:	Human epidermal growth factor receptor 2
HRP:	Horseradish Peroxidase
IC	–Intensity Coverage
IF:	Intermediate filament
IFAP:	IF-associated protein
IHC:	Immunohistochemistry
IP:	Immuno precipitation
JNK:	c-Jun N-terminal kinase

K: Keratin  
 MALDI: Matrix-assisted laser desorption ionization  
 MAPK: Mitogen activated protein kinase  
 MF: Microfilaments  
 MgCl<sub>2</sub>: Magnesium chloride  
 MMP: Matrix Metalloproteinase  
 MS: Mass spectroscopy  
 MT: Microtubules  
 ng: nanogram  
 OSCC: Oral Squamous cell carcinoma  
 PAGE: Polyacrylamide gel electrophoresis  
 PCR: Polymerase chain reaction  
 PG: Plakoglobin  
 PGR: Progesterone receptor  
 pI- Isoelectric point  
 PI3K: Phosphoinositide 3-kinase  
 PKC: Protein kinase C  
 PKP3: Plakophilin 3  
 PMF- Peptide Mass Fingerprinting  
 PMSF: Phenylmethanesulphonyl fluoride  
 PNK: Polynucleotide kinase  
 PRL-3: Phosphatase of regenerating liver-3  
 PVDF: Polyvinylidene difluoride  
 RNA: Ribonucleic Acid  
 RNase: Ribonuclease  
 RT-PCR: Reverse transcriptase Polymerase chain reaction  
 SCC: Squamous cell carcinoma  
 SC-Sequence coverage  
 SDS: Sodium dodecyl sulfate  
 shRNA: Short hairpin RNA  
 TEMED: N, N, N', N' – Tetramethylene diamine  
 TFA: Trifluoroacetic acid  
 TNF- $\alpha$ : Tumor necrosis factor – $\alpha$   
 WB: Western Blot



## LIST OF FIGURES

	Page No.
1. Figure 3.1: Schematic representation of keratin structure.	46
2. Figure 5.1.1: Analysis of K8 and K18 in MCF10A, MDA MB 468 and MDA MB 435 cell lines.	88
3. Figure 5.1.2: Analysis of vimentin expression in MCF10A, MDA MB 468 and MDA MB 435 cell lines	89
4. Figure 5.1.3: Analysis of differentiation status of MCF10A, MDA MB 468 and MDAMB 435 cell lines by lipid droplets staining using Nile red	90
5. Figure 5.1.4: Analysis of soft agar colony forming potential in MCF10A, MDAMB 468 and MDA MB 435 cell lines	91
6. Figure 5.2.1.1: Analysis of K8 and K18 expression in K8 over-expressed MDA MB 435 clones by Western blot and immunofluorescence analysis.	93
7. Figure 5.2.1.2: Analysis of K8 expression by flow cytometry and K8/18 mRNA levels by real time PCR analysis	94
8. Figure 5.2.2: Analysis of K8 and K18 expression in K18 over-expressed) MDA MB 435 cells	95
9. Figure 5.2.3: Analysis of K7expression in K8 over-expressed MDA MB 435 clones	96
10. Figure 5.2.3.2 Analysis of vimentin expression in K8 over-expressed)MDA-MB-435 clones	96
11. Figure 5.2.4: Analysis of differentiation status of MDA MB 435 on K8 up -regulation by lipid droplets staining using Nile red	97
12. Figure 5.2.5: Analysis of changes in soft agar colony forming potential on K8 over-expression in MDA MB 435 cell line	98
13. Figure 5.2.6: Analysis of changes in cell proliferation on K8 over-expression in MDA MB 435 clones	98
14. Figure 5.2.7.1: Analysis of change in motility on K8 over-expression: by wound healing assay in K8 over-expressed MDA MB 435 clones	99
15. Figure 5.2.7.2: Analysis of motility by transwell assay in K8 over-expressed 435 clones	100

16. Figure 5.2.8: Actin organization in K8 over-expressed MDA MB 435 clones	100
17. Figure 5.2.9: Analysis of change in <i>in-vitro</i> invasion in K8 over-expressed clones of MDA MB 435	101
18. Figure 5.2.10: Analysis of change in <i>in-vivo</i> tumorigenicity and metastatic potential in K8 up - regulated MDA MB 435 clones	102
19. Figure 5.2.11: Analysis of K8, K18 and vimentin expression in tumor derived from animals on injection of MDA MB 435 K8 over-expressed and vector control clones	103
20. Figure 5.2.12.: Analysis of E-cadherin expression on K8 over-expression in MDA MB 435 clones	104
21. Figure 5.2.13: Analysis of $\beta 4$ integrin expression on K8 over-expression in MDA MB 435 clones	105
22. Figure 5.3.1.1: Analysis of K8 and K18 expression in K8 down-regulated MDA MB 468 clones by Western blot and immunofluorescence analysis	106
23. Figure 5.3.1.2: Analysis of K8 expression by flow cytometry and K8/18 mRNA levels by real time PCR analysis	107
24. Figure 5.3.2.1: Analysis of K7 expression in K8 down-regulated MDA-MB-468 clones.	108
25. Figure 5.3.2.2: Analysis of vimentin expression in K8 down-regulated MDA MB 468 clones.	109
26. Figure 5.3.3.: Analysis of differentiation status of MDA MB 468 K8 down-regulated clones by lipid droplets staining using Nile red	109
27. Figure 5.3.4: Analysis of changes in soft agar colony forming potential on K8 down-regulation in MDA MB 468 clones	110
28. Figure 5.3.5: Analysis of changes in cell proliferation on K8 down-regulation in MDA MB 468 cells	111
29. Figure 5.3.6.1: Analysis of change in motility on K8 down-regulation in MDA MB 468 cells by wound healing assay	112
30. Figure 5.3.6.2: Analysis of change in motility on K8 down-regulation in MDA MB 468 cells by transwell assay	112
31. Figure 5.3.7: Actin organization in K8 down-regulated MDA MB 468 clones	113

32. Figure 5.3.8. : Analysis of change in <i>in-vitro</i> invasion on K8 down-regulation in MDA MB 468 clones	113
33. Figure 5.3.9: Tumor formation in SCID mice injected with MDA MB 435 K8 down-regulated and vector control clones	114
34. Figure 5.3.10: Analysis of E-cadherin expression on K8 down-regulation in MDA MB 468 clones	115
35. Figure 5.3.11: Analysis of $\beta 4$ expression on K8 down-regulated MDA MB 468 clones:	116
36. Figure 5.4.1.1: Analysis of K8 and K18 expression in K8 down-regulated MCF10A clones by Western blot and immunofluorescence analysis	117
37. Figure 5.4.1.2: Analysis of K8 expression by flow cytometry and K8/18 by real time PCR analysis	118
38. Figure 5.4.2.1: Analysis of K7 expression in K8 down-regulated MCF10A clones	119
39. Figure 5.4.2.2: Analysis of vimentin expression in K8 down regulated MCF10A clones	119
40. Figure 5.4.3: Analysis of differentiation status of MCF10A K8 down-regulated clones by lipid droplets staining using Nile red	120
41. Figure 5.4.4: Analysis of changes in soft agar colony forming potential on K8 down-regulation in MCF10A cells.	121
42. Figure 5.4.5: Analysis of change in proliferation in K8 down-regulated MCF10A clones	122
43. Figure 5.4.6.1.: Analysis of change in motility on K8 down-regulation in MCF10A clones by scratch wound assay	122
44. Figure 5.4.6.2: Analysis of change in motility on K8 down –regulation in MCF10A clones by transwell assay	123
45. Figure 5.4.7: Analysis of change in <i>in-vitro</i> invasion on K8 down-regulation in MCF10A clones	123
46. Figure 5.4.8.: Analysis of change in tumorigenicity in K8 down-regulated MCF10A clones	124
47. Figure 5.4.9. : Analysis of E-cadherin expression on K8 down-regulation in MCF10A clones	125

<b>48.</b> Figure 5.5: Immunohistochemical analysis of K8, 18 and vimentin in primary tumors obtained from non-recurrent and recurrent patients:	128
<b>49.</b> Figure 5.6.2: Real time PCR analysis of K8 over-expressed MDA MB 435 and K8 down-regulated MDA MB 468 clones	135
<b>50.</b> Figure 5.6.3: Up-regulation of CAPG protein on K8 down-regulation in MDA MB 468.	136
<b>51.</b> Figure 6.1: Schematic representation of K8/18 role in oral cancer and breast cancer:	148
<b>52.</b> Figure 6.2: Schematic representation of hypothetical mechanism for the role of K8/18 in (A) MDA MB 435 and (B) MDA MB 468 breast cancer derived cell lines.	149

## LIST OF TABLES

	Page No.
1. <b>Table 3.1</b> Classification of IF and their association with disease.	47
2. <b>Table 3.2:</b> The new human keratin nomenclature	49
3. <b>Table 3.3:</b> Signalling pathways modulated by keratins	55
4. <b>Table 4.1:</b> SDS-PAGE components	72
5. <b>Table 4.2:</b> List of Antibodies used in the study	74
6. <b>Table 4.3:</b> List of Primers and oligonucleotides	78
7. <b>Table 5.1:</b> IHC on tumor sections obtained from primary tumors of patients showing no recurrence and patients showing recurrence using mAbs against K8, K18 and vimentin.	127
8. <b>Table 5.3:</b> Microarray analysis: Differential genes	130
9. <b>Table 5.3.2:</b> Mass spectrometry analysis	166

# ***Introduction***

# 1) Introduction:

---

Breast cancer is the most prevalent form of cancer in women worldwide accounting for 23% of the total cancer cases and ranks second overall (10.9% of all cancers). It is second most common cancer affecting women in India [1]. The two major epithelial cell types found in the breast tissue are basal and luminal epithelial cells [2]. The basal/myoepithelial cells line the basement membrane and the luminal cells are above the myoepithelial cells lining the duct. The basal and luminal cell types can be distinguished based on their cytokeratin profile.

Cytokeratins hereafter referred to as Keratins (K) according to the new nomenclature is the largest family of intermediate filament proteins are epithelia predominant in their expression [3,4]. The filaments are formed by non-covalent coiled coil interaction between one type I acidic (K9-K28) and one type II basic (K1-K8 and K71-K74) keratins which are obligatory heteropolymers [5]. They form cytoplasmic scaffold that emanates from the plasma membrane and spreads throughout the cytoplasm to provide shape and rigidity to the cells [6]. Keratins are tethered to the cell membrane by interacting with desmoplakin at the desmosomal junction [7]. At hemi-desmosome the keratins interact with  $\beta$ -4 integrin via BPAG-1 or plectin [8]. Apart from their structural role, they also provide a platform for various signalling events and form a complex with multiple proteins involved in signalling networks that regulate functions like cell cycle progression, apoptosis, the cellular response to stress, cell size, protein synthesis and membrane trafficking [9-12].

An important feature of keratins is that their expression is regulated by tissue type and also during differentiation [9,13-16]. The basal cells of the stratified epithelia express the keratin pair of K5 and K14. As the basal cells differentiate they express K4/13 in the

internal epithelium and K1/10 in the cornified epithelium [3,17-19]. In breast epithelium the basal/myoepithelial cells (proliferation compartment) express K5 and K14, while the luminal cells (differentiation compartment) express K7, K8, K18 and K19 [3,20]. The strictly regulated tissue and differentiation specific pattern of expression is suggestive of the fact that the keratins may have tissue specific functions.

The keratin pair of K8 and K18 is the first pair to be expressed in embryogenesis, and expression of this pair is restricted later to simple (e.g. liver, pancreas, kidney etc.) [3,12] and mixed (e.g. breast, lungs etc.) epithelia [17,21]. This pair is known to execute various regulatory functions, which include modulation of protein localization, protein targeting/trafficking and apoptosis [11]. Changes in keratin expression are seen during or after malignant transformation and hence these changes can be used for prognostication of different malignancies. Over expression of K8/18 is observed in adenocarcinomas [3,22]. Aberrant expression of this pair is found in squamous cell carcinomas (SCC) irrespective of their site of origin [23-28]. Recent studies from our laboratory have shown that K8/18 mediate neoplastic progression via  $\alpha 6\beta 4$  integrin mediated signalling in oral cancer derived cell line [29] and that K8 is required for the transformation induced by loss of plakophilin 3 in simple epithelia [30].

Keratin expression is used in breast cancer to differentiate between cancer subtypes. The basal type of cancer with poor prognosis expresses keratins K5/14 while luminal subtypes generally express K8/18. There are differing reports about the role of K8/18 pair in breast cancer progression. K8/18 when expressed along with vimentin have been associated with drug resistance, invasion and metastasis in breast cell carcinomas and melanomas [31-34]. Other reports have suggested that the elevation of K18 expression in breast cancer patients correlates with favourable prognosis [35-37] and that the loss of K8 in conjunction with aberrant expression of vimentin correlates with early metastasis



and poor prognosis [38]. Over-expression of K18 in MDA MB 231 breast carcinoma cells, which are invasive and highly metastatic, produced differentiated phenotype [20]. Thus, the role of K8/18 in breast cancer progression is not yet clear.

Along with K8/18 alteration, changes in expression of cell adhesion molecules were seen during breast cancer progression. Alteration in other molecules involved in cell-cell adhesion like E-cadherin is reported in a large number of cancers. E-cadherin along with its interacting proteins is known to be involved in signalling processes and plays a major role in EMT [39]. Change in expression or localization of this protein has been shown to have clinical implications in various cancers like colon, breast etc. and correlated with the clinical outcome of the patient [40].

To understand the role of K8/18 in transformation/ progression of breast epithelial cells three cell lines: non-transformed MCF10A, the transformed and less invasive MDA MB 468 and the highly transformed and invasive MDA MB 435 were used. The levels of K8/18 varied amongst the three cell lines. They were highest in MCF10A but least or undetectable in the MDA MB 435 cells. In MDA MB 468 the levels were lesser than MCF10A and more than MDA MB 435 cells. The levels of K8/18 reflected degree of transformation and invasion in these cells, the non-transformed cell line showing the highest and the invasive cell line showing the least expression. Based on these observations and literature the key questions raised were:

### **KEY QUESTIONS:**

- 1) What is the role of keratins 8 and 18 in transformation/differentiation of mixed epithelia like breast?
- 2) What is the mechanism by which these keratins regulate cell transformation / differentiation?

To answer these key questions the following objectives were undertaken-

## 2) AIMS & OBJECTIVES:

---

1. To transfect K8 gene in MDA MB 435 cells to check if it results in more differentiated phenotype.
2. To knockdown K8 gene in MCF10A and MDA MB 468 cells to understand the role of K8 gene in transformation of these cells.
3. To study molecular changes as a result of either knockdown or introduction of K8 gene using microarray analysis.

# *Review of Literature*

### 3) Review of Literature:

---

#### **3.1. Breast cancer:**

Breast cancer is one of the most common types of cancer seen world-wide. It has highest incidence accounting for 23% of the total cancer cases and stands second overall (10.9% of all cancers) [1]. According to the Globocan 2008 statistics, it ranks second in women in India. Breast cancer is a complex disease which cannot be defined merely by clinical parameters like lymph node involvement and histological grade, or by routinely used biomarkers like estrogen receptor (ER), progesterone receptor (PGR) and epidermal growth factor receptor 2 (HER2) in diagnosis and prognosis [41]. Breast cancer when detected in early stages is not fatal. The major cause of high mortality associated with breast cancer patients is metastasis. Due to high mortality rate there is a need to improve our ability to identify breast cancers that are more likely to recur and molecules that might contribute or prevent recurrence.

Breast cancer arises from the epithelial cells of breast tissue. There are two types of epithelial cells in breast: myoepithelial/basal cells and luminal cells. Myoepithelial cells also called as basal cells lie above the basal layer, constitute the proliferation compartment, while the luminal cells which line the duct constitute the differentiation compartment. These cells can also be classified depending on their keratin expression [42]. Keratins (K) are the intermediate filament of the epithelial cells. The expression of keratins is known to change during or after malignant transformation. The discovery of role of keratins in modulating cancer and their role in tumour metastasis has opened up an important area of research. Understanding the role of these intermediate filament proteins in breast cancer can improve our ability to identify their potential in prognostication and as therapeutic targets.

## **3.2. Intermediate filaments:**

A metazoan cell constitutes of three major fibrillar structures that forms the cytoskeleton. They are microfilaments (MF), micro tubules (MT) and Intermediate filaments (IF). Amongst these, Intermediate filaments acquire their name from the fact that they are intermediate in size about 10nm as compared to micro filaments about 6 nm and microtubules about 25nm as discovered by electron microscopy in skeletal muscle cells cultured from chick embryos [43]. IFs consist of multigene protein family that comprises of 73 unique gene products, thus placing them amongst 100 major gene families seen in humans [44]. IFs can withstand shear stress without breaking due to the lateral alpha helical segments, unlike MT and MFs which are made up of building blocks of globular proteins. Two striking features of IFs are their insolubility to buffers of broad range of ionic strength and that they can spontaneously assemble in physiological buffers without need of any cofactors or tri-nucleosides like ATPs or GTPs as required by MFs or MTs. IFs are completely resistant to extraction with buffers of high ionic strength and high concentrations of non-ionic detergents, such as 1.5 M sodium chloride and 1% Triton X-100. They require harsh conditions to solubilize them, for example, the addition of 8M urea or 3M Guanidinium hydrochloride into the extraction buffer [45].

**3.2.1. IF structure:** All IFs consist of common tripartite structure. The secondary structure is built from a highly conserved alpha helical central rod domain of ~ 310 amino acids with variable N- terminal (head) and C-terminal (tail) domain (Figure 3.1). The rod domain is formed by non-covalent interactions between parallel alpha helical coiled-coil dimers. These interactions occur through long-range heptad repeats of hydrophobic/ apolar residues at first and the fourth residue. This rod domain is subdivided into 1A, 1B, 2A and 2B subdomains, separated with non-helical linkers L1, L12

and L2. The rod domain is flanked by non-helical head and tail domains. The differences seen in the length and primary structure of these head and tail domains are responsible for the heterogeneity seen in all IF types. It is due to the variability of the end domains that IFs proteins exhibit different molecular sizes, charge and antigenicity. The non-helical end domains (head and tail domains) are also divided into subdomains based on homologous (H), variable (V) or end (E) sequences [46,47].

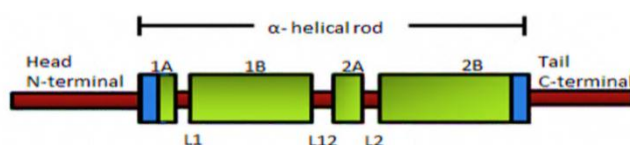


**Figure 3.1: Schematic representation of keratin structure:** Tripartite structure of Intermediate filament with alpha helical rod domain, amino terminal head domain and carboxyl tail domain. Adapted from [48].

**3.2.2. IF Filament assembly:** Filament assembly starts by parallel in-register alignment to form dimers. Dimers then associate in anti-parallel orientation in half staggered manner to form apolar tetramers or protofilaments. Tetramers aggregate into higher order oligomers to form unit length filaments (ULF) 60 nm long, which undergo reorganization and elongation by longitudinal annealing to form immature IF. Further compaction of the filaments results in the 16nm filament to form finally a 10-12 nm diameter filament [46,47].

**3.2.3. IF classification:** The IF proteins are classified into six types based on sequence homology, amino acid sequence identity, net acidic charge, secondary structure predictions etc. Type I-IV and VI are localized in the cell cytoplasm while the type V forms the cytoskeleton of the nucleus. In addition to unique and complex cell distribution of IFs, their importance is reflected in their involvement in several human diseases. The detailed classification of IFs and their association with diseases is described in (Table 3.1).

**Table 3.1** Classification of IF and their association with disease, adapted from [48]

IF name	Type	Size(kDa)	Cell and tissue distribution	Key feature and/or disease association
Cytoplasmic				
Keratins	I ( <i>n</i> = 28)	40–64	K9–K28 (epithelia); K31–K40 (hair/nail)	Types I and II keratins form obligate 1:1 heteropolymers. There are 54 functional keratin genes in the human genome. Mutated in >20 diseases.
	II( <i>n</i> = 26)	52–68	K1–K8, K71–K74 (epithelia); K81–K86 (hair)	
Vimentin	III	55	Mesenchymal	Widely expressed in embryos
Desmin		53	Muscle	Mutated in Cardiomyopathies
GFAP		52	Astrocytes/glia	Mutated in Alexander disease
Peripherin		54	Peripheral neurons	Induced after neuronal injury
Neurofilaments (L,M,H chains)	IV	61-110	CNS neurons	NF-L, M, and H form obligatorily heteropolymers with $\alpha$ -internexin.
$\alpha$ -Internexin		66		Neuronal IFs are key effectors of axonal radial growth
Nestin		177	Neuroepithelial	Markers of “early” progenitor (stem) cells in several tissues.
Syncoilin		54	Muscle	Interacts with $\alpha$ -dystrobrevin.
Synemin		182		$\alpha$ and $\beta$ isoforms; $\beta$ form is also known as desmuslin; binds actin-associated proteins
Nuclear				
Lamins B1, B2 Lamins A/C	V	66–68	Nuclear lamina	Enriched in progenitor cells.
		62–78		Subject to differential splicing; enriched in differentiated cells. Mutated in a progeria condition, muscular dystrophy, and others.
Orphan				
Phakinin (CP49)	undefined	47	Lens	CP49 and filensin form beaded filaments in lens epithelial cells. CP49 mutations cause cataracts.
Filensin		83		

### **3.3. Keratins:**

Keratins is the largest sub-group of IF proteins and constitutes approximately 75% of the total IF proteins. These are epithelia predominant IFs. Genome analysis demonstrated the presence of 54 functional keratin genes which is 28 type I and 26 type II genes in two clusters 17q21.1 and 12q13.13 respectively (27 genes on each cluster). K18 is the only type I keratin gene located in type II keratin gene domain that is chromosome 12q13.13 [5,49]. Keratin polymers are built from heterodimers of obligate pairing between a type I and type II keratin. The type I keratins are acidic low molecular weight (K9-28) and type II keratins are neutral-basic high molecular weight (K1-8 and K71-K80). Like any other IFs, keratins show tissue specific expression and are developmentally regulated. Keratins form the scaffold in an epithelial cell and form an elaborate network in the cytoplasm of most cells, extending from a ring surrounding the nucleus to the plasma membrane to provide shape and rigidity to the cells. Apart from this mechanical function of keratins, they also exhibit several non-mechanical functions [9-11].

**3.3.1. Keratins Classification:** Keratins share the similar tripartite structures seen in all IFs. It has central alpha helical rod domain of about 310 amino acids flanked by amino terminal head domain and carboxyl terminal tail domain. The non-helical head and tail domains consist of subdomains V1, and H1 and H2 and V2 respectively. This epithelial subgroup of IF was classified earlier based on two dimensional gel electrophoresis and SDS-PAGE by Moll and his colleagues in 1982 [3]. They profiled keratins of normal human epithelial tissues, cell cultures and tumors. The first comprehensive classification by them, classified keratins into 19 members: type I acidic (K9-19) and type II neutral to basic (K1-8). Subsequently a large number of hair follicle specific keratins were identified [50,51]. Keratins have been recently classified by Schweizer *et. al.* [5]. This classification included hard keratins- alpha keratins of hair



and nails. The new consensus nomenclature now includes: 28 type I keratins (20 epithelial keratins K9–28 and 11 hair keratins K31–40) and 26 type II keratins (20 epithelial keratins K1–8 and K71–80; and six hair keratins K81–86). The details of Keratin classification are given in table 3.2.

**Table 3.2:** The new human keratin nomenclature [5]

Keratin types	Type I Low molecular weight Acidic	Type II High molecular weight Basic-neutral
Epithelial keratins	K9-K10	K1-K5
	K12-K20	K6a-K6c
	K23-K24	K7-K8
		K76-K80
Hair follicle specific epithelial keratins (root sheath)	K25-K28	K71-K75
Hair keratins	K31-K32	K81-K86
	K33a-K33b	
	K34-K40	

### 3.3.2. Distribution of Keratins:

Keratins are expressed in all types of epithelial cells -simple, stratified (keratinized and non-keratinized), mixed and transitional epithelia [3,52].

**3.3.2.1. Simple Epithelial keratins:** Keratin pair of K8/18 is the first pair seen during embryogenesis [53,54]. They constitute the primary keratin pair in simple epithelial cells, like hepatocytes, pancreatic acinar and islet cells, and kidney cells. K7 and K19 are expressed in some of the simple epithelial cells like lining of ducts, intestine, mesothelium and in luminal (breast) cells, although their expression is variable and low [4].

**3.3.2.1.1. Keratin pair of 8/18:** It is a unique and the most studied pair. Several characteristics of K8 and K18 distinguish them from other members of type I and II keratins. Firstly, they are first IF to be expressed in embryogenesis during mammalian development being associated with the differentiation to the trophoctodermal layer of the blastocyst. K18 gene is the only type I gene present on the type II gene locus i.e. chromosome number 12. Rest of the type I keratins are found on chromosome 17. In addition to this unique feature, K8 and K18 show large number of processed pseudogenes (35 and 62 pseudogenes respectively) [12,59]. This pair is known to execute various regulatory functions, which include modulation of protein localization, protein targeting/trafficking and apoptosis as described previously, cell stress, osmolarity, transformation etc. [12].

**3.3.2.2. Transitional epithelia:** Transitional epithelium (also known as urothelium) is a type of tissue consisting of multiple layers of epithelial cells which can contract and expand. These epithelia exhibit a unique, complex keratin pattern of expression. K8, K18, K19, and K7 are expressed in all cell layers. K5 and K17 are restricted to the basal cell layer. Keratin 13 is expressed in the basal and intermediate cell layers and K20 is specific for the superficial (umbrella) cell layer [55].

**3.3.2.3. Mixed epithelia:** Mixed epithelia of breast and lungs are divided into two cell types: luminal and myoepithelial. In myoepithelial compartment of the breast K5 and K14 and sometimes K17 are expressed, while in the luminal compartment they express K8/18 pair. K7 and K19 expression is also seen in these cells which is low and variable [4].

**3.3.2.4. Stratified epithelial keratins:** Within stratified epithelia, the keratin pair K5/K14 is expressed in the basal proliferative layer. Keratin 19 also is expressed

in basal cells of non-keratinizing epithelia [3,19]. Differentiating suprabasal cells in the post-mitotic layers express a different keratin pair depending on the body site: the epidermal and gingival tissue, examples of keratinized (cornified) epithelia, express keratin pair of K1/10, while non-keratinized epithelia such as buccal mucosa, esophagus, etc. express keratin pair of K4/K13. Suprabasal epithelial cells of the hard palate and gingiva also express K2 [14,56,57].

Keratin pair of K6/16 is not normally expressed in epidermis but are induced during hyperproliferation of keratinocytes e.g. during wound healing [58].

### **3.3.4. Post translational modifications:**

Keratins undergo complex regulation involving post-translational modifications and interactions with self and with various classes of associated proteins. Keratins harbour sites for post translational modifications preferentially within the ‘head’ or ‘tail’ domains. Listed below are important post translational modifications:

**3.3.4.1. Glycosylation:** K8/18 glycosylation occurs as addition of single O-linked  $\beta$ -N-acetylglucosamine (O-GlcNAc) sugar moiety. Keratin glycosylation via O-GlcNAc is a dynamic modification that has been identified in K13, K8 and K18. Three serine glycosylation sites have been identified in the head domain of K18 and it is possible that all keratins are glycosylated [59]. Glycosylation of K8 and K18 regulates its solubility, stability and filament organization [60]. The role of K18 glycosylation was also seen in protecting the pancreatic cells and hepatocytes from epithelial injury as K18–Gly<sup>−</sup> mice are more susceptible to liver and pancreatic injury and apoptosis induced by streptozotocin or to liver injury by combined N-acetyl-D-glucosaminidase inhibition and Fas administration. K18 glycosylation protects the

cells from epithelial injury by promoting the phosphorylation and activation of cell-survival kinases [61].

**3.3.4.2. Phosphorylation:** Phosphorylation and de-phosphorylation are essential for the regulation of IF dynamics by modulating the intrinsic properties of IFs: solubility, conformation, filament organization, the regulation of other post-translational modifications of IF etc. Most of the phosphorylation sites identified so far involve distinct serine (Ser) residues in the head and tail domains of keratins. These Ser phosphorylation sites exhibit various motifs, implying that they constitute targets for several protein kinases, including members of the MAP kinases, p38, ERK, PKC, cAMP and JNK [59]. Several serine phosphorylation sites and some of the relevant kinases have been characterized in K6, K8, and K18. Serine/threonine sites have been identified in K1. Keratin solubility (at least for K8/18) appears to be regulated by 14-3-3 proteins via K18 Ser33 phosphorylation. Phosphorylation of keratins is also closely linked to keratin cytoprotective function during liver injury [62]. Other functions associated with keratin phosphorylation include protection against cell stress, cell signalling, apoptosis, and cell compartment-specific roles.

**3.3.4.3. Keratin transglutamination:** Transglutamination occurs in epidermal and simple epithelial keratins under physiological and pathological conditions. Under physiological condition, this modification provides a compact protective structure, while in the pathologic context of liver disease the role remains ambiguous [59].

**3.3.4.4. Sumoylation in keratins:** Sumoylation is a novel modification reported recently in keratins. This reversible process of addition and removal of Small Ubiquitin-like Modifier (SUMO) polypeptides (SUMO-1, 2 or 3) targets protein lysine residues and affects protein localization, interactions with

binding partners and degradation. During conformational changes induced by keratin natural mutations and extensive tissue injury, hypersumoylation of K8/K18/K19 is observed, which retains keratins in an insoluble compartment, thereby limiting their cytoprotective function [63].

**3.3.4.5. Proteolysis:** Keratins harbour caspase sites which are responsible for proteolysis. Proteolysis of K18 and K19 by caspases occurs during apoptosis, and generates stable keratin fragments that are highly enriched within the cytoskeletal compartment. This apoptosis-associated degradation involves all type I keratins [59]. Keratin fragments are also noted in sera of patients in association with a variety of epithelial tumors and are used as diagnostic markers [64] .

**3.3.4.6. Acetylation:** In a very recent report, Snider *et. al.* have shown role of acetylation in regulating K8 filament organization and solubility. K8 was found to be acetylated at a highly conserved residue- Lys-207. The regulation of K8 acetylation has been shown to be governed by NAD-dependent deacetylase sirtuin 2 (SIRT2) by modulating keratin phosphorylation [65].

**3.3.4.7. Other modifications:** Keratins undergo several other posttranslational modifications including disulfide bond formation (not found in K8/18 due to lack of cysteines) and acetylation of their N-terminal serines [59].

### **3.3.5. Keratins Functions:**

The primary function of keratins is to protect the cell from the mechanical and non-mechanical forces that might result in cell death. Apart from the mechanical functions these static structures are now known to be involved in several non-mechanical functions like cell signalling, regulation of cell cycle, apoptosis, protein synthesis and

protein targeting etc. [66]. They also perform and contribute to cell type specific functions like adhesion, migration etc.

**3.3.5.1. Mechanical functions:** Keratins act as scaffold and play an important role in protecting the epithelial cells from both mechanical and non-mechanical stresses [9]. This is well proven by the fact that point mutations in the keratin genes result in appearance of keratinopathies e.g. Epidermolysis Bullosa simplex and epidermolytic hyperkeratosis have been shown to be a result of single point mutation in K5/14 and K1/10 respectively [67]. Single point mutations in K8 or K18 genes also predispose the liver to chronic and acute degenerative disorders like liver cirrhosis [68-70]. Mutations in cornea specific K3 or K12 result in fragility of the anterior corneal epithelium and intraepithelial microcyst formation (Meesmann's corneal dystrophy) [71]. Further evidence for the mechanical functions of keratins was obtained from murine knockout experiments. K5 null mice survived only for few hours after birth and exhibited extensive skin blistering [72] whereas K14 null mice showed a similar less severe phenotype due to probable compensation with K15. Patients lacking K14 showed similar less severe phenotypes while those lacking K5 is not reported probably due to related lethality. K12 Knockout (KO) mice show corneal erosions [73]. K8 deficiency results in liver haemorrhage and embryonic lethality in C57BL/6 mice [74] along with mechanical fragility and susceptibility to hepatocyte injury during liver perfusion [75]. Keratin 8 knock-out mice demonstrated colorectal hyperplasia, inflammation, rectal prolapse and mild liver injury in FVB strain [74] while in the K18 null mice, clinical phenotypes were less pronounced. The K18 KO mice exhibited late-onset, subclinical liver pathology [76]. Additionally results from transgenic mouse models have underscored the importance of keratins in maintaining the epithelial health preservation. Mice over-expressing human K18 bearing Arg 89 to Cys mutation show liver and pancreatic keratin filament

disruption, hepatocyte fragility, chronic hepatitis [77] and increased susceptibility to stresses like hepatotoxic drug, partial hepatectomy and Fas mediated apoptosis [78-80]. Another mutation K8 Gly-61- to -Cys, (associated with human liver disease) results in stress induced liver injury and apoptosis and similar phenotype is observed in transgenic mice showing over-expression of mutant K8 Ser73-to ala [62]. These observations clearly state the importance of keratins in maintaining the mechanical integrity of cell.

**3.3.5.2. Regulatory functions of Keratins:** In addition to their role in mechanical stability, keratins also impart regulatory functions to the cell. Various regulatory functions include cell size determination and regulation of cell proliferation, vesicle transport and protein targeting, apoptosis, osmolarity etc. Their role in cell signalling is summarised in table 3.3. Their role in cell differentiation, transformation /progression is still emerging.

**Table 3.3: Signalling pathways modulated by keratins, adapted from [81].**

Keratin	Pathway	Reference
K8/18	Fas signalling/apoptosis	Gilbert <i>et. al.</i> 2001
K8/18, K14, K17, K10	TNF $\alpha$ signalling/apoptosis	Caulin <i>et. al.</i> 2000, Inada <i>et. al.</i> 2001, Tong <i>et. al.</i> 2006, Chen <i>et. al.</i> 2006
K18	Cell cycle	Kuno <i>et. al.</i> 2002
K10	PI-3K, Akt pathway/cell proliferation	Paramio <i>et. al.</i> 2001
K17	mTOR pathway/ protein synthesis	Kim <i>et. al.</i> 2006
K10	Notch signalling pathway/ differentiation	Santos <i>et. al.</i> 2005
K6/16	Cell proliferation	Paladini <i>et. al.</i> 1998

**3.3.5.2.1 Keratins in stress response:** Keratins are involved in site-specific phosphorylation and act as scaffolds for key proteins (kinases); and hence also known to act as phosphate “sink” or “sponge”, thereby reducing their adverse effects and hence protect the cells from injury. The most predominant form of keratin mutation which is linked with stress condition of cirrhosis and fibrosis progression is K8 gly -61-Cys [61,79]. The transgenic mice showing this mutant are susceptible to stress induced liver injury and apoptosis. Similar susceptibility to stress was observed in S73A mutation where the phosphorylation site is destroyed. K18 is also involved in protecting the cells from stress by its interaction with Raf-1 [82]. In a lung injury model keratin cytoskeleton disassembled partially in the presence of shear stress coincident with PKC $\delta$  mediated phosphorylation of K8 at K8 S73. Similar role of keratin filaments was also seen in hepatocytes isolated from mice carrying mutated phosphorylation sites including K8 S73 and K18 S33/52 [83]. In mice carrying dominant negative mutation of K18 gene i.e. K18 R89C, resulted in embryonic lethality which was fully rescued by one K18 or K19 allele. In colon carcinoma HT29 and Caco cells alterations in phosphorylation of K8, K18, K19 and K20 were observed under osmotic stress [84].

**3.3.5.2.2. Keratins in organelle transport:** Mutations in K5 or K14 can also result in Dowling-Degos disease. This disease is not related to skin blistering but the patients carrying the mutation exhibit patchy pigmentation due to hypo and hyper pigmentation. It is known that melanosomes (pigment containing granules) produced by melanocytes are transferred to the basal cells, where they are arranged in the distal cap over the nucleus. A defect in the transfer of this melanosomes or their arrangement in keratinocytes leads to changes in skin pigmentation, hence the patchy appearance. The mechanism by which this alteration is brought about is still not



understood. It may involve the interaction of K5 with HSC70 which is a chaperone involved in vesicle uncoating [85]. These observations indicate the role of keratins in organelle transport.

**3.3.5.2.3. Keratins in osmolarity:** Studies conducted to understand the multiple functions of keratins have indicated that keratins modulate processes such as osmolarity. Mice null for K8 show development of colitis, hyperplasia, diarrhoea, and mistargeted jejunal apical markers. Diarrhoea and protein mistargeting were observed 1–2 days after birth while hyperproliferation/inflammation occurred later. Defects in ion transport seen in these mice thus underscore the importance of keratins in maintaining the osmolarity [86].

**3.3.5.2.4. Keratins in apoptosis:** Keratins protect epithelial cells from other cellular stresses that can lead to cell death such as death receptor activation and treatment with chemotherapeutic drugs. E.g. Mice null for K8 lacking complete IF network in hepatocytes were more sensitive to Fas mediated apoptosis. In these mice there was increase in surface Fas receptor while the total Fas receptor remained constant as compared to wild type hepatocytes. Increased Fas receptor on the cell surface of K8 null hepatocytes may predispose them to apoptosis, because over expression of death receptors can trigger the apoptotic cascade even in the absence of ligand [87]. Thus K8/K18 may be involved in the trafficking of Fas receptor from the Golgi to the apical surface of polarized epithelia. Similarly K18 mutation Arg-89-Cys disrupts the keratin filament network and predisposes hepatocytes to Fas mediated apoptosis. This increased sensitivity was associated with a higher and more rapid activation of caspase-3, suggesting that K8/K18 act in events upstream of the

caspase 3 activation [88,89]. These data clearly indicate the role of K8 and K18 in imparting resistance to Fas mediated apoptosis in liver.

Keratins 8 and 18 are capable of binding the cytoplasmic domain of TNFR2 and moderate TNF-mediated NFkB and JNK activation [90]. Type I keratins K18/14/16 and 17 bind to TRADD an adaptor protein and compete with TNFR1 for its binding [91]. Thus cells lacking K8 and K18 were more sensitive to TNF mediated apoptosis.

**3.3.5.2.5. Keratins in epithelial cell growth:** Role of keratins has been shown in protein synthesis and cell growth. There is rapid decrease in K1/10 and up regulation of K6, K16 and K17 during tissue injury. In mice lacking K17 the cultured cells were smaller in size and displayed reduction in total protein synthesis by 20%, accompanied by reduced phosphorylation of kinases. Akt/mTOR signalling pathway and its regulation by 14-3-3  $\sigma$  plays a major role in control of cell size and protein synthesis. The lack of K17 prevented the re-localization of 14-3-3 and further stimulation of Akt/mTOR signalling pathway [92]. Further evidence that keratins may function upstream of mTOR is provided by studies in mice with ablation of all keratin genes. These mice exhibited embryonic lethality which was caused by severe growth retardation and aberrant localization of the glucose transporters and suppression of mTORC1 [93]. Similar role has been shown for K10 and K18 in cell growth in association with 14-3-3 proteins [94,95].

**3.3.5.2.6. Keratins in immune response:** In the simple epithelial lining of the mouse gut, the loss of K8 causes hyperplasia and colitis with increased T-cell recruitment to the colon and upregulation of T-helper (Th) 2 cytokines [96]. Further role of K1 in K1 null mice has been shown by Roth *et. al.*. They have shown the role of K1 in regulation of epidermal immunity and skin barrier function. The serum

levels of the IL-1 superfamily proinflammatory cytokine IL-18 were found to be significantly up-regulated in K1-null mice, suggesting a role for K1 in regulating both local and systemic inflammation [97]. Also previously, K17 have shown to promote keratinocyte growth and proliferation by polarizing the inflammatory response towards Th1 and/or Th17 [98]. Thus it is evident that keratins play role in immune regulation.

**3.3.5.2.7. Keratins in malignant transformation and progression:** The aberrant expression of keratins, their post translational modifications and association with other cellular proteins vis a vis normal and diseased condition is acquiring immense importance in recent years. It is apparent that they are key players in the transformation process and necessary for refinements in cancer management [99]. Previously they were used in the differential diagnosis of carcinomas. For example, to differentiate between an adenocarcinoma and squamous cell carcinoma and also to find the primary site of a metastatic cancer wherever primary was unknown [17,21]. Later studies revealed that keratin expression may change after malignant transformation and the changes are consistent enough to be used as prognostic markers. Based on transgenic mice studies and overexpression in cultured cells, K10 was expected to block cell cycle progression in a retinoblastoma protein dependent manner through sequestration of Akt and PKC $\alpha$ . These K10 null mice showed an increased turnover of skin cells in situ and showed decrease in papillomas formation [100]. Compared to wild type, K10 knockout experiments resulted in induction of 14-3-3 $\sigma$  and K17 in post-mitotic cells [98]. Chimeric experiments by Chen and co-workers demonstrated that K14 rod domain was flanked with K10 head and tail domains showed accelerated papilloma formation on induction of chemical skin carcinogenesis [101]. Study by De Pianto *et. al.* established that tumor associated

keratin K17 promoted cell proliferation and tumor growth by polarizing immune response in skin and established an immune-modulatory role for K17 in Hedgehog (Hh) signaling driven basaloid skin tumors [98]. Role of K8/18 pair is widely reported in various cancers.

**3.3.5.3. Keratins 8/18 in malignant transformation:** Keratin 8/18 pair utilizes similar transcription factors like AP1 and ETS family of transcription factors, which are also utilized by oncogenes of the ras oncogenic pathway [22]. Over expression of keratin 8/18 has been shown in adenocarcinomas. Aberrant expression of these keratins is found in squamous cell carcinomas (SCC) irrespective of their site of origin [23-26,28,102]. When expressed along with vimentin it is known to impart invasive, metastatic and drug resistant properties to the cells [32,33]. The mouse fibroblasts expressing complete K8/18 filaments also have a higher migratory and invasive ability [103]. Previous studies in our laboratory have shown aberrant expression of keratins 8/18 in precancerous lesions and squamous cell carcinomas of oral mucosa [23,25,26,28]. Our laboratory has also shown that aberrant expression of K8/18 contributes to malignant transformation of stratified epithelial cells [104]. Another study has shown similar effects as a result of keratin 8 transgenic expression in the epidermis of mice. In this study K 8 expression in the epidermal cells resulted in hyper-proliferation of these cells and the conversion rate of papillomas to carcinomas on treatment with chemical carcinogen was much higher in these animals [105]. Results from mouse lung epithelial cells (LEC), resistant to chronic exposure to cadmium showed over-expression of K8 and K14 [106]. This resistance was achieved probably by adaptive survival mechanism by attenuating apoptotic response. These observations are suggestive of a role of K8 in tumor progression. Recent studies from our laboratory have demonstrated that K8/18 pair mediates

neoplastic progression via  $\alpha 6 \beta 4$  integrin mediated signalling in oral cancer derived cell line [29] and that K8 is required for the transformation induced by loss of plakophilin3 (PKP3) in simple epithelia. PRL-3 (phosphatase of regenerating liver-3) was found to be up-regulated in metastatic tumors of colorectal cancer [107] and was correlated with decreased phosphorylation of K8 at residue Ser73 and Ser431. In this study authors have concluded that, PRL-3 may play an important role to promote cell migration and metastatic potential of CRC through K8 dephosphorylation [30]. Our laboratory has further shown that loss of keratin 8 phosphorylation leads to increased tumor progression and correlates with clinico-pathological parameters of OSCC patients [108].

### **3.3.6. Keratins in Breast cancer:**

There are two types of epithelial cells in breast: myoepithelial/basal cells and luminal cells. Myoepithelial cells express keratin pair of K5 and K14 and sometimes K17. The luminal cells express primarily keratin pair of K8/ K18 while K7 and K9 are present in less and variable amounts [42].

**3.3.6.1. Keratin 5/14 in breast cancer:** Previous studies have suggested that breast cancer in basal layers is characterized by an expression signature similar to that of the basal/myoepithelial cells and express keratins K5/14 and sometimes K17. They typically do not express estrogen, progesterone or HER-2 receptors (“triple-negative” phenotype). The tumors of this class are often seen in association with a type III intermediate filament protein, vimentin. This group of breast cancer is considered as most aggressive cancer with poorest prognosis [109-111].

**3.3.6.2. Keratins 8/18 in breast cancer:** There are conflicting reports available about the role of keratin 8/18 in tumors derived from mixed epithelial like

breast. Some of the reports support the association of K8/18 in breast cancer with increased transformation and invasive potential and with poor outcome. E.g. Taylor *et. al* showed that the invasive cells from the primary carcinoma of breast exhibited keratin profile of K7,8,18 and 19 [2]. While Thomas *et. al.* showed that the tumors (54 archival postmenopausal tumors) expressing approximately equal amount of keratin 8/18 and vimentin were of poorest prognosis [34]. They also showed in an *in-vitro* experiment that over-expression of vimentin in MCF-7 cell line which expresses high levels of K8/18 resulted in highly motile and invasive phenotype. Reports available from other laboratories revealed opposite role of K8/18 in breast cancer, wherein, K8/18 expression was associated with favourable prognosis. Schaller *et. al.*, in an eight year follow-up study showed that the breast cancer patient showing the elevation of K18 expression irrespective of their stage correlated with favourable prognosis [35,36]. Fuchs *et. al.* further demonstrated that the loss of K8 in conjunction with aberrant expression of vimentin correlated with early metastasis and poor prognosis [38]. Woelfle *et. al.*, using high density micro array studied around 1400 breast tumors. They showed association of down-regulated K18 expression with progression of breast cancer [37]. Other reports also demonstrated high K18 expression in weakly metastatic breast cancer cell lines and low K18 expression in highly metastatic cell lines, suggesting that it may function as a prognostic indicator of breast cancer. Another in-vitro study by Buhler *et. al.* where K18 was over-expressed in MDA MB 231 breast carcinoma cells, produced differentiated phenotype [20]. Gene expression profiling has indicated in metastatic breast cancer, there is frequent down-regulation of K18 [112,113] and this was associated with advanced tumor stage/ grade, bone marrow micrometastasis, shorter

cancer specific survival and overall survival [114]. Thus, these reports indicate that the role of K8/18 in breast cancer is not conclusive.

### **3.3.7. Interactions of keratins with cytoskeletal and membrane proteins:**

Keratins are highly dynamic proteins and they are regulated largely by phosphorylation and de-phosphorylation events. These dynamic filamentous proteins also interact with other key cytoskeletal components i.e. micro tubules and microfilaments, and their many associated proteins via Intermediate Filament associated proteins (IFAPs) [115]. Members of this family have been described as structural linkers between IF and cell–cell or cell–substrate adhesions and as crosslinkers with other cytoskeletal elements. At the cell periphery the keratin filaments anchor into desmosomes which form the cell-cell junction [6,7].

Desmosomal proteins come from three major gene families: (A) Cadherins: Desmoglein (DSG) 1-4 and Desmocollin (DSC) 1-3. (B) Armadillo proteins: Plakophilin (PKP) 1-3 and plakoglobin (PG). (C) Plakins: Desmoplakin (Dp) I, II / Plectin, envoplakin and periplakin [116]. The keratin filaments are integrated into the desmosomal plaque by the plakin-family member desmoplakin [7]. The role of desmosomes in making stable cell-cell contacts is well known and a number of reports have shown their disorganization/perturbation in malignant tissues.

Keratins also interact with hemidesmosomal plaque which forms the junctional complex between cell-extracellular matrix. In hemidesmosomal plaque BPAG1e isoform is an important component which mediates cell adhesion to extracellular matrix in  $\alpha 6\beta 4$  integrin dependent manner. It plays a crucial role in anchoring keratin IFs to hemidesmosomal plaque [117].

**3.3.7.1. Integrins and keratins:** Integrins are the family of transmembrane proteins that mediate adhesion of the cell to the extracellular matrix (ECM). The interaction of integrins with extracellular matrix ligands also results in the generation of intracellular signals and thus play role in fundamental cellular processes like cell growth, differentiation, and death. They are also known to regulate malignant cell growth, metastasis and cancer-induced angiogenesis [118]. Integrins participate in these cellular processes by providing a dynamic physical linkage between the ECM and the actin cytoskeleton. They also interact with keratins (basal keratins) via  $\alpha 6\beta 4$  integrins. The  $\alpha 6\beta 4$  integrin is expressed primarily in epithelial cells and in a few other cell types and is defined as an adhesion receptor for most of the known laminins. A major function of this integrin pair is to link  $\beta 4$  integrin to intermediate filaments in hemidesmosomes. The integrin pair  $\alpha 6\beta 4$  is known to change its expression or modulate signalling cues in various types of cancers. Several reports have indicated that over-expression of this pair is seen in SCC of lung, skin, oral cavity and cervix, while its expression is down-regulated in adenocarcinomas of breast and prostate [119]. Recent studies from our laboratory have shown that K8/18 pair mediates neoplastic progression via  $\alpha 6\beta 4$  integrin mediated signalling in oral cancer derived cell line [29]. K8/18 have been shown to mediate  $\beta 1$  integrin mediated cell adhesion in hepatomas [120]. Adherens junctions and focal adhesions are other types of junctional complexes. Focal adhesions are the sites where integrins interacts with ECM proteins. On the cytoplasmic site of focal adhesions, integrins together with other cytoskeletal proteins link to actin filaments. Recent reports indicate that the keratins are nucleated in the cell periphery at focal adhesions before elongation and integrate into a pre-existing peripheral network [121].



Adherens junctions are protein complexes that occur at cell–cell junctions in epithelial tissues. Adherens junctions serve as a bridge connecting the actin cytoskeleton of the adjacent cells through direct interaction. Adherens junction is composed of cadherins (homodimeric transmembrane proteins), p120,  $\beta$ -catenin or  $\gamma$ -catenin (plakoglobin) and  $\alpha$ -catenin. Alpha-catenin binds the cadherin indirectly via  $\beta$ -catenin or plakoglobin and links the actin cytoskeleton with cadherin [122].

**3.3.7.2. E-cadherin:** It is a well-studied member of the cadherin family and plays key role in epithelial cell–cell adhesion. The extracellular domain of E-cadherin mediates homophilic adhesion while the cytoplasmic domain interacts with the actin cytoskeleton through the  $\beta$ -catenin / plakoglobin– $\alpha$ -catenin complex [123]. E-cadherin mediates cell-cell adhesions, restricts cell motility and establishes apical-basal polarity. The loss of E-cadherin expression and disassembly of E-cadherin adhesion plaques on the cell surface enables tumor cells to dislodge from its primary site and disseminate. Strong evidence indicates that the loss of E-cadherin-mediated adhesion is required for malignant conversion [124] . Previous reports have shown that change in keratin expression was associated with change in E-cadherin, specifically during EMT where cells loose their epithelial marker and gain mesenchymal marker [39,125].

**Thus to summarize the literature provides enough instances that apart from their structural role keratins can be attributed with many other functional roles like their active involvement in cell signalling pathway and other cellular processes like differentiation, migration, and tumorigenicity. The impact of keratin expression in aspect of tumor biology is elusive and further diversification in its role is observed amongst different cell types, which warrants further investigation.**

# ***Materials & Methods***

## 4) Materials & Methods:

---

### 4.1. Routine maintenance of cell lines:

**Reagents:** Powdered medium was dissolved in 1 litre of Milli –Q water. Dulbecco's Modified Eagle's medium (DMEM, GIBCO) (3.7 gm of sodium bicarbonate per litre was added and the pH of medium was adjusted to 7.4), F12 (1.0725 g of sodium bicarbonate per litre was added). The medium was filtered using Millipore assembly – 0.45µM Membrane filter (Whatman). One ml of the filtered medium was added to the sterility test medium and kept at room temperature for 6 days under observation to ensure sterility.

Sterility test medium (14.9 g of Fluid-Thioglycolate was dissolved in approximately 250 ml of water. The volume was made up to 500 ml in measuring flask and boiled. After aliquoting 6 ml of the medium in glass tubes a pinch of calcium carbonate was added to each tube and autoclaved).

### Other reagents:

- a) Phosphate Buffered Saline (PBS): (150mM NaCl, 2mM KCl, 8 mM Na<sub>2</sub>HPO<sub>4</sub>, 1mM KH<sub>2</sub>PO<sub>4</sub>.) The buffer is autoclaved and used.
- b) Trypsin-EDTA: (0.025% Trypsin, 0.2mM EDTA, 5mM D-glucose, 5mM KCL, 0.1M NaCl and 6mM NaHCO<sub>3</sub>) The medium was filtered using Millipore assembly – 0.45µM Membrane filter (Whatman). One ml of the filtered trypsin was added to the sterility test medium and kept at room temperature for 6 days under observation to ensure sterility.
- c) Erythrocin B staining solution: 0.4% Erythrocin B in 1XPBS.
- d) Freezing medium: 90% Fetal Bovine Serum, 10% DMSO.

- e) Complete medium (DMEM or DMEM: F12 with 10% FBS and 1% antibiotic solution (Amphotericin B 20 µg/ml, Penicillin 2500 Units/ml, Streptomycin 800 µg/ml in PBS).

#### **4.1.1. Cell culture:**

The MDA MB 435 breast cancer cell line, derived from the pleural effusion of a 31 year old woman with breast carcinoma [126] was procured from Dr. Lalitha Samant from South Alabama University, USA. The cells were cultured in Dulbecco's Modified Eagle's Medium (DMEM; Gibco, Invitrogen, Carlsbad, CA): Ham's F12 Gibco (1:1), and 10% Fetal Bovine Serum (FBS; Hyclone Thermo Scientific, Lafayette, CO) and standard antibiotic mixture containing penicillin, streptomycin and amphotericin B. The MDA MB 468 breast cancer cell line, isolated from pleural effusion of a 51- year old female with metastatic adenocarcinoma of the breast [126] was procured from Dr. Sushant Kacchyap from John Hopkins University, USA. The cells were cultured in DMEM, supplemented with 10% FBS and standard antibiotic mixture containing penicillin, streptomycin and amphotericin B. MCF10A cell line, derived from fibrocystic non-transformed, immortalized breast epithelial cells [127] was procured from Dr. Kalpana Joshi from Nicholas Piramal, Mumbai, India. The cells were cultured in DMEM: Ham's F12 (1:1) Gibco, 10% FBS, Supplement cocktail (10 µg/ml Insulin, 0.5 µg/ml Hydrocortisone, 20ng/ml EGF all from Sigma-Aldrich, USA) from Sigma-Aldrich, USA) and standard antibiotic mixture containing penicillin, streptomycin and amphotericin B. All cell lines were cultured at 37°C and 5% CO<sub>2</sub> atmosphere.

#### **Protocols:**

**a) Revival of cells:** A frozen vial from liquid nitrogen cylinder was removed and placed into a 37-40°C water bath for thawing. The thawed cell suspension was mixed

gently and transferred into a sterile test tube. 5 ml of complete medium was added drop wise with intermittent shaking every 30 seconds. The cell suspension obtained was centrifuged for 10' at 1500 rpm at RT. The supernatant was discarded and the pellet was dislodged by finger tapping. Three ml of complete medium was then added drop wise to the test tube with continuous shaking followed by centrifugation at 1500 rpm for 10' at RT. The supernatant was discarded and the pellet was dislodged by tapping and re-suspended in 1ml of complete medium. Total cell count and the percent viability were calculated by dye exclusion method using Erythrocin B dye on a haemocytometer in an inverted microscope. The medium was mixed by pipetting and the 100mm petri plates were seeded with  $1 \times 10^6$  cells. The cells were incubated in a humidified CO<sub>2</sub> (5%) incubator at 37°C and their growth was observed each day under inverted microscope.

**b) Subculture/Trypsinization and transfer of cells:** The cells were washed with PBS twice and trypsin-EDTA was added to the culture plate. Excess trypsin-EDTA was discarded and the plate was incubated till the cells were partially detached. Complete medium was added to inhibit the trypsin activity and the resulting cell suspension was mixed by pipette to make a single cell suspension. Total cell count was taken and appropriate amount of cells depending upon cell type were seeded in culture plates. The plates were incubated in humidified CO<sub>2</sub> incubator at 37°C.

**C) Freezing and cryopreservation of cells:** Log phase cells were trypsinised and single cell suspension was obtained. After determining the total cell count, the cell suspension was spun at 1500 rpm for 10' at RT. The supernatant was discarded and the pellet was dislodged by tapping. One ml of freezing medium was added into the tube drop wise and mixed gently by pipette. The cells suspension was then transferred to freezing vials. The freezing vials were then placed in bio-freezer with 3 rings. First ring

was removed after 90', the second ring was removed after 120' and third ring was removed after 150'. The vials were then kept in liquid nitrogen freeze boxes at -196°C for long term storage.

#### **4.2. Stable Transfections:**

Reagents: DNA plasmids, Lipofectamine Plus (Invitrogen), Icafectin 441 (Eurogenetic), Superfect (Qiagen) transfection reagent, puromycin, G418 sulphate.

Protocol: To determine the effect of K8 over-expression, K8- expression vector, K8 – pCND A3 or its empty vector pCND A3, were transfected in MDA MB 435 cells (P-54). The stable clones were selected in 1200 µg/ml G418 sulphate containing medium. To determine effect of inhibition of K8 expression on cells transformation potential, the shRNA construct of K8 K8shRNA 8.2 (previously designed and validated, sequence given in table 4.2) or its empty vector pTU6-puro were transfected in MCF10A (P-9) and MDA MB 468 (P-15) cells using Icafectin 441 and Superfect respectively according to manufacturer's protocol. The stable clones of MCF10A or MDA MB 468 clones were selected in puromycin (0.5µg/ml) containing medium. Single cell clones were isolated, expanded and screened for the inhibition or overexpression of K8 gene levels by Laser Confocal microscopy, Real time-PCR and Western blot analysis.

#### **4.3. Preparation of whole cell lysates:**

Reagents: SDS lysis buffer (5mM EGTA, 5mM EDTA, 0.4% SDS and protease inhibitor cocktail (Calbiochem, 1X solution contains 500µM AEBSF, 500µM EDTA, 1µM E-64, 1 µM Leupeptin and 1 µg/ml Aprotinin, Cat no. 539131) in 25mM TrisHCl pH 7.2. SDS lysis buffer without protease inhibitor cocktail was stored at 4°C. 1X Sample Buffer (1M Tris pH 6.8 50mM, Glycerol (SD fine) 10%, 10% SDS 2%, Bromophenol blue (Sigma) 0.1% and before use, to 950µl of 1X buffer add 50µl of β-mercaptoethanol).

Protocol: The cells were grown upto 80-90% confluency in tissue culture dish. The cells were suspended in SDS lysis buffer for 40 min. The cell suspension was then sonicated followed by centrifugation at 13,000 rpm for 15' to remove cell debris. The supernatant was then aliquoted and stored at -80°C for further use.

#### **4.4. High salt extraction:**

Reagents: 10mM Tris pH 7.6, 140mM NaCl, 5mM EDTA, Tritox-100, Protease inhibitor

Protocol: The high salt extraction for keratins was performed as previously described [128]. Briefly, MDA MB 468 cells were trypsinised and lysed in detergent buffer (10 mM Tris pH 7.6, 140 mM NaCl, 5 mM EDTA, 1% Triton X-100) with protease inhibitors and incubated for 30' on ice. The lysates were centrifuged and supernatant was suspended in high salt buffer (10 mM Tris pH 7.6, 140 mM NaCl, 1.5 M KCl 0.5% TritonX-100) with protease inhibitors and stirred for 1–3 hours at 4°C. The insoluble material was washed thrice in 10 mM Tris pH 7.6, the pellet suspended in 2% SDS and 50 mg of protein loaded on SDS-PAGE gels followed by staining with Coomassie brilliant blue.

#### **4.5. Protein estimation by modified Lowry's method [129]:**

**Reagents:** 1mg/ml BSA, Copper Tartarate Carbonate (CTC) solution: 0.1 % copper sulphate(w/v), 0.2 % potassium tartarate (w/v), 10 % Sodium carbonate (w/v); Solution A: Equal volumes of CTC solution, 10 % SDS (w/v), 0.8 N NaOH (w/v) and distilled water (1: 1: 1: 1 proportion); Solution B (2N Folin and Ciocalteau's Phenol Reagent (FC reagent) diluted 1:5 (v/v) with distilled water (1 part of FC reagent and 5 parts of distilled water).

Protocol: One ml of 5 µg/ml to 25 µg/ml of BSA with Blank were taken in test tubes in duplicates as standard. Five µl of whole cell lysates were added in test tubes in duplicates and volume was made up to 1 ml by distilled water. 1 ml of solution A was added to each test tube and the tubes were vortexed followed by incubation at RT for 10'. 500µl Solution

B was added to each tube. The tubes were vortexed and incubated at RT for 30' in dark and optical density was read at 750 nm using a spectrophotometer. The readings obtained with BSA standards were used to plot the standard curve. The protein concentration of the sample was determined by using BSA standard curve.

#### **4.6. SDS PAGE:**

Reagents: 30% Acrylamide (29.2 Acrylamide and 0.8 Bis Acrylamide), 1.5M Tris (pH 8.8), 1 M Tris (pH 6.8), 10% SDS, 10% APS, TEMED and PAGE sample buffer (62.5mM Tris HCl pH 6.8, 25% Glycerol w/v, 2% SDS, 0.5% Bromophenol blue).

Protocol: The samples were dissolved in PAGE sample buffer and were run at constant volt and separated on 6-15% SDS PAGE depending on the molecular weight of the proteins being analyzed with 3.9% stacking gel. The composition of 10% resolving gel and 5% stacking gel is given in table 4.1.

**Table 4.1: SDS-PAGE composition**

Component	10% Resolving gel (5ml)	5% stacking gel (2 ml)
Mili Q	1.9	1.4
30% accrylamide	1.7	0.33
1.5 M Tris (pH 8.8)	1.3	-
1.0 M Tris (pH 6.8)	-	0.25
10% SDS	0.05	0.02
10% APS	0.05	0.02
TEMED	0.002	0.002
Total Volume	5ml	2ml



#### **4.7. Western blotting:**

Reagents: Transfer Buffer (190mM Glycine, 20% methanol, 0.05% SDS, 25mM Tris base), Tris-buffered saline (150mM NaCl, 10mM TrisHCl pH 8.0), Tris-buffered saline TWEEN 20 (TBST) (0.1% TWEEN 20 (v/v), 150mM NaCl, 10mM TrisHCl pH 8.0), Ponceau Staining solution (0.2% Ponceau stain in 5% acetic acid), Blocking buffer (3% BSA in TBS or 5% Milk powder in 1XTBS), Antibodies dilutions were made in 0.5% BSA in TBS, ECL+ Kit from ( RPN2132 GE Healthcare).

Protocol: After SDS-PAGE, the gel with resolved proteins and the activated PVDF membrane were placed in form of the sandwich and wet electro-blotting was carried out at 100V for 1 hour. Transfer of proteins was visualized using Ponceau-S staining for 2 min, and later rinsed with MilliQ water. Ponceau-S stain was completely removed by washing the blot with 1X TBST. The blot was incubated in blocking solution for 1 hour at RT on a rocker. After blocking the blot was incubated with diluted primary antibody for 1 hour at RT on the rocker. The blot was then washed four times with TBST followed by incubation with horseradish peroxidase (HRPO) conjugated secondary antibody for 1 hour at RT on the rocker. The secondary diluted antibody was removed and the blot was washed four times with TBST. Excess buffer was drained and chemiluminescence solution (ECL+) was added on the blot for 4 min. The ECL+ solution was prepared according to the manufacturer's protocol. The X-ray film (Carestream, Kodak) was exposed to the blot in the dark and incubated for various time intervals depending on the signal strength. The signal was visualized by developing the X-ray film in an automated developing machine Promax X-ray film processor. The list of antibodies is given in table 4.2.

**Table 4.2:** List of Antibodies used in the study

Antibody Dilution	Clone	Origin	Company	Catalogue No.
K14	1:100 (IF) clone LL002	mouse monoclonal	Serotec, UK	ab58744
K5	1:4000 (WB) clone XM26 1: 200 (IF)	mouse monoclonal	Novacastra, UK	NCL-CK5
K8	1:4000(WB) clone M20 1: 200 (IF)	mouse monoclonal	Sigma,USA	C5301
K18	1:4000(WB) clone CY- 90 1: 200 (IF)	mouse monoclonal	Sigma,USA	C 8541
$\beta$ Actin	1:8000 (WB) clone AC-74	mouse monoclonal	Sigma, USA	A 5316
$\beta$ 4 Integrin	1:1000 (WB)	Rabbit polyclonal	Santacruz, USA	sc9090
E-Cadherin	1:5000 (WB)	mouse monoclonal	BD Transduction Lab	H-101
K7	1:1000 (WB)	Mouse monoclonal	ThermoScientific Pierce UK	RCK105
CAPG	1:1000 B-9 (WB)	Mouse monoclonal	Santacruz Biotechnology	Sc-365473
HRPO	1:8000 (WB)	Whole ab (sheep) Antimouse	GE healthcare UK	NA931
Alexafluor 568	1:200 (IFM)	Whole ab (goat) Anti-mouse Anti- rabbit	Invitrogen, USA	A11001

#### **4.8. Coomassie staining:**

Reagents: Coomassie staining solution (0.25% coomassie brilliant blue R 250, 45% methanol and 10% acetic acid in distilled water), Destainer (45% methanol (v/v) and 10% acetic acid (v/v) in distilled water).

Protocol: For Coomassie blue staining, the gel was stained with coomassie staining solution by incubating it for 2 hours at RT. The gel was destained to remove the background staining using destainer and the gels were stored in distilled water.

#### **4.9. Mass spectrometry analysis:**

Reagents:  $\text{NH}_4\text{HCO}_3$ , Acetonitrile, Dithiotreitol, Iodoacetamide, TFA.

Protocol: Keratins extracted using high salt buffer were run on SDS-PAGE. The bands from Coomassie stained gels were excised for the mass spectrometry analysis. Briefly, for the analysis, the gel pieces were washed with water and after thoroughly rinsing, the gel pieces were gradually dehydrated using 50 mM  $\text{NH}_4\text{HCO}_3$ :Acetonitrile (1:1) for 15' and then with 100% Acetonitrile. The gel pieces were then vacuum dried and further incubated with 10mM Dithiotreitol at 56°C for reduction and with 55mM Iodoacetamide in dark at room temperature for alkylation. The gel pieces were then washed with 1:1 ratio of  $\text{NH}_4\text{HCO}_3$ : Acetonitrile. The final wash with 100% Acetonitrile was given to dehydrate the gel pieces were vacuum dried followed by an overnight digestion with 10ng/μl trypsin in 25mM  $\text{NH}_4\text{HCO}_3$ . After digestion, the peptides were extracted using 50% Acetonitrile and 5% TFA (Tri fluoro acetic acid) solution. The tryptic protein digests were reconstituted using 10% Acetonitrile and 0.1% TFA solvent before subjecting to mass spectrometry analysis. A reconstituted sample and Matrix  $\alpha$ -CyanoHydroxyCinnamic acid (CHCA) (1:1) were mixed properly and were loaded onto the ground steel MALDI plate and subjected to mass spectrometry (MS) analysis on Ultraflex-II MALDI TOF-TOF (Brucker Daltonics) machine.

#### **4.10. RNA extraction:**

Reagents: Tri reagent (sigma), Chloroform, Isopropanol, 70% ethanol in DEPC treated water and DEPC treated water.

Protocol: The RNA from cell lines was isolated by Tri reagent as per manufacturer's instructions. Briefly medium was removed and cells were lysed by adding 1 ml/100cm<sup>2</sup> plate of Tri reagent. The lysate was transferred into an eppendorf tube and 100 µl of chloroform was added and incubated for 2' at RT. The phase was separated by centrifugation at 12,000 rpm and supernatant was transferred to a new eppendorf tube. RNA was precipitated by adding isopropanol and spun at 12000rpm. The pellet was washed by 70% ethanol made in DEPC treated water; air dried and dissolved in 50 µl of DEPC treated water. RNA was estimated by measuring absorbance at 260 nm and 280 nm.

#### **4.11. Reverse transcriptase:**

Reagents: RT PCR kit (MBI fermantas), Taq 2X mix.

Protocol: cDNA synthesis was carried out as per the manufacturer's protocol (MBI fermantas). Briefly 1µg of total RNA and 0.2 µg (100 pmol of random hexamer in a volume of 12 µl were incubated at 70°C for 5' and chilled on ice and centrifuged. Reaction buffer, RiboLock™ RNase Inhibitor and dNTP Mix were added to final concentration of 1X, 1 unit/ µl and 1mM each respectively and incubated at 25°C for 5'. RevertAid™ H Minus M-MuLV Reverse Transcriptase (200 units) was added and the reaction mixture was incubated at 25°C for 10' followed by 42°C for 1 hr. The reaction was terminated by heating at 70°C for 10'.

#### **4.12. Microarray analysis:**

The K8 over-expressed and control vector transfected MDA MB 435 clones and K8 down-regulated and control vector transfected MDA MB 468 clones were assessed for changes in gene expression as result of K8 modulation by microarray analysis. The stably transfected clones were analysed by services offered by Genotypic (Bangalore) using Human whole genome 8 x 60 K format Agilent platform microarray by Cy3 labelled single colour hybridization. The data normalization and analysis was done using Gene spring 11.2 software. The differential expression of a select set of genes was validated by real time RT-PCR analysis.

#### **4.13. Real-Time Quantitative PCR:**

Reagents: SYBR green Master 2X mix (ABI), Primers (Table 4.3).

Protocol: A total of 2µg of RNA was reverse transcribed using pdN6 random primers as described previously. Real time PCR analysis was performed on 10ng of cDNA using gene specific primers and SYBR green based real-time quantitative PCR was performed on the ABI 7900HT Fast Real Time PCR System (Applied Biosystems, Foster, CA, USA). The relative gene expression was quantified by comparative Ct method using GAPDH as house keeping control.

Plasmid copy number of all the clones was determined by real time PCR analysis on the genomic DNA isolated from the clones and parental cells. To determine the plasmid copy number of K8 over-expressed clones, real time PCR was performed for neomycin resistant gene, and for K8 knockdown clones, real time PCR was performed for puromycin resistant gene. GAPDH primer recognizing genomic GAPDH gene was used as reference to determine the copy number.

**Table 4.3:** List of Primers and oligonucleotides

Sr. No.	Gene	Sequence
1.	K8	Forward primer-5' AGATGAACCGGAACATCAGC-3' Reverse primer- 5'TCCAGCAGCTTCCTGTAGGT-3'
2.	K18	Forward primer: 5'-TGAGACGTACAGTCCAGTCCTT-3' Reverse primer-5.' GCTCCATCTGTAGGGCGTAG-3'
3.	GAPDH	Forward primer -5'-TCAACGACCACTTTGTCAAGC-3' Reverse primer-5'-TACTTTATTGATGGTACATGACAAGG - 3'
4.	Neomycin	Forward primer: 5'-CGTTGGCTACCCGTGATATT-3' Reverse primer 5'-AAGAAGGCGATAGAAGGCGA-3'
5.	Puromycin	Forward-5' CGCAGCAACAGATGGAAGGC-3' Reverse primer: 5'-CCGCTCGTAGAAGGGGAGGT-3'
6.	GAPDH (genomic)	Forward primer: 5' AGGGTCTACATGGCAACTG-3' Reverse primer: 5'- CGACCACTTTGTCAAGCTCA-3'
7.	FGFRL1	Forward primer: 5'CCTGAGCGTCAACTACACCC-3' Reverse primer: 5'ATCTTGGAGGGCTGTGTGAA-3'
8.	TUBB6	Forward primer: 5' CGGCACCAAGTTTTGGGAAG-3' Reverse primer: 5'CTGGGCACATATTTCTGAGACG-3'
9.	MMP11	Forward primer: 5' GTGTAGACAGTCCCGTGCC-3' Reverse primer: 5' AAAGTTCCAGTAGAGGCGGC-3'
10.	CAPG	Forward primer: 5'CCAGGTGAAGGGGAAGAAGA-3' Reverse primer: 5'TGTTGCGTTCCAGGATGTTG-3'
11.	MGP	Forward primer: 5' TGGAGAGTGGCAGAAAGAAG-3' Reverse primer: 5'TGCTGAGGGGATATGAAGGT-3'
12.	THBS2	Forward primer: 5' AGAGTCACTTCAGGGGTTTGCT-3' Reverse primer: 5' TGTTCTCACTGATGGCGTTG- 3'

13.	shRNA 8.2	5'CCGGCATCACCGCAGTTACGGTCAAAGTTCTCTTGA CCGTAAGTGCAGGTGATGCCTTTTTTC 3' & 5'TCGAGAAAAAAGGCATCACCGCAGTTACGGTCAAG AGAACTTTGACCGTAACTGCGGTGATG 3'
-----	-----------	--

#### 4.14. Immunofluorescence:

Reagents: PBS, Chilled methanol or 4% paraformaldehyde in PBS, 0.3% Triton X 100 in PBS, antibodies.

Protocol: Cells were grown on glass cover slips for 48 hours till they reached a confluency of 60-70%. Adhered cells were washed twice with PBS for 10' each. The cells were fixed either with chilled 100% methanol in -20°C or 4% paraformaldehyde at RT for 10' and 15' respectively. After fixation, coverslips were washed thrice with 1X PBS for 10' each. The cells were then permeabilised using 0.3% Triton X-100 for 90 seconds in case of methanol fixation and 10' in 0.5% Triton X-100 when cells were fixed with paraformaldehyde. Coverslips were again washed thrice with PBS for 5' each. Coverslips were then placed in a small humidified chamber and 5% BSA was layered over the cells for blocking the non-specific sites and incubated for 1 hour. BSA was drained and the cells were layered with 50 µl of primary antibody diluted in PBS and incubated for 1 hour. The coverslips were washed thrice with 1XPBS for 10' each followed by incubation with 100 µl of anti-mouse (Alexa Fluor 488) or anti-rabbit (Alexa Fluor 568) conjugated secondary antibody for 1 hour and later washed with PBS thrice for 10' each. After washing the coverslips were stored in dark at 4°C overnight. The next day coverslips were washed twice and inverted. The coverslips were then mounted using anti-quenching agent and sealed with nail paint. Confocal images were obtained using a LSM 510 Meta Carl Zeiss Confocal system with an Argon 488 nm and Helium/Neon 543 nm lasers. All images were obtained using an Axio Observer Z.1

microscope numerical aperture (NA 1.4) at a magnification of 63X with 2X optical zoom. For measuring the intensity of the cells the 4% laser with emission filter band pass of 505-550 was used. All the scanning conditions of gain offset and laser percentage were kept same and applied for all images with secondary control as threshold.

#### **4.15. Phalloidin staining:**

Reagents: PBS, 4% paraformaldehyde, Phalloidin-FITC

Protocol: To analyze changes in actin filamentous organization, the 48 hours old grown culture cells on cover slip were fixed with 4% paraformaldehyde in PBS. The cells were incubated with FITC labeled Phalloidin (Sigma Aldrich, P5282) antibody for 30' in a humidified chamber. The cells were then washed with PBS thrice. Mounted using Vectasheild mounting medium and observed under LSM 510 Carl Zeiss Confocal system.

#### **4.16. Flow cytometry:**

The cells were grown for 48 hours and were harvested by trypsinization. For the assay,  $1 \times 10^6$  cells were fixed in 1% paraformaldehyde for 15 minutes at 4°C. The cells were then treated with FACS buffer (PBS with 1%FBS, 0.02% Sodium azide and 0.1% triton X-100) for 5'. The cells further were incubated with anti- K8 (M20 clone) monoclonal antibody for 45 minutes at 4°C. After incubation with primary antibody, cells were washed three times with FACS buffer. The cells were then incubated with Alexa-Fluor-488-conjugated anti-mouse-IgG secondary antibody (Molecular Probes) for 45' at 4°C. Cells were then analysed with FACS Calibur (Becton Dickinson, San Jose, CA) flow cytometer. The mean fluorescence intensity was measured in arbitrary units using Msiy Cell Quest software.



#### **4.17. Nile red staining:**

Reagents: PBS, Nile red dye

Protocol: Cells were stained with Nile red for lipid droplets (marker of cell differentiation). Briefly, the stock solution of Nile red 1mg/ml in acetone was diluted in PBS (1:1000). The fixed cells (4% paraformaldehyde) were incubated with diluted Nile red for 5' at room temperature, rinsed with PBS and observed for the presence of lipid droplets by confocal microscopy. All the scanning conditions of gain offset and laser percentage were kept same and applied for all images with secondary control as threshold.

#### **4.18. *In- vitro* wound healing assay for migration:**

Reagents: 1mg/ml Mitomycin C dissolved in PBS.

Protocol:  $1 \times 10^4$  cells were seeded in 35mm petriplates and grown to 95% confluency. Cells were replaced with fresh medium, containing 10  $\mu$ g/ml mitomycin-C for 3 hours. After incubation, medium was discarded and two parallel wounds were scratched with the help of sterile 2 $\mu$ l pipette tip. The cells were fed with fresh medium and observed under an Axiovert 200 M Inverted Carl Zeiss microscope fitted with a stage maintained at 37°C and 5% CO<sub>2</sub>. Cells were observed by time lapse microscopy, and images were taken every 10' for 20 hours using an AxioCamMRm camera with a 10X phase 1 objective. Migration was measured using Axiovision software version 4.5 (Zeiss).

#### **4.19. Transwell motility assay:**

Reagents: 8 $\mu$ m-pore-size polycarbonate membrane filters, hematoxilin (H), eosin (E) and 4% paraformaldehyde in PBS (pH- 7.0)

Protocol: For assessing motility by transwell assay  $2 \times 10^5$  cells were seeded into the top chamber with serum-free medium containing 0.1% BSA. Medium containing 10% serum

was added to the lower chamber of the Boyden chamber (polyvinyl pyrrolidone-free polycarbonate filter with 8- $\mu$ m pore size inserts, BD Pharmingen, San Diego, CA). The cells were incubated for 16 hours. Motility of cells to the underside of the membrane was detected by wiping the upper side with cotton swab and staining the underside cells with Mayer's Hematoxylin and Eosin (H&E) solution. The cells were counted under microscope in five random fields after staining. The assay was repeated thrice with 3 replicates each time.

#### **4.20. Boyden chamber cell invasion assay:**

Reagents: Matrigel (BD Biosciences), 8 $\mu$ m-pore-size polycarbonate membrane filters, hematoxilin (H), eosin (E) and 4% paraformaldehyde in PBS (pH- 7.0).

Protocol: The invasion potential of the cells was determined by Boyden chamber invasion assay. 40 $\mu$ l Matrigel (1mg/ml; BD Biosciences,) was applied to 8 $\mu$ m-pore-size polycarbonate membrane filters and the bottom chamber was filled with 0.6 ml of DMEM medium with 10% FBS.  $1 \times 10^5$  cells were seeded in the upper chamber in serum-free medium with 0.1% BSA, and then incubated for 16 hours at 37°C. The cells on the upper surface were carefully removed with a cotton swab. The membranes containing invaded cells were fixed with 4% paraformaldehyde prepared in PBS (pH 7.0) and stained with H&E. The invasion potential was quantified by counting 5 random fields under a light microscope. Data obtained from three separate experiments was shown as mean values.

#### **4.21. Cell proliferation/MTT (3-(4,5-Dimethylthiazol-2-yl)-2,5-Diphenyltetrazolium Bromide) viability assay [130]:**

Reagents: Acidified SDS (10% SDS in 0.01N HCl), MTT solution (5 mg/ml MTT in PBS).

Protocol: For the assay, 1500 cells were seeded per well, in triplicate in a 96-well microtitre plate in 100µl complete medium. Proliferation was studied every 24 hours up to a period of 5 days using MTT assay. At the desired time points, 100µl of the medium was discarded and 20µl MTT solution with 80 µl of medium was added to each well. Plate was incubated at 37°C in a CO<sub>2</sub> incubator for 4 hours, then 100µl of acidified SDS was added to each well and incubated overnight at 37°C. Next day, the optical density was measured on an ELISA plate reader at 540 nm against a reference wavelength of 690 nm. Growth curve was prepared from three independent experiments by plotting OD at 540 nm (on Y axis) against time (on X axis).

#### **4.22. Soft agar colony forming assay:**

Reagents: 2% Low melting agarose (Sigma)

Protocol: One milliliter of the basal layer of 1 % agar in complete medium (IMDM with 10% FCS and antibiotics) was prepared in 30 mm Petri plates, 1000 cells in complete medium containing 0.4% agar were seeded over the basal layer. Plates were fed with complete medium on alternate day and incubated at 37°C in a 5% CO<sub>2</sub> incubator for 15 days. Opaque and dense colonies were observed and counted microscopically on day 15. The assay was done in triplicates.

#### **4.23. Tumor formation in immune-compromised (nude/SCID) mice:**

Protocol: To test the tumorigenicity of the cells 6–8 weeks old NIH nude mice or NOD-SCID mice were used. Cells were injected in the mammary fat pad of SCID mice (6–8 weeks old). Five mice were injected for each clone and observed for tumor to reach 1-2cm. The ellipsoid volume formula  $\frac{1}{2} \times L \times W \times H$  was used to calculate the tumor volume [131]. After the tumor reached the volume of 1-2 cm, the tumor was surgically excised and the wound was stitched and the animals were observed for 4 weeks following

which animals were sacrificed and all the vital organs were collected. All protocols for animal studies were reviewed and approved by the Institutional Animal Ethics committee (IAEC) constituted under the guidelines of the CPCSEA, Government of India. Approval number - 09/2008.

#### **4.24. Histology and immunohistochemistry:**

Reagents: Buffered formalin (10 % formalin, 0.025 M sodium dihydrogen phosphate and 0.046 M disodium hydrogen phosphate in distilled water), Poly-L-Lysine (0.01% Poly-L-Lysine in Milli Q water), Xylene, Alcohol, Paraffin, Haematoxylin and Eosin stain, Methanol, TBS pH 7.2 (0.05M Tris, 0.8% NaCl), 0.1M Citrate buffer, 0.08% DAB with 3% H<sub>2</sub>O<sub>2</sub> in TBS.

Protocol: Formalin fixed paraffin embedded blocks of breast tumors were collected from department of pathology, Tata Memorial Hospital, Parel, Mumbai and ethical clearance was obtained from ACTREC/TMC-IRB (Intramural Review Board) DD/IRG-2010/11220/2010). For analysis of human breast tumors the levels of K8, K18 and vimentin were determined using semi quantitative IHC analysis. This study was a double blind study. Five micron thick sections of formalin fixed and paraffin embedded tissues were stained with Hematoxylin/eosin for histology. Immunohistochemical staining was performed according to previously described method [28]. The tissues were permeabilized for antigen retrieval by microwave treatment. The sections were then blocked with pre-immune horse serum for 30' at RT. Following this the sections were incubated overnight with respective primary antibodies and then incubated with secondary and tertiary antibody. Signals were detected by an avidin-biotin based immunoperoxidase technique (Elite ABC Kit; Vector laboratories; USA) using DAB as chromogen. The negative control was kept with tris-buffered saline instead of primary antibody, to determine any non-specific staining by the secondary antibody. Analysis was

done on the basis of signal intensity. The tumor samples were categorized based on percentage positive cells and staining intensity. Similar procedures were carried out for tumors obtained from animals injected with K8 modulated cells.

#### **4.25. Statistical analysis:**

Two groups of data were statistically analysed by student's t-test. A p value less than 0.05 was considered statistically significant.

# *Results*

## 5. RESULTS:

---

The role of Keratin 8/18 pair in breast cancer progression is not well understood and the available literature is inconsistent. To determine whether this Keratin pair plays a role in regulating tumor progression in breast tissue, three breast derived cell lines - MCF10A (immortalised but not transformed), MDA MB 468 (transformed but less invasive) and MDA MB 435 (transformed, highly invasive and metastatic) served as model systems in this study. K8 levels were modulated in the three cell lines to understand the role of K8/18 in transformation of these cells.

### **5.1. Characterization of the cell lines used for the study:**

#### **5.1.1. Expression of keratins in breast derived non-transformed**

**/transformed cell lines:** To determine if K8 and K18 levels in these cells correlate with the degree of transformation, the levels of K8/18 were determined in the three cell lines using Western blot and immunofluorescence analysis. K8 and K18 levels were found to decrease from MCF10A to MDA MB 435 cells. K8 and K18 levels were highest in MCF10A, lower in MDA MB 468 and less or undetectable in MDAMB 435 cells (Figure 5.1.1A). From the Western blot data, the fold change was calculated using Image J software. To determine the fold intensity, Intensity of the band was normalized using  $\beta$ -actin as internal control. Relative intensity was measured by considering band intensity of MCF10A for K8 and K18 as 1. MDAMB 468 showed 2 fold less K8 and K18 as compared to MCF10A cells while in MDA MB 435 K8 expression was negligible and K18 expression was 5 fold lesser than MCF10A (Figure 5.1.1B). Immunofluorescence analysis revealed that K8/18 filaments were abundant in MCF10A as compared to MDA MB 468 cells, while the highly invasive MDA

MB 435 cells showed no K8 filaments and very sparse K18 filaments (Figure 5.1.1C). These results suggested that the levels of K8 and K18 reflect the degree of transformation and invasion in these cells, with the non-transformed cell line showing the highest and the invasive cell line showing the lowest expression.

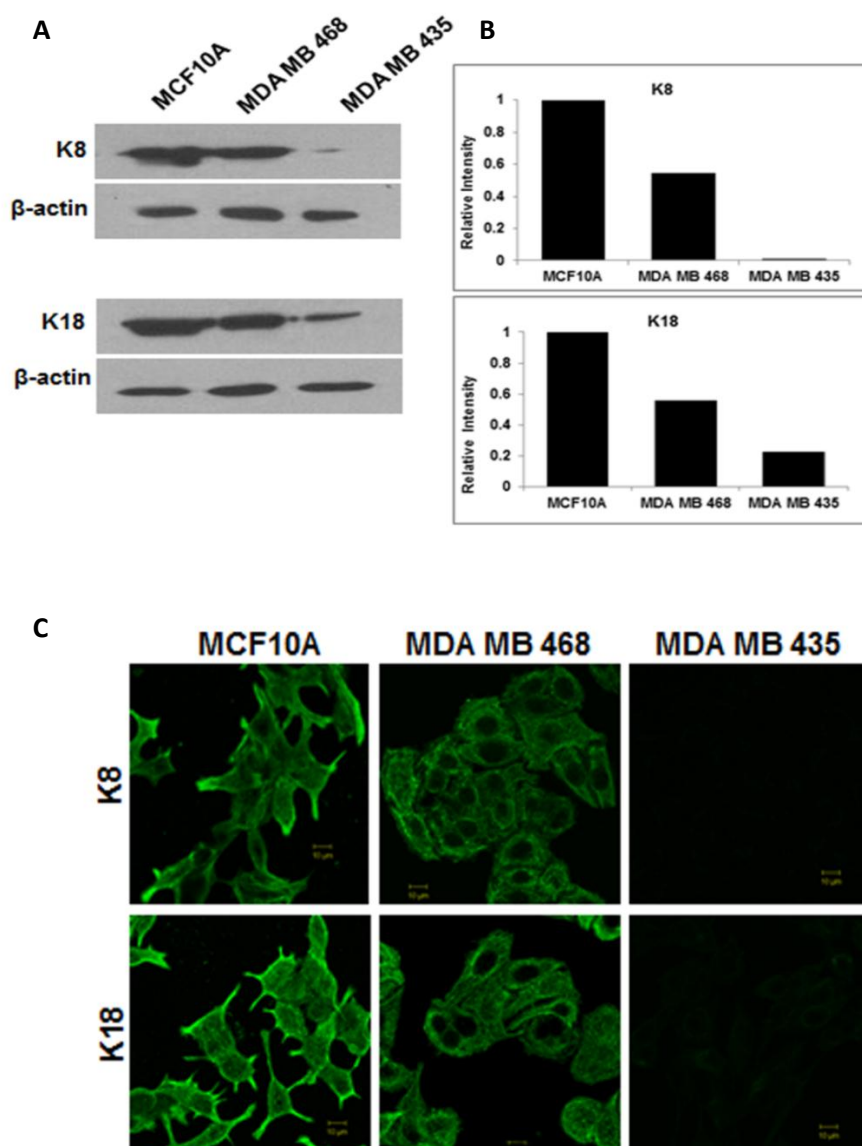


**Figure 5.1.1: Analysis of K8 and K18 in MCF10A, MDA MB 468 and MDA MB 435 cell lines:** (A) Western blot analysis of K8 and K18 using mAb to K8 and K18 respectively. β-actin was taken as loading control. (B) Histogram showing relative intensity of K8 and K18 in the cell lines. (C) Representative confocal images of K8 and K18 filaments using mAb to K8 and K18 respectively. **Scale bar:** 10μm. **Note:** Sequential decrease in K8, K18 expression from MCF10A to MDA MB 435 cells.



### 5.1.2. Expression of vimentin in breast derived non-transformed

**/transformed cell lines:** Vimentin, a mesenchymal marker is often co-expressed in various carcinomas along with keratins. Previous reports have also showed reciprocal expression between keratins and vimentin. Therefore vimentin levels were analysed in the cell lines used for the study. MDA MB 435 cells demonstrated high expression of vimentin, while it was weak or undetectable in MDA MB 468 and MCF10A cells (Figure 5.1.2 A& B).

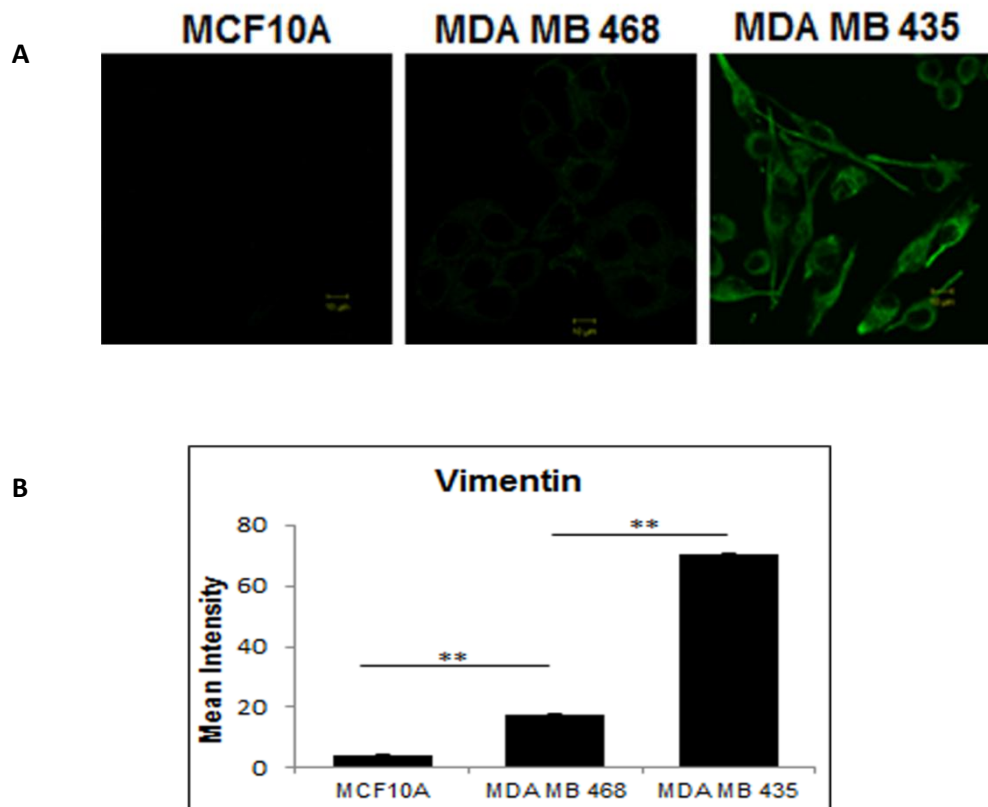


**Figure 5.1.2: Analysis of vimentin expression in MCF10A, MDA MB 468 and MDA MB 435 cell lines:** (A) Representative confocal images of vimentin. **Scale bar:** 10µm. (B) Histogram showing mean intensity of vimentin. The mean fluorescence intensity ( $\pm$  SE) of vimentin was calculated per cell by measuring fluorescence intensity of 20 cells of each experiment (using LSM10 software; Carl Zeiss MicroImaging GmbH, Jena, Germany). This was repeated thrice. Results are mean of  $\pm$  SE of three independent experiments performed. **Note:** Sequential increase in vimentin expression from MCF10A to MDA MB 435 cells.

**5. 1. 3. Determination of Lipid droplet levels, the differentiation marker of breast epithelial cells:** A differentiated mammary gland exhibits a specific secretory function of producing milk. Human milk is mainly constituted of fat globules containing triglycerides. Triglycerides are neutral lipids that can be stained by Nile red. To understand the correlation of K8/18 levels with the differentiation status of breast epithelial cells, the levels of lipid droplets were determined. The levels of lipid droplets were found to sequentially decrease from the non-transformed MCF10A to highly invasive MDA MB 435 cell lines (Figure 5.1.3 A and B).

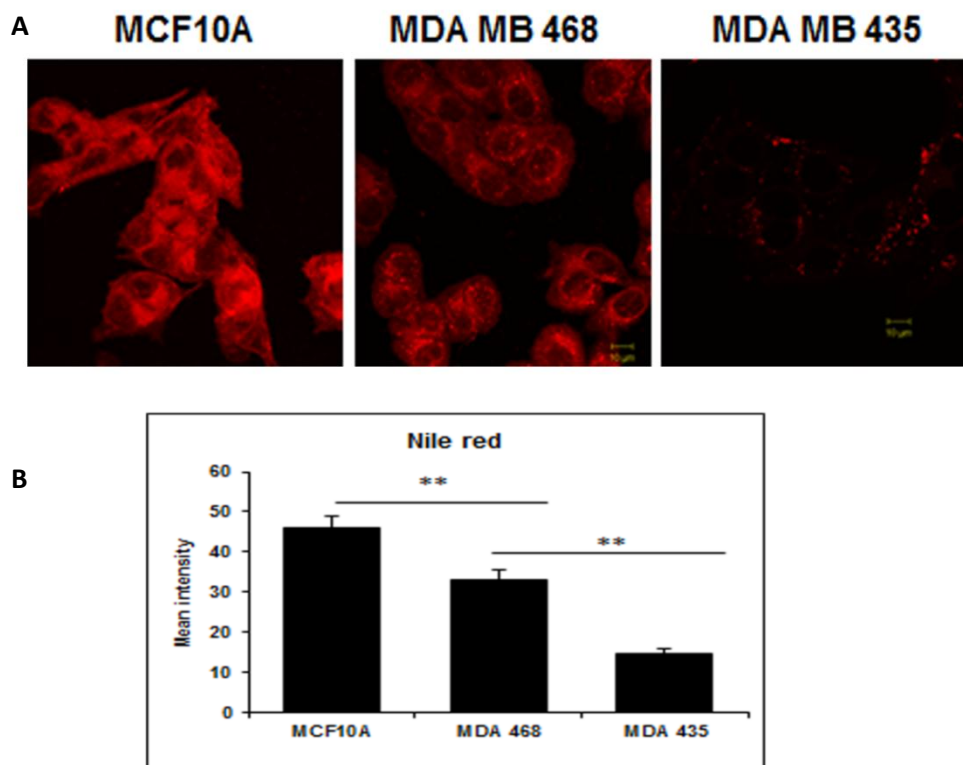


**Figure 5.1.3: Analysis of differentiation status of MCF10A, MDA MB 468 and MDAMB 435 cell lines by lipid droplets staining using Nile red:** (A) Representative confocal images of lipid droplets staining using Nile red. **Scale bar:**10µm. (B) Histogram showing the mean intensity. The mean fluorescence intensity ( $\pm$  SE) of lipid droplets was calculated per cell by measuring fluorescence intensity of 20 cells of each experiment (using LSM10 software; Carl Zeiss MicroImaging GmbH, Jena, Germany). This was repeated thrice. Results are mean of  $\pm$  SE of three independent experiments performed. **Note:** Sequential significant decrease in lipid droplet staining intensity from MCF10A to MDA MB 435 cells.

**5. 1. 4. Analysis of Soft agar colony forming potential:** Soft agar colony forming assay or determination of anchorage independence was performed to determine *in-vitro* tumorigenic potential of the cells. The number and size of the soft agar colonies was found to significantly increase from MCF10A to MDA MB 435 cell lines ( $p<0.05$ ) (Figure 5.1.4 A, B and C). It was maximum for MDA MB 435 cells, which showed significantly big an more number of colonies, while MDA MB 468 cells showed significantly smaller and lesser colonies than MDA MB 435 but greater than MCF10A cells. MCF10A the non-transformed cell line demonstrated significantly smaller and least number of colonies

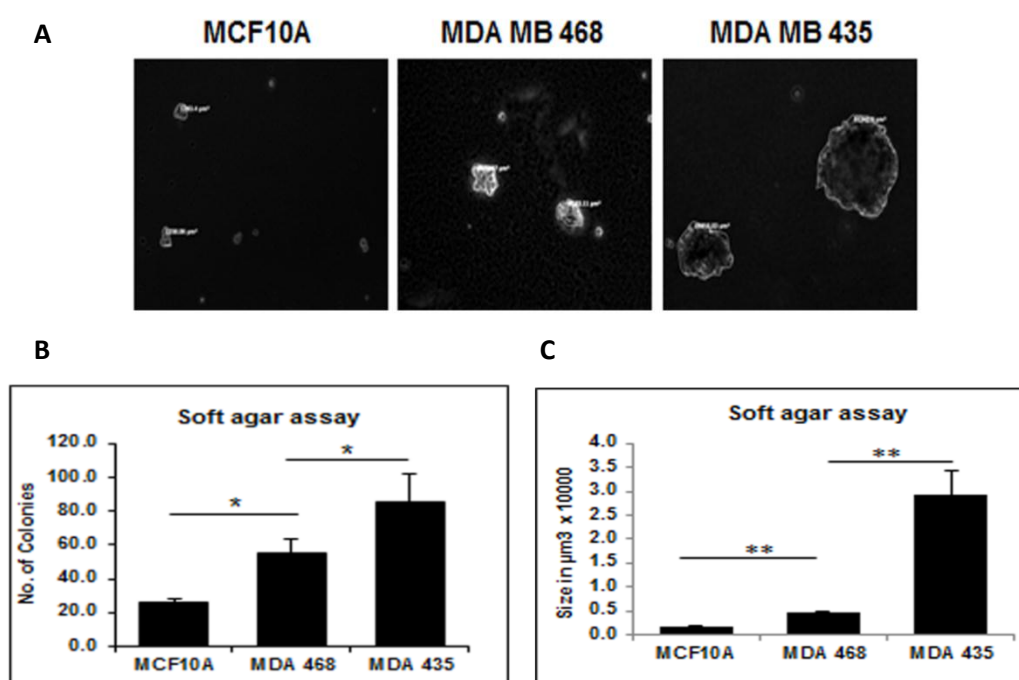


**Figure 5.1.4: Analysis of soft agar colony forming potential in MCF10A, MDAMB 468 and MDA MB 435 cell lines:** (A) Representative phase contrast images (10X) of colonies formed in soft agar per plate. (B) Histogram showing number of colonies formed in soft agar. (C) Histogram showing volume of colonies formed in soft agar. Size of the colonies was determined using Axiovision software (\* $p<0.05$  by student's t-test). Results are mean of  $\pm$  SE of three independent experiments performed. **Note:** Sequential increase in number

and volume of soft agar colonies formed from non-transformed MCF10A to invasive MDA MB 435 cell lines.

*In summary, K8/18 levels decreased with increasing transformation potential also reflecting the degree of the differentiation of the cells, while vimentin levels correlated with transformation potential.*

## **5.2.Generation of stable K8 over-expressing MDA MB 435 cells:**

To determine if expression of the K8/18 pair inhibits transformation in breast epithelia, MDA MB 435 cells were transfected with either vector alone (pCDNA3) or K8 expression construct (K8- pCDNA3).

### **5.2.1 Expression of K8/18 in K8 over-expressed clones:**

**5.2.1.1. Western blot and immunofluorescence analysis of K8 over-expressed clones:** Three stable clones expressing K8 (K8C1, C2 and C3) and empty vector transfected (K8Vc) clones of MDA MB 435 cells were obtained (Figure 5.2.1.1 A). The plasmid copy number was determined for the MDA MB 435 clone which was found close to 1. The K8 over-expressed clones showed up-regulation of its binding partner K18. The immunofluorescence analysis revealed K8/18 filaments in K8 over-expressed clones (Figure 5.2.1A and B). The clones K8C1 and C2 along with the vector control K8Vc were selected for further analysis.

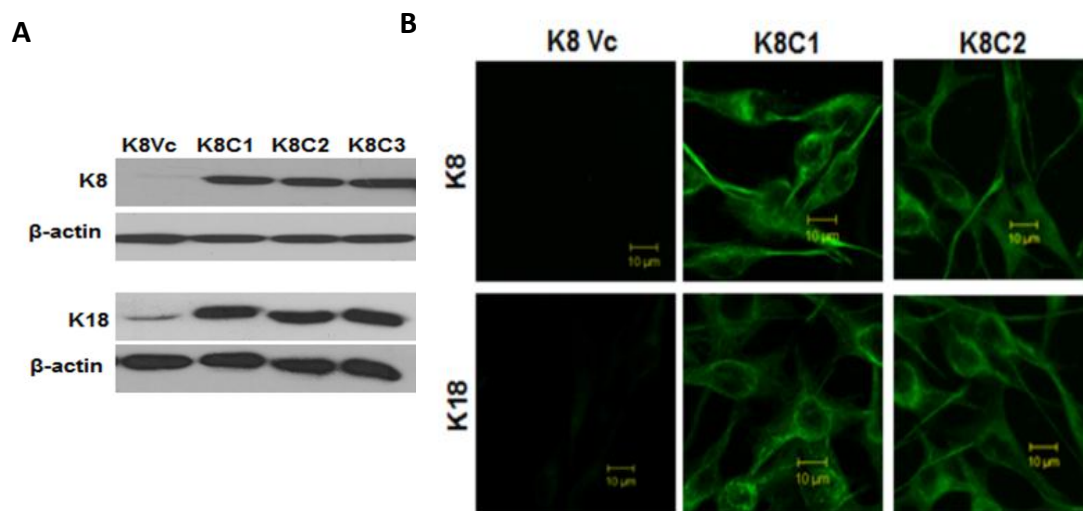


**Figure 5.2.1.1: Analysis of K8 and K18 expression in K8 over-expressed MDA MB 435 clones by western blot and Immunofluorescence:** (A) Western blot analysis of K8/18 using mAbs to K8 and K18 respectively in K8 over-expressed (K8C1, C2 and C3) and vector control (K8Vc) clones. (B) Representative confocal images of K8 and K18 filaments in K8 over-expressed (K8C1, C2) and vector control (K8Vc) clones. **Scale bar:** 10μm. **Note:** Formation of K18 filaments in K8 over-expressed MDAMB 435 clones.

### 5.2.1.2. Flow cytometric and real time PCR analysis of K8 over-expressed clones:

Over-expression of K8 in MDA MB 435 clones as compared to vector control clone and parental cells was also confirmed using flow cytometry analysis with antibody to K8 (M 20 clone, sigma). The K8 over-expressed clones showed up-regulation of its binding partner K18 without much change in their mRNA levels (Figure 5.2.1.2 A, B and C).

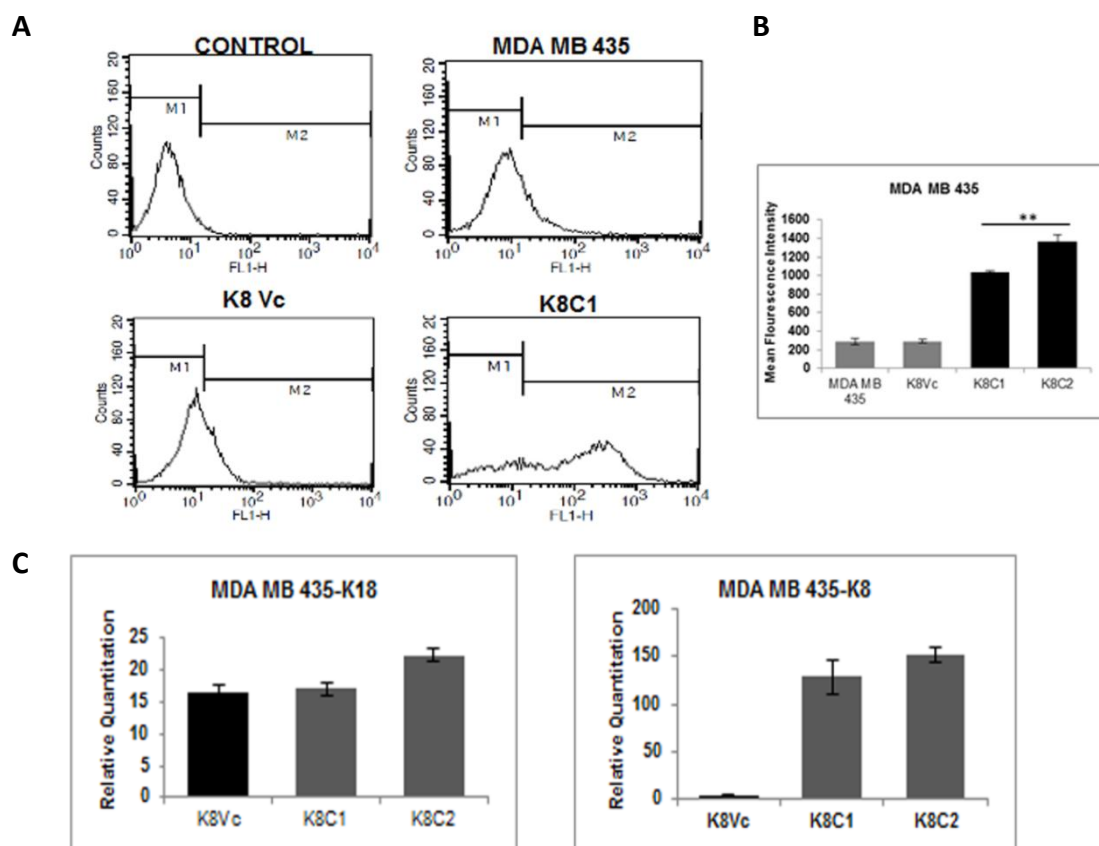


**Figure 5.2.1.2. Analysis of K8 expression by flow cytometry and K8/18 mRNA levels by real time PCR:** (A) Flow cytometric analysis of K8 expression in MDA MB 435 parental, vector control clone (K8Vc) and K8 over-expressed (K8C1) representative clone. (B) Histograms showing mean fluorescence intensity of K8 ( $\pm$  S.E.) for three independent experiments in K8 over-expressed clones (K8C1 and C2) as compared to parental MDA MB 435 and vector control clone (K8Vc) as analysed by flow cytometry. (C) Real time PCR analysis of K8 and K18 genes in K8 over-expressed (K8C1 and C2) and vector control (K8Vc) clones using *GAPDH* as internal control. Results are mean of  $\pm$  SE of three independent experiments performed. **Note:** No. significant difference in m-RNA levels of K18 on K8 over-expression as compared to vector control.

### 5.2.2. Keratin 18 over-expression in MDA MB 435 cells resulted

**in aggregate formation:** Previous studies have shown the importance of K8 and K18 filaments (1:1) ratio for proper filament formation. Transient over-expression of K18-YFP in MDA MB 435 cells did not result in up-regulation of its binding partner K8 but resulted in non-filamentous aggregates, unlike what was observed on K8 over-expression (Figure 5.2.2).

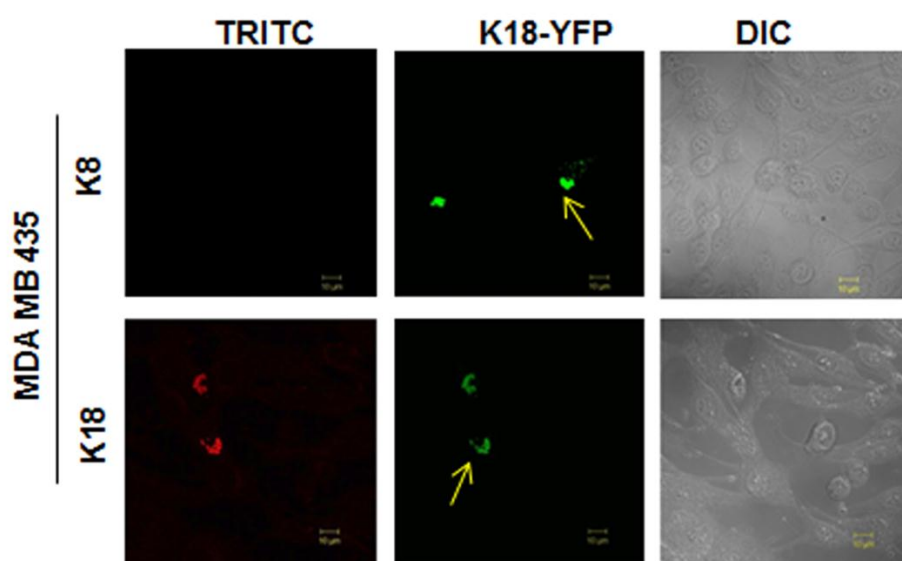


**Figure 5.2.2: Analysis of K8 and K18 expression in K18 (over-expressed) MDA MB 435 cells:** Representative confocal images of MDA MB 435 K18-YFP transiently transfected cells using mAb to K8 and K18 and anti-mouse TRITC secondary antibody. Fluorescence micrograph showing aggregates of K18 in MDA MB 435 K18-YFP transfected cells and DIC of the cells. **Scale bar:** 10 $\mu$ m. **Note:** K18 non-filamentous aggregates and no induction of K8 on K18-YFP over-expression.

### 5.2.3. Effect of K8 over-expression on the levels of other keratins and vimentin:

**5.2.3.1. Analysis of keratin 7 in K8 over-expressed clones:** A cell can exhibit various pairs of keratins, and breast epithelial cell is known to express K7 in variable amount. Also K7 is known to pair with K18 in absence of K8. Hence K7 expression was analyzed in the cells by western blot analysis, which

remained undetected in vector control transfected and K8 over-expressed MDA MB 435 (K8C1, C2) and vector control (Vc) clones (Figure 5.2.3.1).

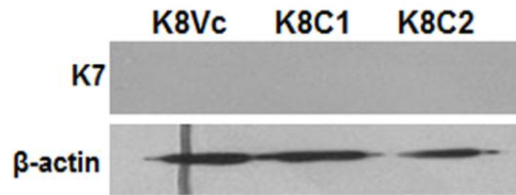


**Figure 5.2.3.1: Analysis of K7 expression in K8 over-expressed MDA-MB-435 clones:** Western blot analysis of K7 in K8 over-expressed (K8C1 and C2) and vector control (K8Vc) clones. **Note:** Absence of K7 in K8 over-expressed and vector control clones

#### 5.2.3.2. Analysis of vimentin expression in K8 over-expressed clones:

Previous reports have shown reciprocal expression between keratins and vimentin. Therefore vimentin levels were analysed in MDA MB 435 clones.

Vimentin levels remained unchanged in these cells (Figure 5.2.3.2).

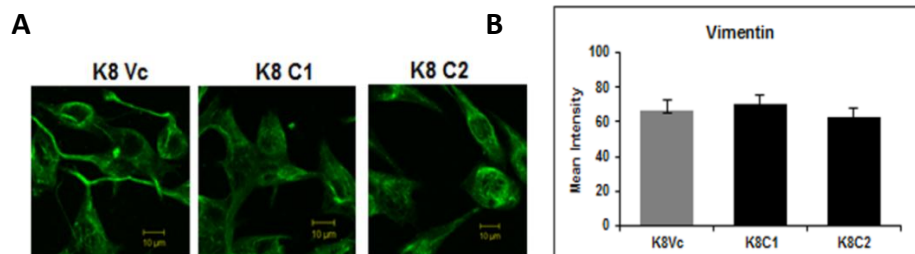


**Figure 5.2.3.2: Analysis of vimentin expression in K8 over-expressed MDA MB 435 clones:** (A) Representative confocal images of vimentin filaments K8 over-expressed (K8C1 and C2) and vector control (K8Vc) clones. **Scale bar:** 10μm. (B) Histograms showing mean fluorescence intensity of K8 (± S.E.) for three independent experiments. The mean fluorescence intensity of 20 cells of three independent experiments was calculated. Results are mean of ± SE of three independent experiments performed **Note:** No change in vimentin expression or filament formation on K8 over-expression.

#### 5.2.4 Effect of K8 over-expression in MDA MB 435 on

**differentiation status:** To determine if change in K8 levels affected

differentiation, the levels of lipid droplets were measured in the K8 over-



expressed clones. The K8 over-expressing MDA MB 435 clones (K8C1 and C2) did not show any significant change in lipid droplet levels as compared to the vector control clone (K8Vc) (Figure 5.2.4 A and B), indicating no change in the differentiation status of MDA MB 435 cells on K8 over-expression.

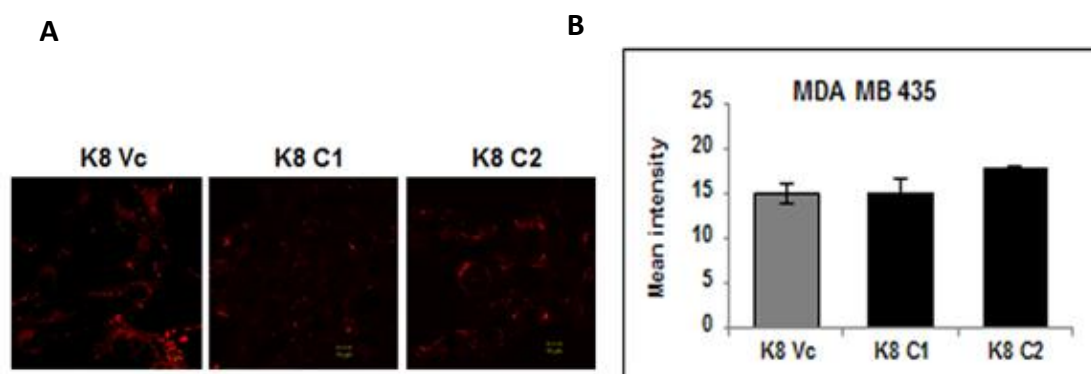


**Figure 5.2.4.1: Analysis of differentiation status of MDA MB 435 on K8 over-expression by lipid droplets staining using Nile red:** (A) Representative confocal images of lipid droplets staining K8 over-expressed (K8C1, C2) and vector control (K8Vc) clones. **Scale bar:** 10μm. (B) Histogram showing the mean intensity of K8 over-expressed (K8C1 and C2) and vector control (K8Vc) clones. The mean fluorescence intensity ( $\pm$  SE) of lipid droplets was calculated per cell by measuring fluorescence intensity of 20 cells of each experiment (using LSM10 software; Carl Zeiss MicroImaging GmbH, Jena, Germany). This was repeated thrice. Results are mean of  $\pm$  SE of three independent experiments performed. **Note:** No change in lipid droplet staining intensity in any of the clones on K8 over-expression.

### 5.2.5. Effect of K8 over-expression in MDA MB 435 on soft agar

**colony forming potential:** In order to assess the effects of K8 over expression on tumorigenic potential *in-vitro*, soft agar colony forming assays were performed. The MDA MB 435 K8 over-expressing clones (K8C1 and C2) did not show any significant change in the size and the number of colonies formed in the soft agar as compared to the vector transfected clone (K8Vc) (Figure 5.2.5A and B).

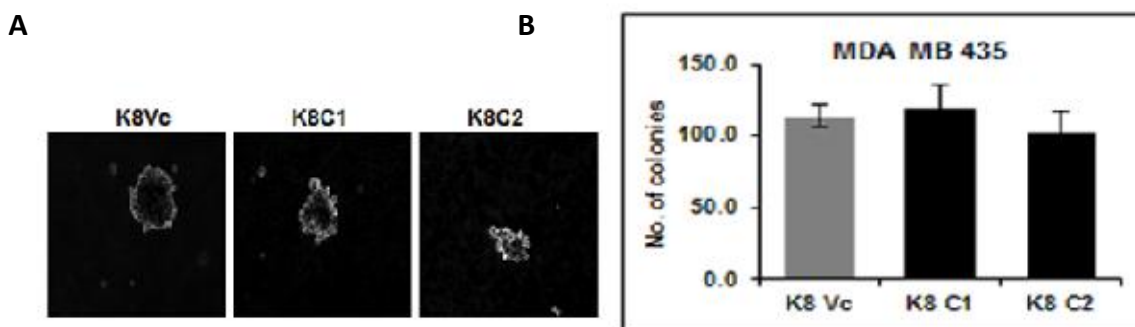


**Figure 5.2.5: Analysis of changes in soft agar colony forming potential on K8 over-expression in MDA MB 435 cell line:** (A) Representative phase contrast images (10X) of colonies formed in soft agar K8 over-expressed (K8C1, C2) and vector control (K8Vc) clones. (B) Histogram showing number of colonies of K8 overexpressed (K8C1, and C2) and vector control (K8Vc) clones. Results are mean  $\pm$  SE of three independent experiments performed in triplicate. **Note:** No change in anchorage independent growth.

### 5.2.6. Effect of K8 over-expression on proliferative potential of

**the cells:** To determine if an alteration in K8 levels led to changes in proliferation, MTT assays were performed. The K8 over-expressed MDA MB 435 clones (K8C1, C2) showed significant decrease in growth as compared to the vector control clone (K8Vc) (Figure 5.2.6)

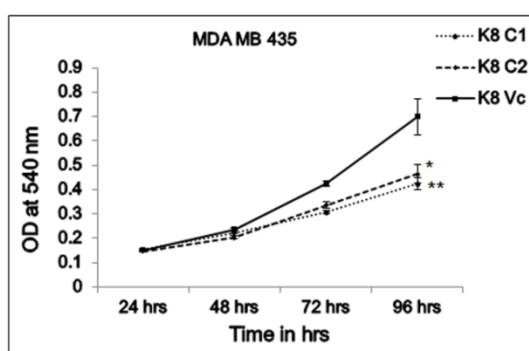


**Figure 5.2.6: Analysis of changes in cell proliferation on K8 over-expression:** Cell proliferation curves of K8 overexpressed (K8C1, C2) and vector control (K8Vc) clones. Cell proliferation was plotted against time. Results are mean  $\pm$  SE of three independent experiments performed in triplicate (\*p<0.05, \*\*p<0.01). **Note:** Decrease in proliferation in K8 over-expressed clones of MDA MB 435 as compared to vector control clone.

**5.2.7. Decrease in Motility on K8 over-expression:** Previously published results from our laboratory and others have suggested that alterations in K8 expression lead to changes in motility. To determine whether changes in motility would be observed in the cell systems used in this report, motility was assessed by performing wound healing as well as transwell assays.

**5.2.7.1 Analysis of motility by scratch wound assay:** Decrease in motility was observed in MDA MB 435 (K8C1 and C2) as compared to vector control clone (K8Vc). However, the decrease in motility was not statistically significant when compared to vector control clone when analysed by wound healing assay (Figure 5.2.7.1 A and B). This indicates that K8 over-expression inhibits motility.

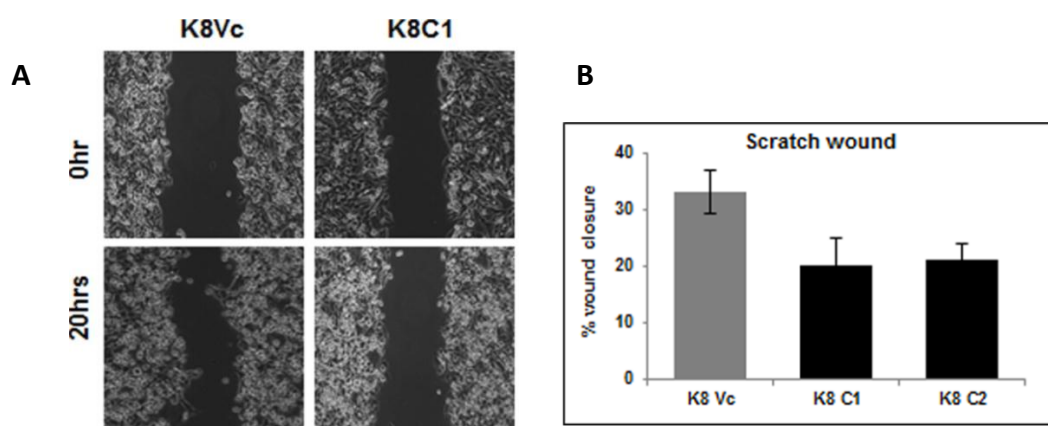


**Figure 5.2.7.1: Analysis of change in motility on K8 over-expression in MDA MB 435 clones: Motility of K8 up -regulated clones by wound healing assay:** (A) Representative Phase contrast images (10X) of time lapse microscopy at 0 hour and 20 hours showing wound healing in K8 over-expressed (K8C1) and vector control (K8Vc) clones. (B) Histogram showing % wound closure at the end of 20 hours of K8 over-expressed (K8C1 and C2) and vector control (K8Vc) clones. Results are mean of  $\pm$  SE of three independent experiments performed. Migration rate was calculated by AxioVision software.

**5.2.7.2. Analysis of motility by transwell assay:** The decrease in motility by scratch wound assay showed decrease in motility, but the decrease was statistically non-significant, while transwell assay demonstrated significant

decrease in motility in K8 over-expressed clones (Figure 5.2.7.2 A and B). These results indicated that K8 over-expression and K8/18 filament formation impeded motility in MDA MB 435 clones.

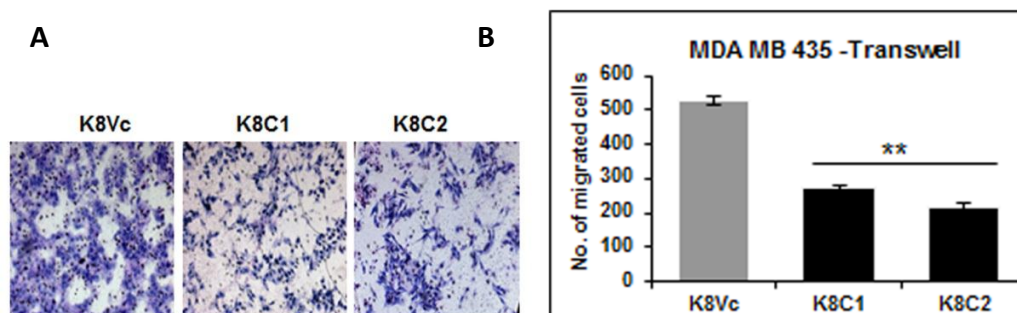


**Figure 5.2.7.2: Analysis of Motility by transwell assay K8 over-expressed MDA MB 435 clones:** (A) Representative images of H &E stained migrated cells of K8 over-expressed (K8C1, C2) and vector control (K8Vc) clones. (B) Histogram showing number of migrated cells at the end of 16 hours of over-expressed (K8C1 and C2) and vector control (K8Vc) clones (\* $p < 0.05$ ) **Note:** Significant decrease in motility in K8 over-expressed MDA MB 435 clones by transwell assay.

**5.2.8. No significant change in actin organization observed in K8 over-expressed clones:** No obvious change in the actin filament organization was observed in the K8 over-expressed clones of MDA MB 435 (K8 C1 and C2) clones as compared to vector control clone (K8Vc) (Figure 5.2.8).

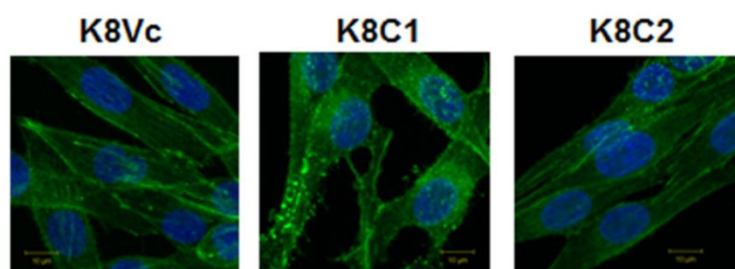


**Figure 5.2.8: Actin organization in K8 over-expressed MDA MB 435 clones:** Representative images of phalloidin stained actin filaments in K8 over-expressed (K8C1 and C2) and vector control (K8Vc) clones. Scale bar: 10µm. **Note:** No obvious changes in actin organization.

### 5.2.9. K8 over-expressed clones show decreased invasion *in-vitro*:

Our previous results have demonstrated that changes in K8 expression lead to changes in metastatic progression. To determine if changes in K8 expression led to changes in invasion, matrigel invasion assays were performed. The K8 overexpressing clones (K8C1 and C2) exhibited significant reduction in invasion as compared to vector control clone (K8Vc) (Figure 5.2.9A and B)

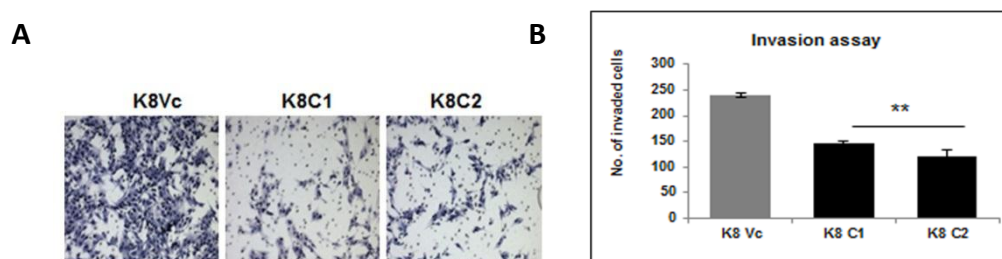


**Figure 5.2.9: Analysis of change in *in-vitro* invasion in K8 over-expressed clones of MDA MB 435:** (A) Representative images (10X) of H&E stained membrane showing invaded cells K8 over-expressed (K8C1, C2) and vector control (K8Vc) clones. (B) Histogram showing number of invaded cells of K8 overexpressed (K8C1 and C2) and vector control (K8Vc) clones (\*\*p < 0.01) **Note:** Significantly decreased invasion in K8 over-expressed MDA MB 435 clones.

### 5.2.10. K8 over-expression in an invasive cell line resulted in

#### decreased tumor volume and metastasis *in-vivo*:

The K8 over-expressed clones of MDA MB 435 (K8 C1 and C2) and vector control (K8Vc) clones were injected in the orthotopic site i.e. mammary fat pad of SCID mice to determine the tumorigenic potential of these cells. K8 transfected clones demonstrated delay in the onset of the tumor development as compared to the vector control cells. Significant decrease in the tumor volume was seen in K8 transfected clones as compared to animals injected with vector control clone (Figure 5.2.10A and B). Metastatic lesions were observed all over the lungs in all the animals injected with vector control transfected clone whereas only two

out of five animals injected with K8 transfected clone showed metastasis which was drastically reduced to few islands (Figure 5.2.10 C and D). Thus the K8 transfected cells demonstrated decrease in invasion as well as metastasis.

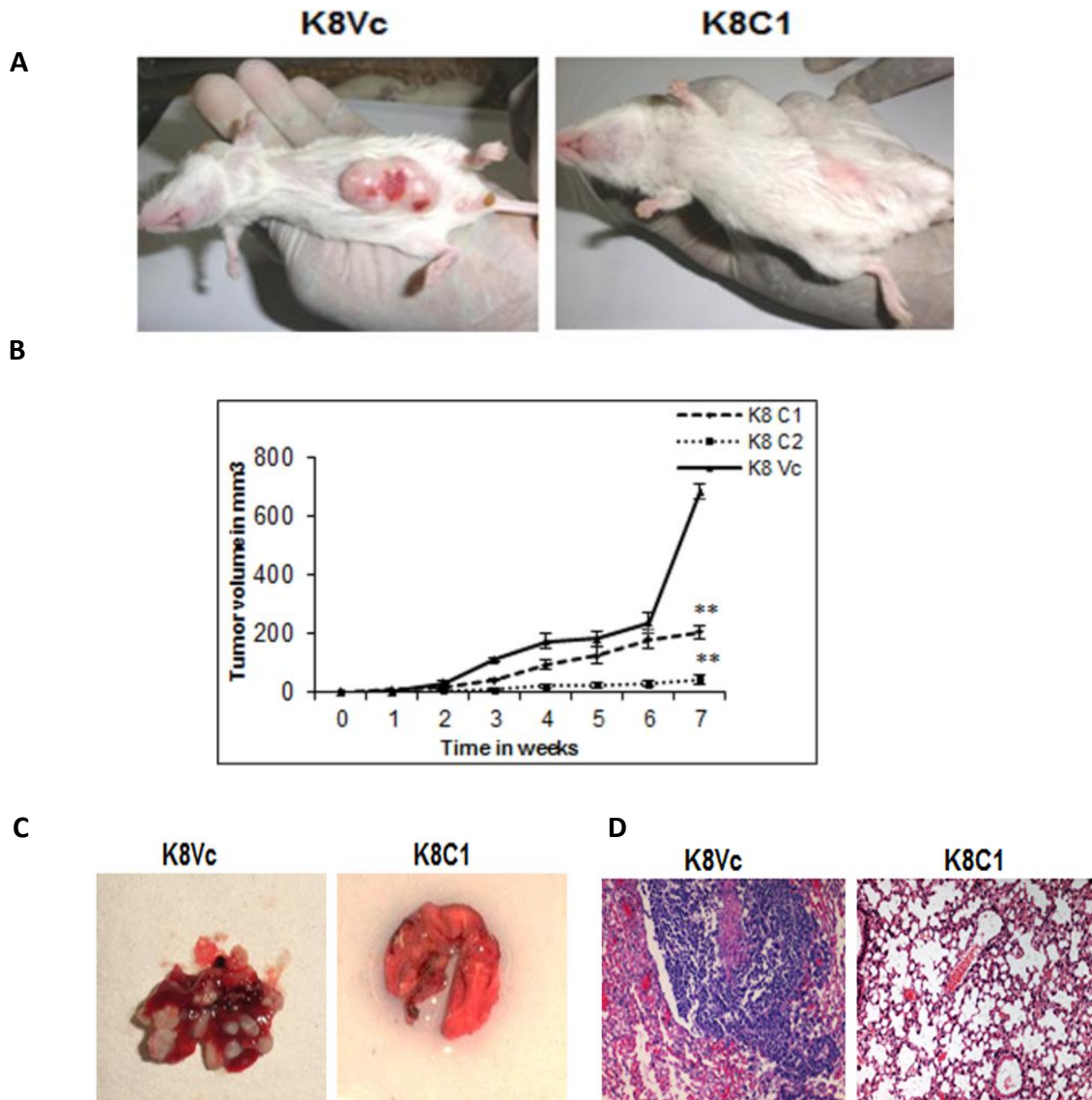


**Figure 5.2.10: Analysis of change in *in-vivo* tumorigenicity and metastatic potential in K8 up - regulated MDA MB 435 clones:** (A) Representative images of NOD-SCID mice bearing tumors of K8 over-expressed (K8C1) and vector control (K8Vc) clones, 7 weeks after the injection in mammary fat pad. (B) Tumor growth was plotted against time (\* $p < 0.05$ , \*\* $p < 0.01$ ). Results are mean of  $\pm$  SE for five animals injected for each clone. (C) Representative images of excised lungs of animals injected with K8 over-expressed (K8C1) and vector control (K8Vc) clones. (D) H&E stained lung sections of animals injected with MDA MB 435 K8 over-expressed clone (K8C1) showing no metastasis and vector control clone (K8Vc) showing metastatic foci throughout the lungs. **Note:** Very less or no metastasis in animals injected with K8 over-expressed MDA MB 435 clones.



**5.2.11. Immunohistochemical (IHC) analysis of tumors excised from animals injected with K8 over-expressed clones and vector control clone:** IHC was performed on the tumors excised from the animals injected with K8 over expressing MDA MB 435 (K8 C1 and C2) clones and vector control clone (K8Vc) using mAb to K8, 18 and vimentin. The tumors from animals injected with vector control derived MDAMB 435 clones showed no expression of K8, low expression of K18 and abundant expression of vimentin, while the tumors excised from animals with K8 overexpressed clones showed up-regulation of K8 K18 and marginal decrease in vimentin expression (Figure 5.2.11).

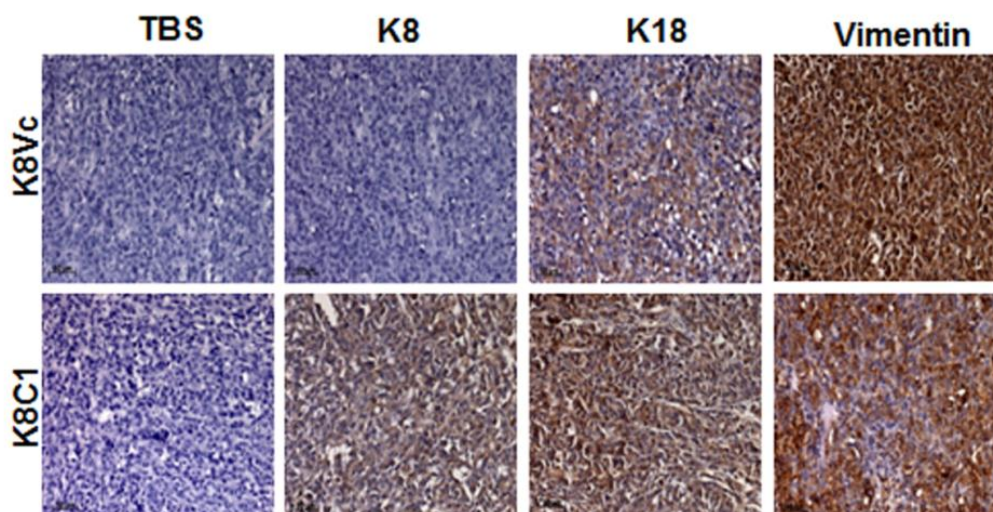


**Figure 5.2.11: Analysis of K8, K18 and vimentin expression in tumor derived from animals on injection of MDA MB 435 K8 over-expressed and vector control clones:** Representative IHC images of tumor sections derived from injection of K8 overexpressed (K8C1) and vector control (K8Vc) clones using mAb to K8, 18 and vimentin respectively. **Note:** K8, K18 up-regulation is reflected in tumors obtained from injecting K8 over-expressing clones.

### 5.2.12. Analysis of E-cadherin expression in K8 over-expressed

**clones:** E-cadherin expression is known to change during malignant transformation. Previous reports on breast cancer showed concurrent up-regulation of E-cadherin with keratins 8/18. Hence change in E-cadherin levels and localization was assessed in K8 over-expressed MDA MB 435 clones (K8 C1 and C2) and vector control clone (K8Vc). E-cadherin remained undetected after K8 over-expression. MCF-7 cells were taken as a positive control (Figure 5.2.12 A and B).

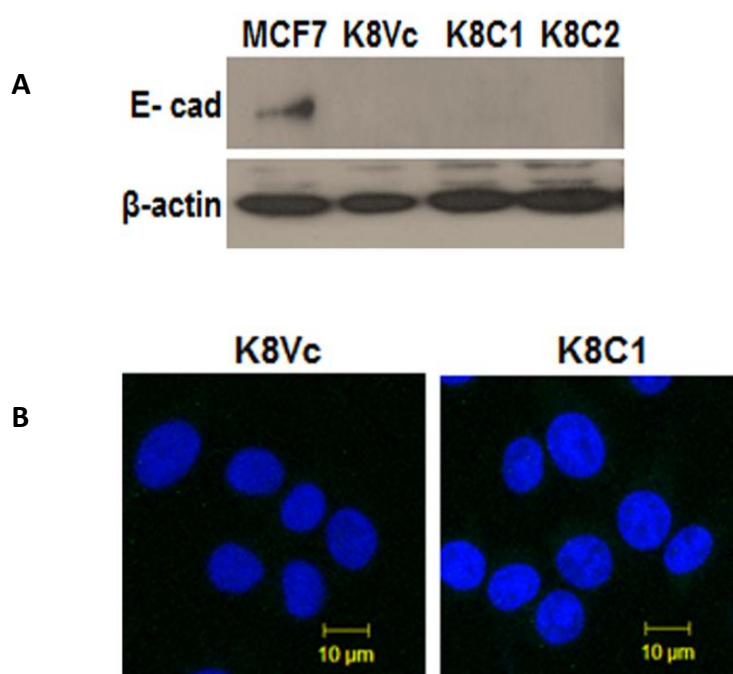


**Figure 5.2.12.: Analysis of E-cadherin expression on K8 over-expression in MDA MB 435 clones:** (A) Western blot analysis of E-cadherin in K8 over-expressed (K8C1, C2 and C3) and vector control (K8Vc) clones. MCF7 served as positive control.  $\beta$ -actin was taken as loading control. (B) Representative confocal images of E-cadherin in K8 over-expressed (K8C1) and vector control (K8Vc) clones. **Scale bar:** 10 $\mu$ m. **Note:** No change in E-cadherin levels on K8 over-expression.

### 5.2.13. Keratin 8 over-expression did not result in any change in the

**expression of  $\beta$ 4 integrin:** Previous reports from our laboratory showed the involvement of  $\beta$ 4 integrin mediated pathway on K8 down-regulation in human



oral SCC derived cell lines. Therefore to understand whether  $\beta 4$  integrin mediated signalling has any role in transformation /progression of breast cancer derived cell lines, its expression levels were analysed in K8 over-expressed MDA MB 435 (K8 C1 and C2) clones and vector control clone (K8Vc).  $\beta 4$  integrin was not detected in either K8 over-expressed or vector control clones (Figure 5.2.7).

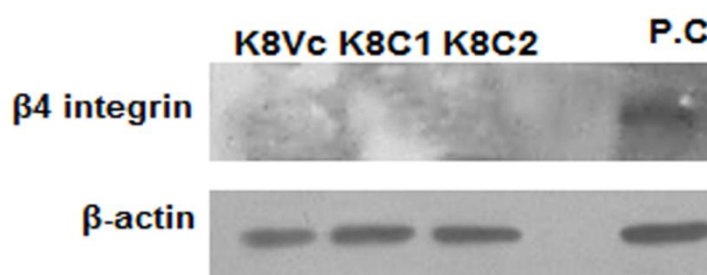


**Figure 5.2.13: Analysis of  $\beta 4$  integrin expression on K8 over-expression in MDA MB 435 clones:** Western blot analysis of  $\beta 4$  integrin in K8 over-expressed (K8C1 and C2) and vector control (K8Vc) clones.  $\beta$ -actin was taken as loading control. Positive control (P.C.):Lysate of MDA MB 468 cells. **Note:** Absence of  $\beta 4$  integrin in K8 over-expressed and vector control clones.

*In summary, the over-expression of K8 in an invasive MDA MB 435 cell line resulted in the significant decrease in proliferation, in-vitro motility, in-vitro invasion, and tumor volume and metastasis in-vivo. Keratin 7, E-cadherin and beta4 integrin were not detected in vector control or K8 over-expressed clones.*

### **5.3. Generation of stable K8 knockdown MDA MB 468 clones:**

To determine whether loss of K8 leads to an increase in transformation in the MDA MB 468 clones, a previously described and validated shRNA construct to K8, shRNA8.2 [29] or the empty vector control pTU6-puro were transfected to generate stable clones.

#### **5.3.1. Expression of K8/18 in K8 knock-down clones:**

**5.3.1.1. Western blot and immunofluorescence analysis of K8/18 in K8 down-regulated clones:** MDA MB 468 K8 knockdown clones (ShC1, C2, and C3) exhibited efficient down regulation in K8 levels (undetectable) as compared to the vector control transfected clone (Vc) (Figure 5.3.1.1 A and B). There was no change in K18 levels in K8 down-regulated clones, in contrast to what has been observed previously by us and others ((Figure 5.3.1.1A) [29,30]. Immunofluorescence analysis revealed no K8 filaments, yet K18 filaments were observed (Figure 5.3.1.1B) indicating that K18 formed filaments possibly by binding with some other type II keratin like K7, as shown previously [76].

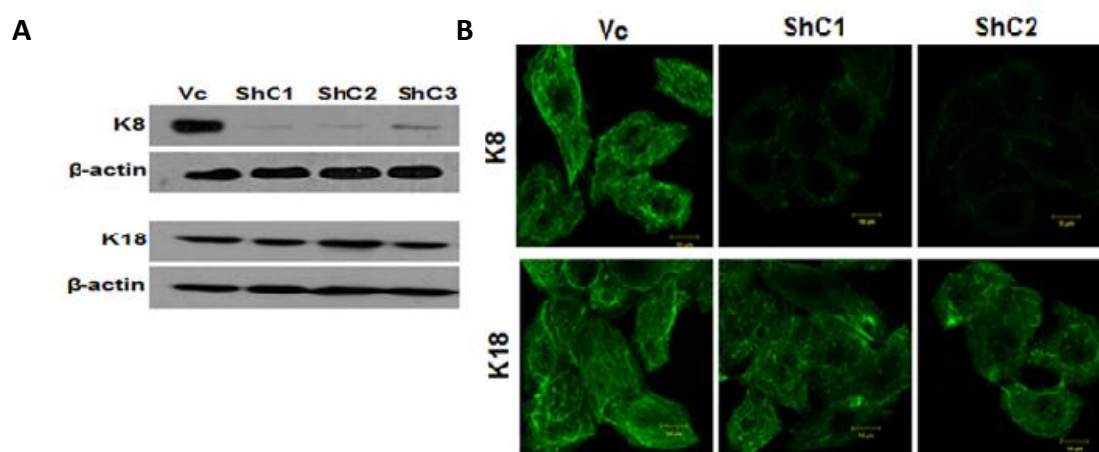


**Figure 5.3.1.1: Analysis of K8 and K18 expression in K8 down-regulated MDA MB 468 clones by western blot and immunofluorescence :** (A) Western blot analysis of K8 and 18 using mAbs to K8 and K18 respectively in K8 down-regulated (ShC1, C2 and C3) and vector control (Vc) clones. β-actin was used as loading control (B) Representative confocal images of K8 and K18 filaments in K8 down-regulated (ShC1, C2) and vector control (Vc) clones. **Scale bar:** 10 μm. **Note:** No change in K18 filaments in K8 down-regulated MDA MB 468 clones

**5.3.1.2. Flow cytometric and real time PCR analysis of K8 down-regulated clones :** Down-regulation of K8 in MDA MB 468 clones as compared to vector control clone and parental cells was also confirmed using flow cytometric analysis with antibody to K8 (M-20 clone, Sigma) (Figure 5.3.1.2A and B). Real time PCR analysis did not show any significant decrease in K18 levels (Figure 5.3.1.2C). Plasmid copy number was found to vary from 1-2 for MDA MB 468 clones

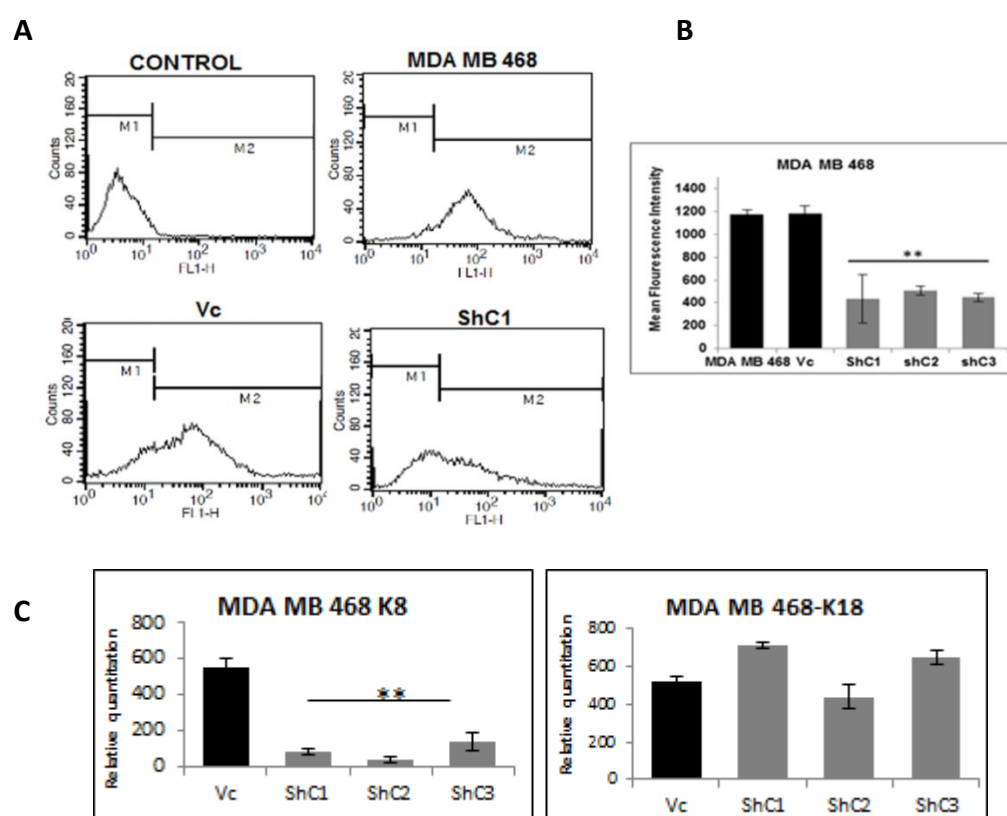


**Figure 5.3.1.2: Analysis of K8 expression by flow cytometry and K8/18 mRNA levels by real time PCR in MDA MB 468 clones:** (A) Flow cytometric analysis of K8 expression in MDA MB 468 parental, vector control clone (Vc) and K8 down-regulated (ShC1) a representative clone. (B) Histograms showing mean fluorescence intensity of K8 ( $\pm$  S.E.) for three independent experiments in K8 down-regulated (ShC1, C2 and C3) as compared to parental MDA MB 468 and vector control clone (Vc) as analysed by flow cytometry. (C) Real time PCR analysis of K8 and K18 genes in K8-down-regulated clones (ShC1, C2 and C3) as compared to vector control clone (Vc) using *GAPDH* as internal control. Results are mean of  $\pm$  SE of three independent experiments performed. **Note:** No significant difference in K18 mRNA levels on K8 down-regulation.

## 5.3.2 Effect of K8 knockdown on the levels of other keratins and vimentin:

**5.3.2.1. Analysis of K7 expression in K8 down-regulated clones:** High salt extraction was done to enrich the keratin pool. The mass spectrometric (MS) analysis of the high salt extracted proteins (keratins) revealed presence of K7, K18 along with K19 in both K8 down regulated MDA MB 468 clones (ShC1, C2, and C3) and vector control clone (Vc), while K8 (52 kDa band) was present only in vector control clone (Vc) and absent in K8 down-regulated clones (Figure 5.3.21.A and Appendix Table 5.3.2), showing specificity of shRNA. Further Western blot analysis using mAb to K7 showed up-regulation of K7 in the K8 down-regulated clones (Figure 5.3.2.1 B).

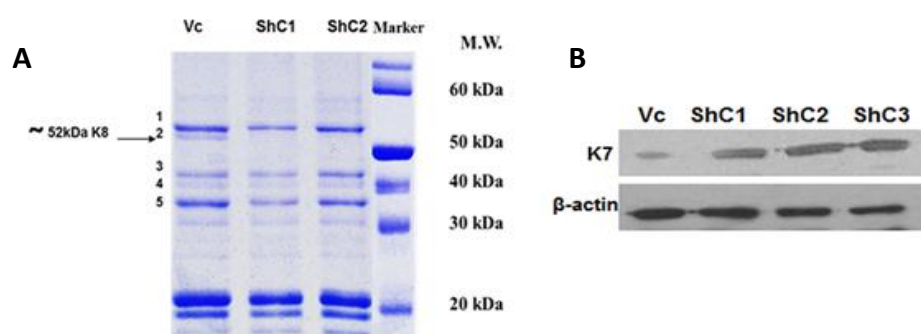


**Figure 5.3.2.1: Analysis of K7 expression in K8 down-regulated MDA-MB-468 clones:** (A) **High salt Keratin extraction:** The keratin profile of MDA MB 468 K8 down-regulated (ShC1 and C2) and vector control (Vc) clones after high-salt extraction. The arrow indicates position of K8 band on the gel at molecular weight (M.W. ~52 kDa). The numbers indicated on the left hand side indicates the gel pieces taken for the mass spectrometry analysis. **Note:** Keratin 8 was observed to be down-regulated in the K8 knockdown clones as compared to vector control. (B) **Western blot analysis of K7** using mAb to K7 in K8 down-regulated (ShC1, C2 and C3) and vector control (Vc) clones. **Note:** K7 up-regulation in K8 down-regulated clones. **Note:** Up-regulation of K7 in K8 down-regulated clones of MDA MB 468

**5.3.2.2. Analysis of vimentin expression in K8 down-regulated MDA-MB-468 clones:** To understand if any change in K8 expression resulted in change in vimentin expression, it was analysed. K8 down-regulation in cells did not result

in any change in vimentin levels and levels were comparable in all the clones (Figure 5.3.2.A&B).

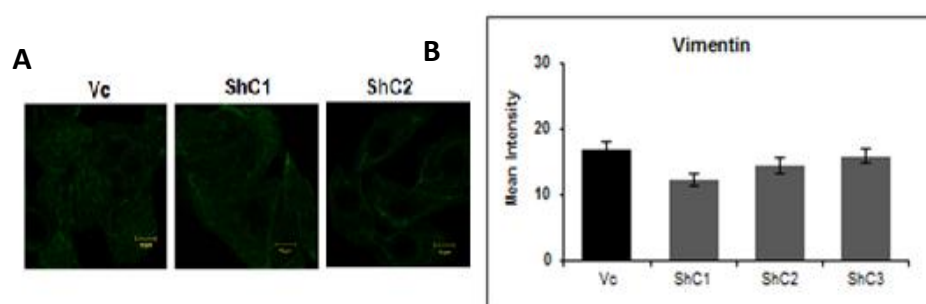


**Figure 5.3.2.2: Analysis of vimentin expression in K8 down regulated MDA MB 468 clones:** (A) Representative confocal images of vimentin filaments in K8 down-regulated (ShC1, C2) and vector control (Vc) clones. **Scale bar:** 10 $\mu$ m. (B) Histograms showing mean fluorescence intensity of vimentin in K8 down-regulated (ShC1, C2 and C3) and vector control (Vc) clones. The mean fluorescence intensity of 20 cells was calculated. Results are mean of  $\pm$  SE for three independent experiments performed. **Note:** No change in vimentin expression or filament formation on K8 down-regulation.

### 5.3.3 Effect of K8 down-regulation cells on differentiation status:

To determine if change in K8 levels affected differentiation, the levels of lipid droplets were measured. The MDA MB 468 derived K8 knockdown clones (ShC1, C2 and C3) did not show any significant change in the lipid droplet levels as compared to the vector control clone (Vc) (Figure 5.3.3.A & B).

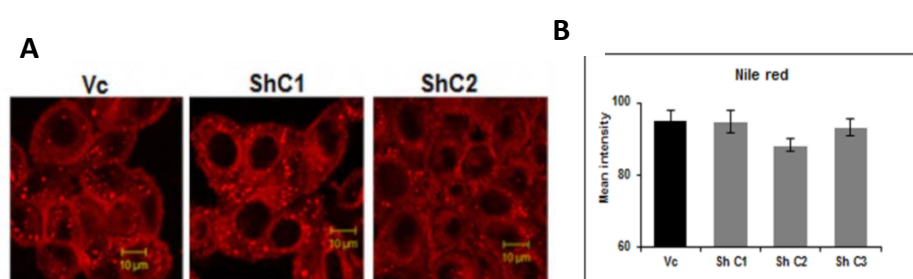


**Figure 5.3.3.: Analysis of differentiation status of MDA MB 468 K8 down-regulated clones by lipid droplets staining using Nile red:** (A) Representative confocal images of lipid droplets staining in K8 down-regulated (ShC1, C2) and vector control (Vc) clones. **Scale bar:** 10 $\mu$ m. (B) Histogram showing the mean intensity of K8 down-regulated (ShC1, C2 and C3) and vector control (Vc) clones. The mean fluorescence intensity ( $\pm$  SE) of lipid droplets was calculated per cell by measuring fluorescence intensity of 20 cells of each experiment (using LSM10 software This was repeated thrice. Results are mean of  $\pm$  SE of three independent experiments performed.

**Note:** No change in lipid droplet staining intensity in any of the clones on K8 down-regulation.

#### 5.3.4. Effect of K8 down-regulation on soft agar colony forming

**potential:** In order to assess the effect of K8 expression on tumorigenesis *in-vitro*, soft agar colony forming assays were performed. The K8 knockdown clones of MDA MB 468 (ShC1, C2 and C3) demonstrated a significant increase in size and number of colonies compared with vector control clone (Vc) (Figure 5.3.4 A & B).

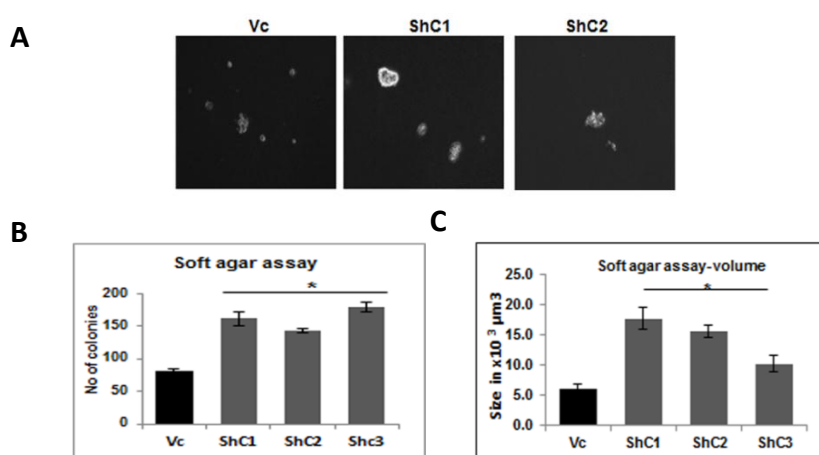


**Figure 5.3.4: Analysis of changes in soft agar colony forming potential on K8 down-regulation in MDA MB 468 clones:** (A) Representative phase contrast images (10X) of colonies formed in soft agar in K8 down-regulated (ShC1, C2) and vector control (Vc) clones. (B) Histogram showing number of colonies of K8 down-regulated (ShC1, C2 and C3) and vector control (Vc) clones (\* $p < 0.05$ ). **Note:** Significant Increase in soft agar colonies formed in K8 down-regulated MDA MB 468 clones.

#### 5.3.5. K8 down-regulation did not change the proliferative

**potential of the cells:** Previous reports have shown that alterations in K8 lead to changes in the cell proliferation. To determine the change in proliferation potential, MTT assays were performed on K8 knockdown clones. The MDA MB 468 K8 knockdown clones (ShC1, C2 and C3) did not demonstrate significant difference in the proliferation as compared to vector control clone (Vc) (Figure

5.3.5), although K8 down-regulated cells showed growth at high density. High density cell growth is one of the hall marks of transformed cells, indicating increased transformation potential of K8 down-regulated clones.

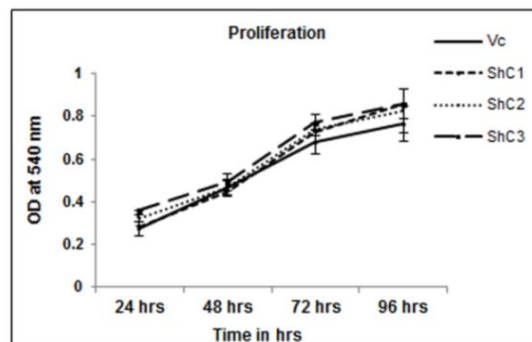


**Figure 5.3.5: Analysis of changes in cell proliferation on K8 down-regulation in MDA MB 468 cells:** Cell proliferation curves of K8 down-regulated (ShC1, C2 and C3) and vector control (Vc) clones. Cell proliferation was plotted against time. Results are mean  $\pm$  SE of three independent experiments performed in triplicate. **Note:** No significant decrease in proliferation in K8 down-regulated clones of MDA MB 468 as compared to vector control.

**5.3.6. Increase in Motility on K8 down-regulation:** To determine whether the changes in motility would be observed on K8 down-regulation in MDA MB 468 cells, motility was assessed by performing wound healing as well as transwell assays. as well as transwell assay was observed(Figure 5.3.6.A , B, C& D)

**5.3.6.1. Analysis of motility by scratch wound assay:** A significant increase in the motility in MDA MB 468 derived K8 knockdown clones (ShC1, C2 and C3) as compared to vector control clone (Vc) by scratch wound assay.



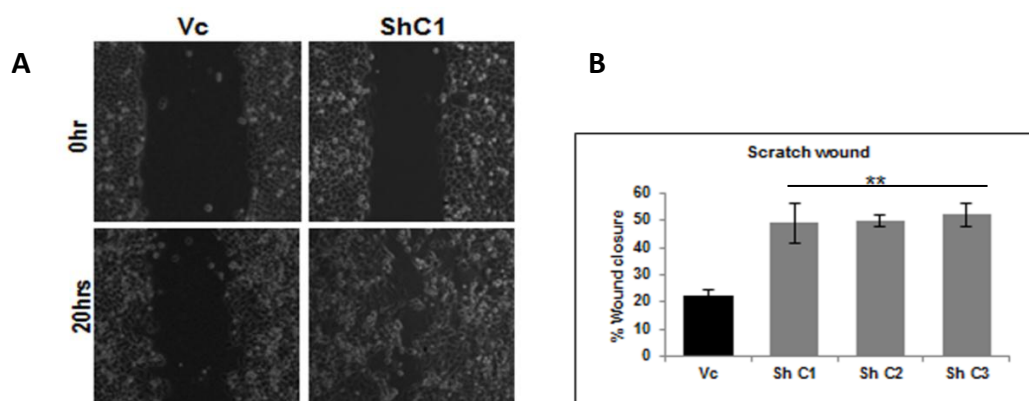


**Figure 5.3.6.1: Analysis of change in motility on K8 down-regulation in MDA MB 468 cells by wound healing assay:** (A) Representative Phase contrast images (10X) of time lapse microscopy at 0 hour and 20 hours showing wound healing in K8 down-regulated (ShC1) and vector control (Vc) clones. (B) Histogram showing % wound closure at the end of 20 hours. Results are mean of  $\pm$  SE of three independent experiments performed. Migration rate was calculated by AxioVision software.

**5.3.6.2. Analysis of motility by transwell assay:** Significant increase in the motility in MDA MB 468 derived K8 knockdown clones (ShC1, C2 and C3) as compared to vector control clone (Vc) by transwell assay

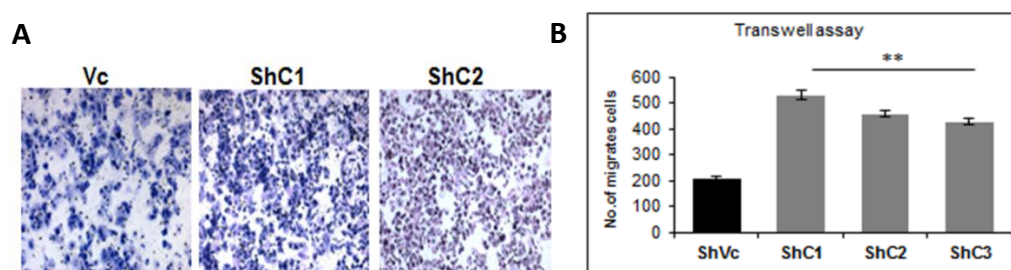


**Figure 5.3.6.2: Analysis of change in motility on K8 down-regulation in MDA MB 468 cells by transwell assay:** (A) Representative images (10X) of H &E stained migrated cells in K8 down-regulated (ShC1, C2) and vector control (Vc) clones. (B) Histogram showing number of migrated cells at the end of 16 hours of K8 knockdown clones (ShC1, C2 and C3) and vector control (Vc) clone (\*  $p < 0.05$ , \*\* $p < 0.01$ ) **Note:** Significant increase in motility in K8 down-regulated MDA MB 468 clones by both scratch wound and transwell assay.

**5.3.7. Changes in actin organization on K8 down-regulation:** To understand whether the changes seen in motility of the cells were accompanied with alterations seen in the actin organisation, the cells were analysed by



phalloidin staining. K8 down-regulated clones MDA MB 468 (ShC1, C2 and C3) demonstrated increased lamellipodia formation as compared to vector control clone (Vc) (Figure 5.3.7).

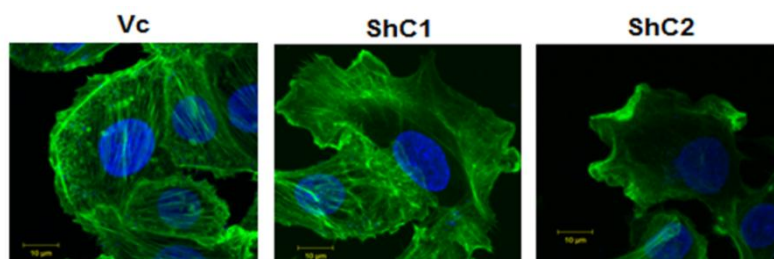


**Figure 5.3.7: Actin organization in K8 down-regulated MDA MB 468 clones:** Representative images of phalloidin stained actin filaments in K8 down-regulated (ShC1 and C2) and vector control (Vc) clones. **Scale bar:** 10µm **Note:** Increase in lamellipodia formation was seen in K8 down-regulated clones.

### 5.3.8. K8 down-regulated clones show increased invasion *in-vitro*:

To determine if changes in K8 expression led to changes in invasion, matrigel invasion assays were performed. There was significant increase in invasion in the MDA MB 468 derived K8 knockdown clones (ShC1, C2 and C3) as compared to the vector control clone (Vc) (Figure 5.3.8 A&B).

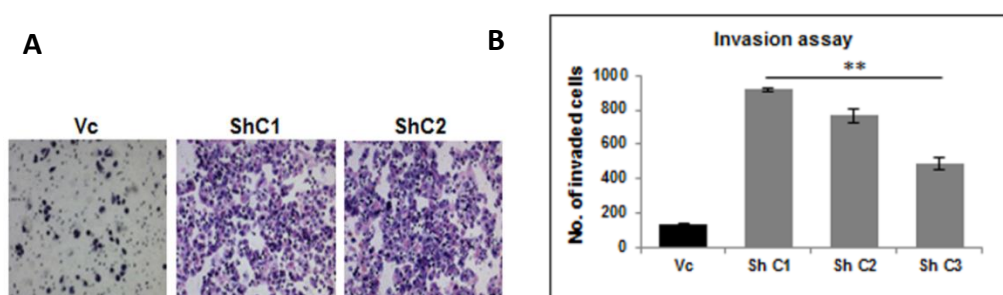


**Figure 5.3.8: Analysis of change in *in-vitro* invasion on K8 down-regulation in MDA MB 468 clones:** (A) Representative images (10X) of H&E stained membrane showing invaded cells in K8 down-regulated (ShC1, C2) and vector control (Vc) clones. (B) Histogram showing number of invaded cells of K8 down-regulated (ShC1, C2 and C3) and vector control (Vc) clones ( $p < 0.05$ ). **Note:** Significant increase in *in-vitro* invasion in K8 down-regulated MDA MB 468 clones.

**5.3.9: Analysis of change in *in-vivo* tumorigenicity and metastatic potential on K8 down-regulation:** Four million cells of MDA MB 468 K8

down-regulated (ShC1, C2 and C3) and vector control clone (Vc) were injected in the mammary fat pad of the 5 SCID/Nude mice per group. The tumor size was not uniform in the SCID mice. After the tumor sized reached 1-1.5cm the tumor was excised the wound was sealed and animals were observed for 4 weeks. After 4 weeks the animals were sacrificed. The histological examination of the lungs of all the SCID mice showed severe congestion. The same experiment was later repeated in Nude mice. The animals were observed for tumor formation for 8-12 weeks. There was no tumor seen in the Nude mice injected with MDA MB 468 clones. All the Nude mice died within a month's time and the experiment had to be abandoned.

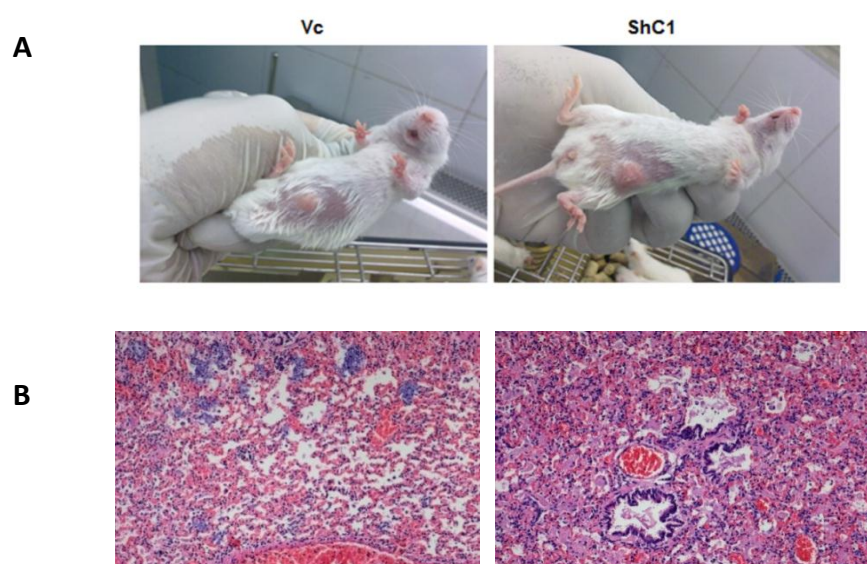


**Figure 5.3.9: Tumor formation in SCID mice injected with MDA MB 435 K8 down-regulated and vector control clones:** (A) Representative images of animals injected with K8 down –regulated clone (ShC1) and vector control clone (Vc). (B) Representative H & E stained images of lungs of the animals injected with K8 down-regulated (ShC1) and vector control (V) clones. **Note:** Congestion and haemorrhage due to infection in lungs was observed, therefore this experiment was abandoned.

### 5.3.10. Changes in E-cadherin localization on K8 down-regulation:

Western blot was performed to determine whether down-regulation of K8 has any effect on levels of E-cadherin. The results showed that there was no change in the

levels of E-cadherin in the K8 down-regulated clones (ShC1, C2 and C3) as compared to vector control clone (Vc) (Figure 5.3.10 A). We observed Change in localization of E-cadherin from membrane to cytoplasm in K8 down-regulated clones of MDA MB 468 while the vector control clone demonstrated membrane staining (Figure 5.3.10.B).

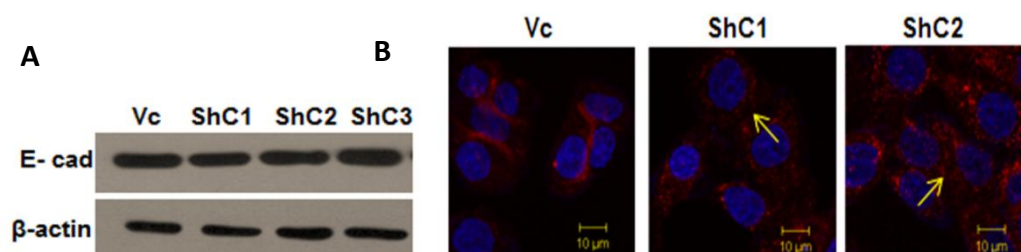


**Figure 5.3.10: Analysis of E-cadherin expression on K8 down-regulation in MDA MB468 clones:** (A) Western blot analysis of E-cadherin in MDA MB 468 K8 down-regulated (ShC1, C2 and C3) and vector control (Vc) clones.  $\beta$ -actin was taken as loading control. **Note:** No change in E-cadherin levels. (B) Representative confocal images of E-cadherin in MDA MB 468 K8 down-regulated (ShC1, C2) and vector control (Vc) clones. **Scale bar:** 10  $\mu$ m. Nuclei (blue) are stained with DAPI. **Note** Cytoplasmic localization of E-cadherin in K8 down-regulated MDA MB 468 clones.

### 5.3.11. Keratin 8 down-regulation did not result in any change in

**the expression of  $\beta$ 4 integrin:** To assess if  $\beta$ 4 integrin mediated signalling pathway is involved in the change in transformation potential observed in the MDA MB 468 K8 down-regulated clones (ShC1, C2 and C3) and vector control clone (Vc), we determined  $\beta$ 4 integrin levels in these cells. We did not see any significant change in the levels of  $\beta$ 4 integrin on K8 down-regulation (Figure 5.3.11).

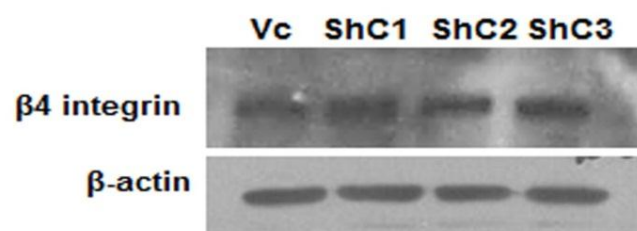


**Figure 5.3.11: Analysis of  $\beta 4$  expression on K8 down-regulated MDA MB 468 clones:** Western blot analysis of  $\beta 4$  integrin in K8 down-regulated (ShC1, C2 and C3) and vector control (Vc) clones.  $\beta$ -actin was taken as loading control. **Note:** No change in levels of  $\beta 4$  integrin.

*In summary down-regulation of K8 in MDA MB 468 cells resulted in up-regulation of K7, significant increase in soft agar colony formation, in-vitro motility and invasion. K8 down regulation also resulted in change in E-cadherin localization to cytoplasm without change in its protein levels, while there was no change in  $\beta 4$  integrin levels.*

## **5.4. Generation of stable K8 knockdown MCF10A clones:**

To determine whether loss of K8 leads to transformation in the MCF10A cells, shRNA8.2 [29] or the empty vector control pTU6-puro were transfected to generate stable clones.

### **5.4.1. Expression of K8/18 on K8 down-regulation:**

**5.4.1.1. Western blot and Immunofluorescence analysis of K8/18 expression in K8 down-regulated clones:** MCF10A stable K8 knockdown clones (MShC1, C2 and C3) demonstrated 80% and 60% down-regulation in K8 and K18 protein levels respectively as compared to the vector control clone (MVc) (Figure 5.4.1 A, B & C). The immunofluorescence analysis revealed formation of diffused filaments in the K8 knockdown MCF10A clones as compared to the vector control clone (Figure 5.4.1D). Plasmid copy number was found to vary from 1-2 for MCF10A clones.

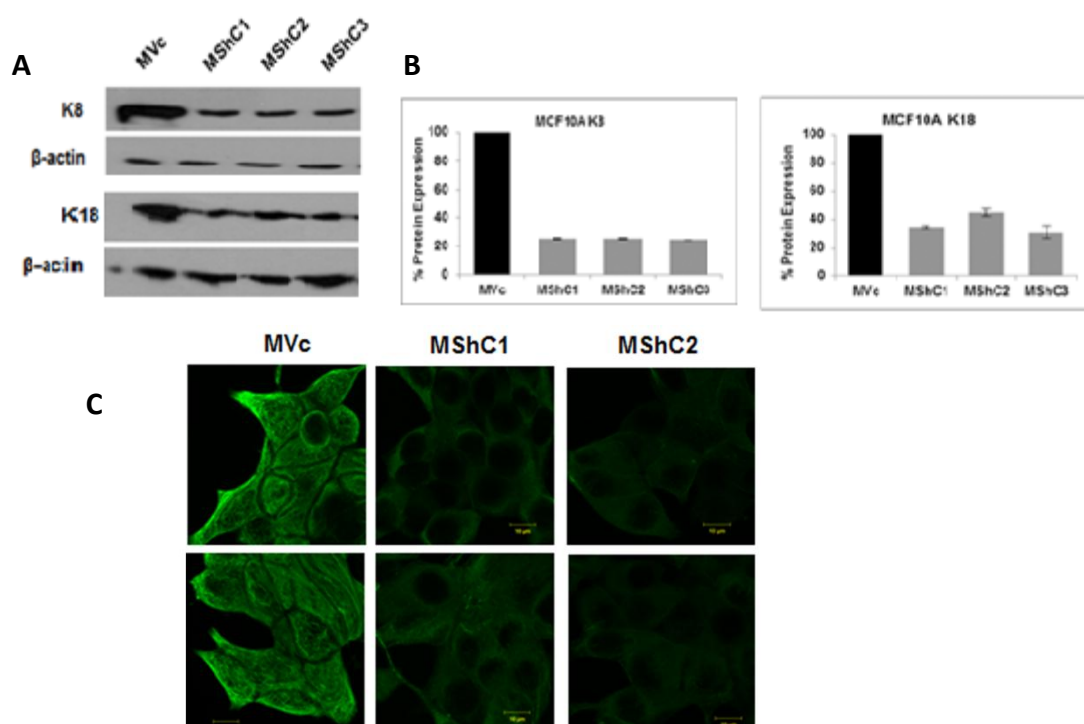


**Figure 5.4.1.1: Analysis of K8 and K18 expression in K8 down-regulated MCF10A clones by Western blot and immunofluorescence:** (A) Western blot analysis of K8/18 using mAbs to K8 and K18 respectively in MCF10A K8 down-regulated (MShC1, C2 and C3) and vector control (MVc) clones. β-actin was taken as loading control. (B) Histogram showing % protein expression ( $\pm$  S.E.) for three independent experiments of K8 and K18 in MCF10A K8 down-regulated (MShC1, C2 and C3) and vector control (MVc) clones. The percentage of protein expression was determined by Image J software. The intensity of

the K8 or K18 expression was normalized with  $\beta$ -actin. Intensity of vector control clone (MVc) was considered as 100% expression. **Note:** ~60% down-regulation in K18 levels on K8 down-regulation. **(C)** Representative confocal images of K8 and K18 filaments in MCF10A K8 down-regulated (MShC1, C2) and vector control (MVc) clones. **Scale bar:** 10  $\mu$ m.

#### 5.4.1.2. Flow cytometric and real time PCR analysis of K8 down-regulated

**clones:** Down regulation of K8 in MCF10A clones as compared to vector control clone and parental cells was also confirmed using flow cytometric analysis with antibody to K8 (M-20 clone, Sigma) (Figure 5.4.1.2 A and B). Real time PCR analysis showed down-regulation of both K8 and K18 (Figure 5.4.1.2 C).

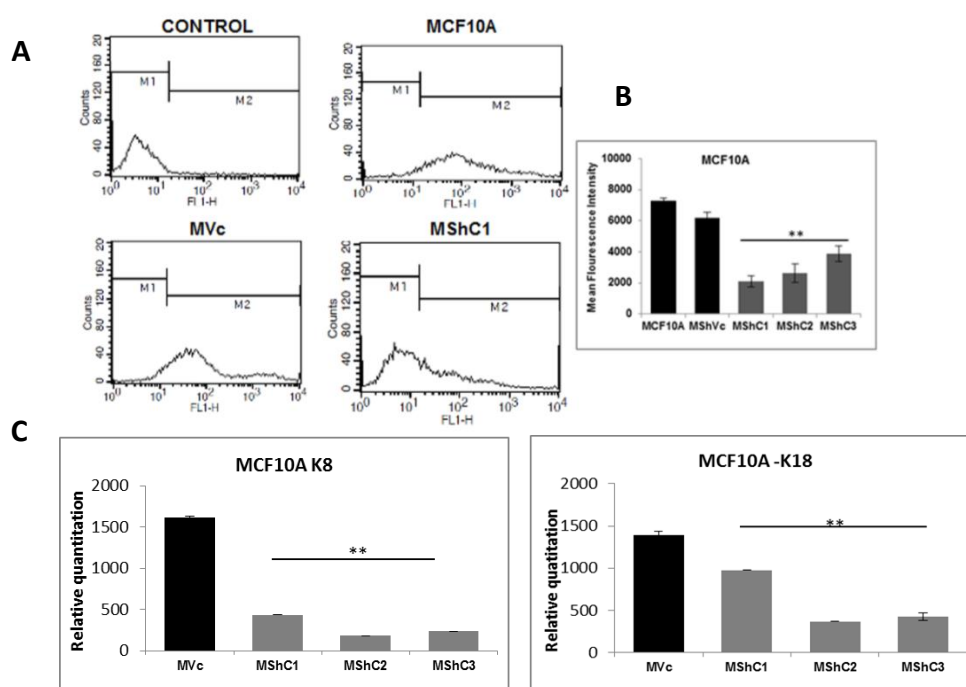


**Figure 5.4.1.2: Analysis of K8 expression by flow cytometry and K8/18 mRNA levels by real time PCR:** (A) Flow cytometric analysis of K8 expression in MCF10A parental, vector control clone (Vc) and K8 down-regulated (MShC1), representative clone. (B) Histograms showing mean fluorescence intensity of K8 ( $\pm$  S.E.) for three independent experiments in K8 down-regulated clones (MShC1, C2 and C3) as compared to parental MCF10A and vector control clone (MVc) as analysed by flow cytometry. (C) Real time PCR analysis of K8 and K18 genes in K8-down-regulated MCF10A clones (MShC1, C2 and C3) as compared to vector control clone (MVc) using *GAPDH* as internal control. Results are mean of  $\pm$  SE of three independent experiments performed. **Note:** Decrease in K8 and K18 protein and mRNA levels and also diffused filament formation in K8 down-regulated MCF10A clones.



## 5.4.2. Effect of K8 knockdown on the levels of other keratins and vimentin:

**5.4.2.1. Analysis of Keratin 7 expression on K8 down-regulation:** Keratin7 is known to pair with K18 in absence of K8 and was found to be previously up-regulated in K8 down-regulated MD MB 468 clones. Hence K7 expression was analysed in MCF10A K8 down-regulated clones (MShC1, C2 and C3) as compared to the vector control clone (MVc) by western blot analysis. Keratin 7 remained undetected in K8 down-regulated clones and vector control transfected clone (Figure 5.4.2 A).

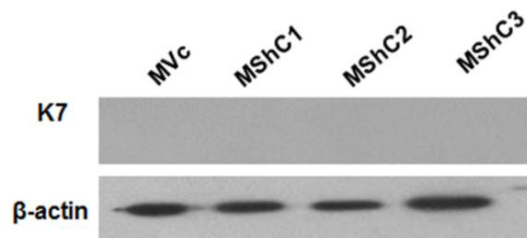


**Figure 5.4.2.1: Analysis of K7 expression in K8 down-regulated MCF10A clones:** Western blot analysis of K7 using mAb to K7 in MCF10A K8 down-regulated (MshC1, C2 and C3) and vector control (MVc) clones. β-actin was taken as loading control. **Note:** No change in K7 levels in K8 down-regulated MCF10A clones.

**5.4.2.2. Analysis of vimentin expression on K8 down-regulation:** Vimentin expression was analysed in MCF10A K8 down-regulated clones (MShC1, C2 and C3) as compared to the vector control clone (MVc). Vimentin, remained absent in K8 down-regulated clones (Figure 5.42 B & C).

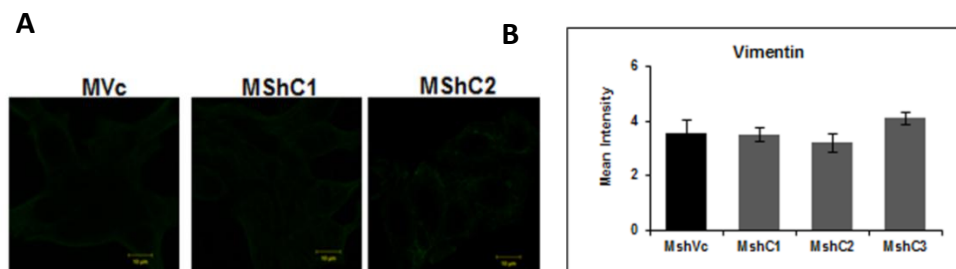


**Figure 5.4.2.2: Analysis of vimentin expression in K8 down-regulated MCF10A clones:** (A) Representative confocal images of vimentin filaments in MCF10A K8 down-

regulated (MshC1, C2) and vector control (MVc) clones. Scale bar: 10  $\mu$ m. **(B)** Histograms showing Mean fluorescence intensity of vimentin ( $\pm$  S.E.) for three independent experiments. The mean fluorescence intensity of 20 cells was calculated (using LSM10 software; Carl Zeiss MicroImaging GmbH, Jena, Germany). Results are mean of  $\pm$  SE of three independent experiments performed. **Note:** No change in vimentin expression or filament formation in K8 down-regulated MCF10A clones

**5.4.3. Effect of K8 down-regulation on differentiation status:** To determine if change in K8 levels affected differentiation, the levels of lipid droplets were measured in the K8 down-regulated MCF10A and vector control clones. MCF10A (MShC1, C2 and C3) derived K8 knocked down clones did not show any significant change in the lipid droplet levels as compared to the vector control clone (MVc) (Figure 5.4.3A &B). These results indicate that change in levels of K8 did not have any effect on the differentiation status of the cells.

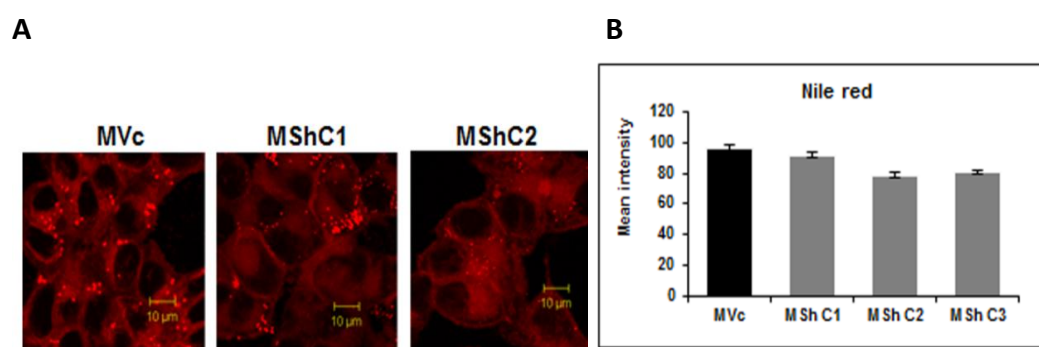


**Figure 5.4.3: Analysis of differentiation status of MCF10A K8 down-regulated clones by lipid droplets staining using Nile red:** Representative confocal images of lipid droplets staining in MCF10A K8 down-regulated (MShC1, C2) and vector control (MVc) clones. **(B)** Histogram showing the mean intensity of MCF10A K8 down-regulated (MShC1, C2 and C3) and vector control (MVc) clones. **Scale bar:** 10 $\mu$ m. The mean fluorescence intensity ( $\pm$  SE) of lipid droplets was calculated per cell by measuring fluorescence intensity of 20 cells in each experiment (using LSM10 software). Results are mean of  $\pm$  SE of three independent experiments performed. **Note:** No change in lipid droplet staining intensity in MCF10A K8 down-regulated clones as compared to vector control clone.

**5.4.4. Effect of K8 down-regulation on soft agar colony forming potential:** In order to assess if K8 down-regulation resulted in change in anchorage independence, soft agar colony forming assays were performed. There



was no change in the number or volume of the soft agar colonies formed in MCF10A K8 knockdown clones (MShC1, C2 and C3) as compared to the vector control clone (MVc) (Figure 5.4.4A & B).

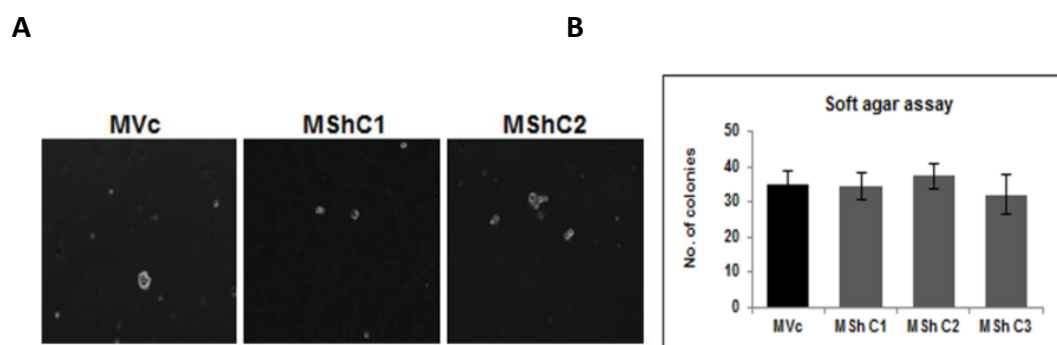


**Figure 5.4.4: Analysis of changes in soft agar colony forming potential on K8 down-regulation in MCF10A cells:** (A) Representative phase contrast images (10X) of colonies formed in soft agar in K8 down-regulated (MShC1, C2) and vector control (MVc) clones. (B) Histogram showing number of colonies of K8 down-regulated (MshC1, C2 and C3) and vector control (MVc) clones (right hand side). **Note:** No significant change in the number or volume of soft agar colonies in MCF10A K8 down-regulated clones.

#### 5.4.5 K8 down-regulation did not result in any change in

**proliferation:** To determine whether down-regulation of K8 results in change in proliferation in the cells, proliferation was analysed in the MCF10A K8 down-regulated (MShC1, C2 and C3) and vector control clones (MVc). The change in K8 levels did not result in any significant change in the proliferative potential of the cells (Figure 5.4.6).

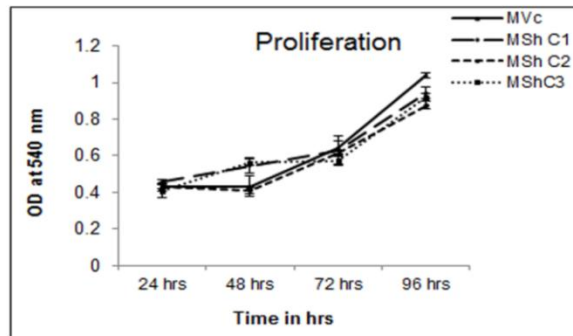


**Figure 5.4.5: Analysis of change in proliferation in K8 down-regulated MCF10A clones:** Cell proliferation curves of K8 down-regulated (MShC1, C2 and C3) and vector control (Vc) clones. Cell proliferation was plotted against time. Results are mean  $\pm$  SE of three independent experiments performed in triplicate. **Note:** No significant decrease in proliferation in K8 down-regulated clones of MCF10A as compared to vector control.

**5.4.6. K8 down-regulation did not result in any change in the motility of the cells:** To determine whether K8 down-regulation can result in change in motility in the non-transformed MCF10A cell line. It was analysed in K8 down regulated clones (MShC1, C2 and C3) and vector control clone (MVc). The change in K8 levels did not result in any change in motility as assessed by transwell (Figure 5.4.6A &B) and scratch wound assays (Figure 5.4.6 C &D).

**5.4.6.1. Analysis of change in motility by Scratch wound assay:** The scratch wound assay did not show change in motility on K8 down-regulation in MCF10A cell line.

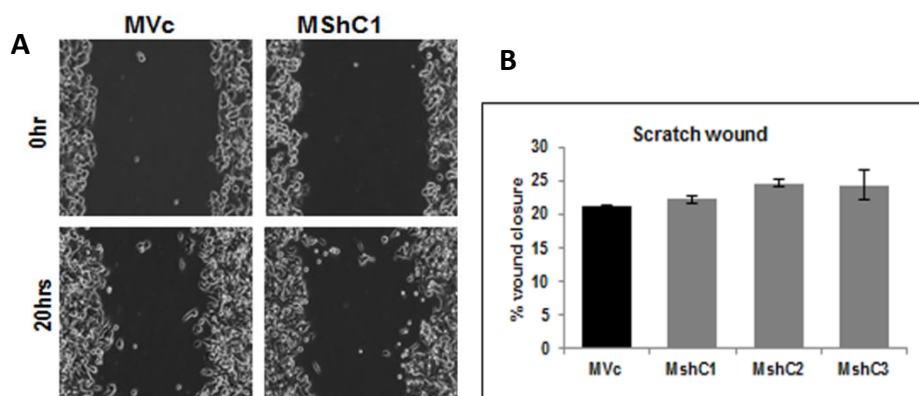


**Figure 5.4.6.1.: Analysis of change in motility on K8 down-regulation in MCF10A clones by wound healing assay:** (A) Representative Phase contrast images (10X) of time

lapse microscopy at 0 hour and 20 hours showing wound healing in K8 down-regulated (MShC1) and vector control (MVc) clones. **(B)** Histogram showing % wound closure at the end of 20 hours of K8 down-regulated (MShC1, C2 and C3) and vector control (MVc) clones. Results are mean of  $\pm$  SE of three independent experiments performed. Migration rate was calculated by AxioVision software.

**5.4.6.2. Analysis of change in motility by transwell assay:** The transwell assay did not show change in motility on K8 down-regulation in MCF10A cell line

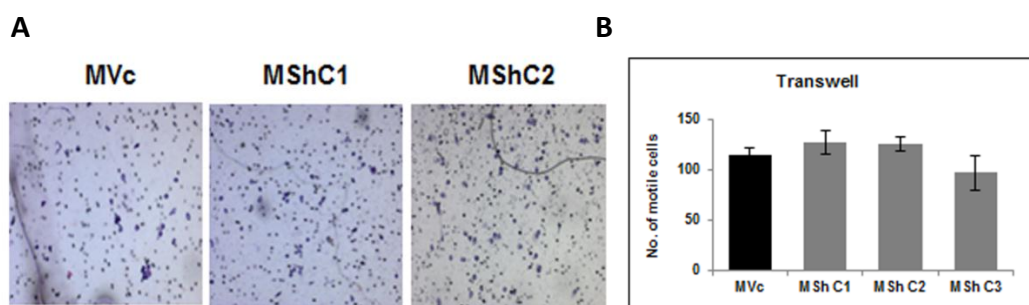


**Figure 5.4.6.2: Analysis of change in motility on K8 down-regulation in MCF10A clones by transwell assay:** (A) Representative images (10X) of H & E stained migrated cells in K8 down-regulated (MShC1, C2) and vector control (MVc) clone. **(B)** Histogram showing number of migrated cells of K8 down-regulated (MShC1, C2 and C3) and vector control (MVc) clones. Results are mean of  $\pm$  SE of three independent experiments performed. **Note:** No change in motility of K8 down-regulated MCF10A clones as compared to vector control.

#### 5.4.7. K8 down-regulation did not result in change in *in-vitro*

**invasion:** *In-vitro* matrigel invasion assays were performed to determine any change in the invasiveness of MCF10A clones on K8 down-regulation. There was no change in invasive potential in MCF10A derived K8 knockdown clones (MShC1, C2 and C3) as compared to vector control clone (MVc) (Figure 5.4.7A & B).

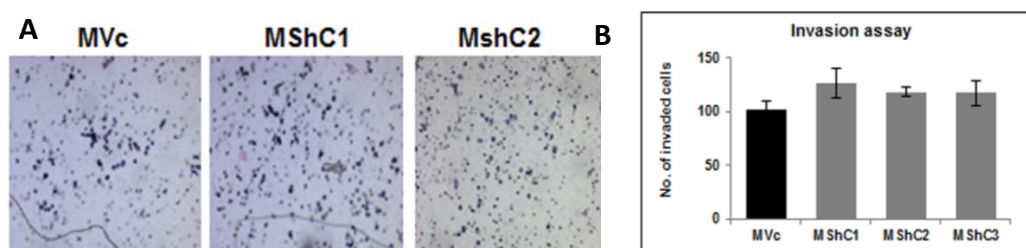


**Figure 5.4.7: Analysis of change in *in-vitro* invasion on K8 down-regulation in MCF10A clones:** (A) Representative images (10X) of H&E stained membrane showing invaded cells in K8 down-regulated (MShC1, C2) and vector control (MVc) clones. **(B)** Histogram showing

number of invaded cells of K8 down-regulated (MShC1, C2 and C3) and vector control (MVc) clones. Results are mean of  $\pm$  SE of three independent experiments performed. **Note:** No change in *in-vitro* invasion in MCF10A K8 down-regulated clones as compared to vector control.

**5.4.8. No change in tumor formation on K8 down-regulation:** NOD-SCID mice injected with MCF10A K8 down-regulated (MShC1, C2 and C3) and vector control (MVc) clones did not form any tumors, confirming no change in the transformation potential of these cells (Figure 5.4.8).



**Figure 5.4.8.: Analysis of change in tumorigenicity in K8 down- regulated MCF10A clones:** Representative images of NOD-SCID mice injected with K8 down-regulated (MShC1) and vector control (MVc) clones, 7 weeks after the injection in mammary fat pad. **Note:** No tumor formation in K8 down-regulated MCF10A and vector control clones.

#### **5.4.9. Analysis of E-cadherin expression on K8 down-regulation:**

To assess if down-regulation of K8 in MCF10A cells resulted in change in localization or levels of E-cadherin the K8 down-regulated clones (MShC1, C2 and C3) as compared to the vector control clone (MVc) were analysed for the E-cadherin expression and localization. The Western blot and immunofluorescence analysis showed no change in levels or localization of E-cadherin (Figure 5.4.9A&B).

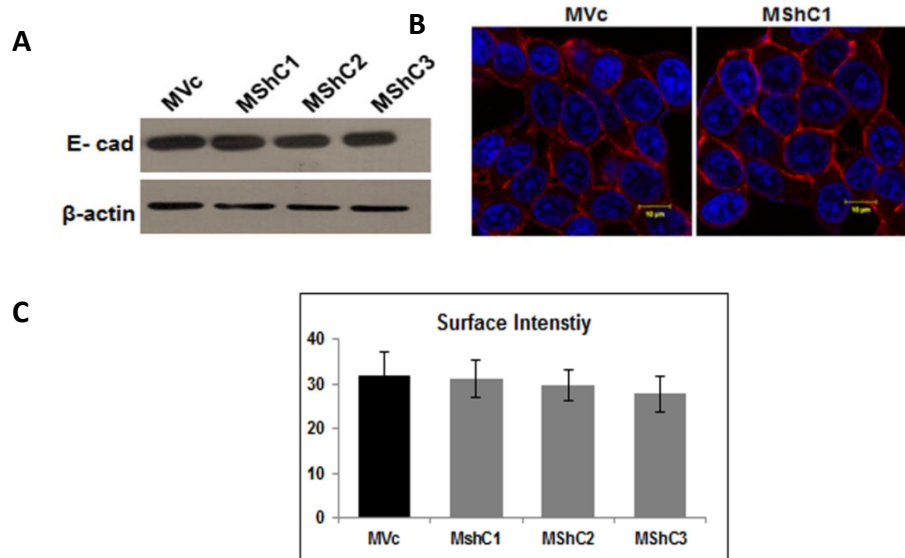


**Figure 5.4.9: Analysis of E-cadherin expression on K8 down-regulation in MCF10A clones:** (A) Western blot analysis of E-cadherin: K8 down-regulated (MshC1, C2 and C3) and vector control (MVc) clones.  $\beta$ -actin was used as loading control. (B) Representative confocal images of E-cadherin in K8 down-regulated (MshC1) and vector control (MVc) clones. **Scale bar:** 10  $\mu$ m. Nuclei (blue) are stained with DAPI. (C) Histogram showing mean fluorescent intensity of surface staining of E-cadherin in K8 down-regulated (MShC1, C2 and C3) clones as compared to vector control clone (MVc). **Note:** No change in E-cadherin localization or levels on K8 down-regulation.

*Thus in summary K8 down-regulation in MCF10A did not result in any phenotypic alterations.*

**SUMMARY:** The results of this study have demonstrated that K8 over-expression in invasive cell line led to decrease in motility and invasion while K8 down-regulation in less invasive transformed cell line led to a more transformed motile and invasive phenotype, with no effect on the non-transformed cell line.

## **5.5. Expression of K8, K18 and vimentin proteins in human breast tumors:**

**IHC analysis:** In order to confirm our in vitro data, a retrospective preliminary study using primary tumors (invasive ductal carcinoma) from patients showing recurrence and patients showing no recurrence was undertaken. The levels of K8, K18 and vimentin were analyzed in these tumors using semi quantitative IHC analysis. The tumor samples were categorized based on percentage positive cells and staining intensity.

A total of 51 non-recurrent and 43 recurrent tumors were analysed for K8, K18 and vimentin expression. Amongst the non-recurrent tumors 19.6% and 5.88% of tumors were negative for K8 and K18 respectively, while the recurrent tumors showed 25.58% and 20.93% negative staining for K8 and K18 respectively. The % of tumors showing 40-100% cells with moderate to high K8 and K18 staining intensity was 66.66 and 82.35 respectively in non-recurrent tumors and 51.16 and 67.44 in the recurrent tumors. The % of tumors negative for both K8 and K18 were 11.76 in non-recurrent tumors and 23.25 in the recurrent tumors. As against this, the % of tumors showing 40-100% cells with moderate to high staining for both K8 and K18 was 68.62 in non-recurrent tumors and 48.83 in the recurrent tumors. We also determined vimentin levels in the non-recurrent and recurrent tumors. Tumors of patients showing no recurrence showed 78.43% negative staining for vimentin while it was 55.81% for the recurrent tumors. The % of tumors showing 40-100% cells with moderate to high vimentin staining was 17.64 and 23.25 in the non-recurrent and recurrent tumors respectively.

**Table 5.1:** IHC on tumor sections obtained from primary tumors of patients showing no recurrence and patients showing recurrence using mAbs against K8, K18 and vimentin.

Sr. No.	Protein	Non-recurrent tumors (n=43) (%)	Recurrent tumors (n=51) (%)
1	K8 (Negative)	19.6	25.58
2	K18 (Negative)	5.88	20.93
3	K8/18 (Negative)	11.76	23.25
4	K8 (40-100% positive)	66.66	51.16
5	K18 (40-100% positive)	82.35	67.44
6	K8/18 (40-100% positive)	68.62	48.83
7	Vimentin (Negative)	78.43	55.81
8	Vimentin(40-100% positive)	17.64	23.25

The IHC data indicates that percentage of tumors showing higher expression of K8, K18 or K8/18 was more in the non-recurrent tumors, while the percentage of tumors in which K8, K18 or K8/18 were not detected was more in recurrent tumors than the non-recurrent tumors. We did not find any correlation between vimentin non-expression or expression with recurrence or non-recurrence of the tumors. We were not able to statistically analyse our data because of the small sample size.

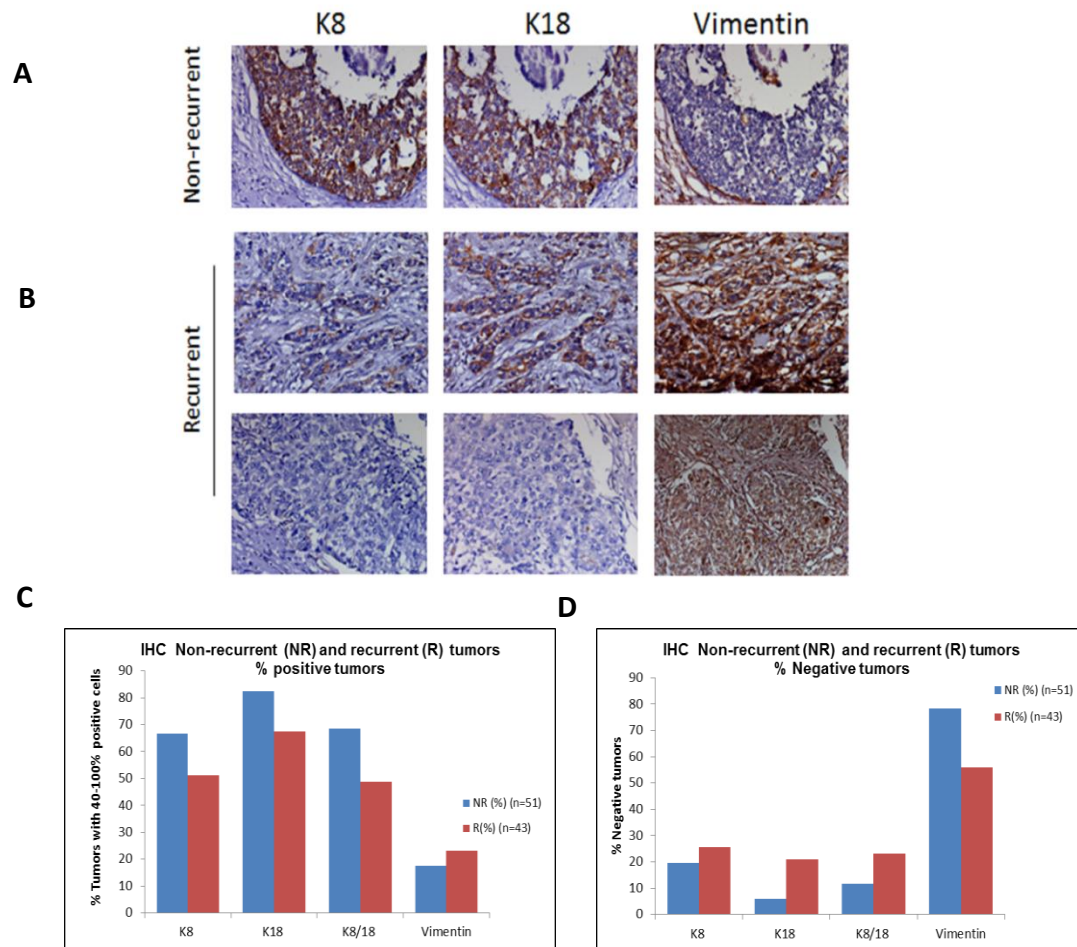


**Figure 5.5: Immunohistochemical analysis of K8, 18 and vimentin in primary tumors obtained from non-recurrent and recurrent patients:**(A) Representative IHC images (20X) of breast tumor sections from patients showing no-recurrence using mAb against K8, K18 and Vimentin respectively (B) Representative IHC images (20X) of breast tumor sections from patients showing recurrence using mAb against K8, K18 and Vimentin respectively (C) Histogram of percentage tumors showing strong (40-100% cells) presence of K8, K18, K8/18 and vimentin proteins respectively and (D) Histogram of percentage of tumors showing absence K8, K18, K8/18 and vimentin proteins respectively.



**5.6. To understand the molecular changes associated with K8 up-/Down-regulation, Microarray analysis was carried out.**

**5.6.1 Microarray analysis:** To understand the mechanism underlying the effect of K8 expression on growth and malignant behaviour, genome wide expression profiles of the K8 modulated and the vector control transfected clones of the two breast cancer cell lines (MDA MB 435 and MDA MB 468) were analyzed. MCF10A clones were not analyzed because they did not show any significant phenotypic changes on K8 down-regulation. The differentially expressed genes on K8 up-/down-regulation were selected based on the fold change and Gi processed signal values (Table 5.3). The genes associated with change in transformation, motility and invasive phenotype were selected. The genes showing up-regulation on K8 over-expression in MDA MB 435 (K8 C1 and C2) clones were TUBB6, RASSF4, THBS2 while the genes that showed down-regulation were CSPG4, PRKACB and LEF1. The analysis of differentially expressed genes on K8 down-regulation in MDA MB 468 clones (ShC1, C2 and C3) demonstrated up-regulation of FABP6, CAPG, BMP7, MMP11 and Wnt11 and down-regulation of FGFR1 and PTPRM as compared to vector control clone (Vc).

**Table 5.3: Microarray analysis: Differential genes**

Sr. No.	Gene Symbol	Description	Fold change		Gi Processed Signal		
			K8C1	K8C2	K8Vc	K8C1	K8C2
1	<i>ASRGL1</i>	Asparaginase like 1	4.62	1.98	400.2	8686.8	1475.2
2	<i>TUBB6</i>	tubulin, beta 6 class V	4.50	4.85	304.4	6111.1	7396.4
3	<i>POMT1</i>	Protein-O-mannosyltransferase 1	2.99	3.52	162.2	1140.4	1971.6
4	<i>PRDM7</i>	PR domain containing 7	2.76	1.41	230.4	1381.3	518.0
5	<i>THBS2</i>	Thrombospondin 2	2.68	2.51	526.7	2982.6	2453.9
6	<i>AR</i>	Androgen receptor	2.23	1.96	116.1	481.2	382.2
7	<i>ADSSL1</i>	Adenylosuccinate synthase like 1	2.19	1.18	424.4	1716.8	1024.5
8	<i>IGFBP7</i>	Insulin-like growth factor binding protein 7	2.12	1.40	2861.4	10988.3	4720.2
9	<i>TYRP1</i>	Tyrosinase-related protein 1	1.90	1.83	113.1	374.5	463.1
10	<i>QPRT</i>	Quinolate phosphoribosyltransferase	1.83	2.80	1622.3	5122.8	13520.3
11	<i>PDE4B</i>	Phosphodiesterase 4B, cAMP-specific	1.79	1.77	888.5	2714.6	2430.3
12	<i>CBS</i>	Cystathionine-beta-synthase	1.59	1.42	122.4	327.1	363.4
13	<i>SPHK1</i>	Sphingosine kinase 1	1.52	1.01	3998.2	10142.0	9860.1
14	<i>FAM83H</i>	Family with sequence similarity 83, member H	1.50	1.96	114.5	285.7	548.4
15	<i>PRKAR2B</i>	Protein kinase, cAMP-dependent, regulatory,	2.13	2.00	187.1	723.5	686.6

Table 5.3...continued

		type II, beta					
16	<i>RASSF4</i>	Ras association (RalGDS/AF-6) domain family 4	1.02	0.91	285.2	510.7	406.0
17	<i>CSPG4</i>	Chondroitin sulfate proteoglycan 4	-0.73	-0.79	5294.7	2821.5	3492.5
18	<i>LEF1</i>	Lymphoid enhancer- binding factor 1	-1.42	-1.05	14187.4	7731.0	10250. 5
19	<i>PRKAC</i> <i>B</i>	Protein kinase, cAMP- dependent, catalytic, beta	-1.00	-0.99	460.0	175.8	418.3
20	<i>AK5</i>	Adenylate kinase 5	-4.28	-5.58	2584.7	118.0	51.6
21	<i>MGP</i>	Matrix Gla protein	-3.15	-6.50	7050.5	702.5	94.8
22	<i>LDB3</i>	LIM domain binding 3	-2.60	-2.58	2669.5	389.3	346.2
23	<i>TRAPP</i> <i>C6A</i>	Trafficking protein particle complex 6A	-1.85	-2.55	1984.9	486.7	356.7
24	<i>PLA2G4</i> <i>A</i>	Phospholipase A2, group IVA (cytosolic, calcium-dependent)	-1.34	-1.17	604.7	211.3	222.4
25	<i>DTX3</i>	Deltex 3 homolog (Drosophila)	-5.41	-2.67	5139.5	106.7	832.8
26	<i>TMEM1</i> <i>36</i>	Transmembrane protein 136	-3.12	-0.81	3128.9	318.2	1502.6
27	<i>CEACA</i> <i>M1</i>	Carcinoembryonic antigen-related cell adhesion molecule 1 (biliary glycoprotein)	-2.89	-2.46	965.7	115.5	139.2
28	<i>MAT1A</i>	Methionine adenosyltransferase I, alpha	-2.73	-1.76	12141.0	1621.9	2777.2

Table 5.3...continued

29	<i>TMEM173</i>	Transmembrane protein 173	-2.70	-2.83	1672.5	227.8	222.1
30	<i>RENBP</i>	Renin binding protein	-2.63	-1.27	1381.3	197.5	481.5
31	<i>CITED2</i>	Cbp/p300-interacting transactivator, with Glu/Asp-rich carboxy-terminal domain 2	-2.44	-0.85	2283.8	371.4	856.4
32	<i>EVI2A</i>	Ecotropic viral integration site 2A	-2.26	-1.18	806.5	149.4	406.2
33	<i>USP36</i>	Ubiquitin specific peptidase 36	-2.17	-1.14	990.7	195.6	425.2
34	<i>SLC12A7</i>	solute carrier family 12 (potassium/chloride transporters) member 7	-1.79	-1.97	985.1	252.7	256.6
35	<i>CHCHD6</i>	coiled-coil-helix-coiled-coil-helix domain containing 6	-1.58	-1.79	42922.9	12753.1	12966.2
36	<i>DNAH2</i>	dynein, axonemal, heavy chain 2	-1.56	-1.26	1324.0	397.1	532.5
<b>MDA MB 468</b>							
Sr. No.	Gene Symbol	Description	Fold change		GiProcessed signal		
			ShC 1	ShC 2	Vc	ShC1	ShC2
1	<i>LGI2</i>	Leucine-rich repeat LGI family, member 2	3.22	1.17	113.2	924.7	191.4
2	<i>AB014766</i>	mRNA for DERP12 (dermal papilla derived protein 12)	1.10	1.27	170.1	300.7	352.1
3	<i>ASB13</i>	Ankyrin repeat and	1.71	2.01	742.4	1995.1	2551.6

Table 5.3...continued

		SOCS box-containing 13					
4	<i>MMP11</i>	Matrix metallopeptidase 11 (stromelysin 3)	2.33	1.47	53.91	238.45	112.41
5	<i>FMO3</i>	Flavin containing monooxygenase 3	1.56	4.43	53.9	139.6	872.4
6	<i>CAPN12</i>	Calpain 12 (CAPN12)	1.61	1.78	27.7	69.8	81.7
7	<i>MGP</i>	Matrix Gla protein	1.63	0.66	80897.3 3	188241. 4	81387. 2
8	<i>CAPG</i>	Capping protein (actin filament), gelsolin-like	1.52	1.01	22359.4	49944.2	38566. 4
9	<i>WNT11</i>	Wingless-type MMTV integration site family, member 11	1.76	1.33	28.30	84.39	53.32
10	<i>LAT</i>	Linker for activation of T cells	-1.38	-0.72	448.1	142.2	232.2
11	<i>SNRA61</i>	Small nucleolar RNA, H/ACA box 61	-1.31	-1.29	997.7	323.3	499.1
12	<i>LIF</i>	leukemia inhibitory factor differentiation factor)	-1.12	-3.73	28853.9	10907.5	1858.1
13	<i>GPC2</i>	Glypican 2	-1.03	-1.13	1719.1	696.2	670.4
14	<i>TPM2</i>	Tropomyosin 2 (beta)	-1.61	-4.67	1934.7	558.2	56.9
15	<i>GOLGA8</i> A	golgin A8 family, member A	-3.21	-4.02	237.8	22.5	11.0
16	<i>FRMD4A</i>	FERM domain containing 4A	-0.94	-1.90	1675.9	717.5	384.9
17	<i>DGCR8</i>	DiGeorge syndrome critical region gene 8	-1.86	-0.91	1292.6	293.1	589.8

Table 5.3...continued

18	<i>FKBP11</i>	FK506 binding protein 11, 19 kDa	-1.38	-0.64	1040.9	329.5	572.3
19	<i>CCDC18</i>	Coiled-coil domain containing 18	-0.98	-2.65	1236.4	517.6	168.1
20	<i>SLC7A5</i>	Solute carrier family 7 (amino acid transporter light chain, L system), member 5	-1.02	-0.78	603.7	245.4	301.4
21	<i>NAT11</i>	N(alpha)- acetyltransferase 40, NatD catalytic subunit, homolog ( <i>S. cerevisiae</i> )	-0.89	-1.04	411.2	183.2	170.7
22	<i>CCNL1</i>	Cyclin L1	-0.82	-1.08	5684.9	2649.1	2309.5
23	<i>KIAA164</i> <i>1</i>	ankyrin repeat domain 36B	-0.68	-1.64	677.9	349.0	186.2
24	<i>ING3</i>	Inhibitor of growth family, member 3	-0.65	-2.77	972.9	512.3	121.8

### 5.6.2. Validation of differentially expressed genes using Real time

**PCR:** The real time PCR data demonstrated significantly increased expression of THBS2 (Figure 5.2.6 A) and TUBB6 (Figure 5.2.6 B) in K8 over-expressed MDA MB 435 clones (K8 C1 and C2) as compared to vector control clone (Vc). LEF-1 transcription factor was found to be significantly down-regulated in K8 over-expressed clones (Figure 5.2.6 C). CAPG, an actin binding protein was significantly up-regulated in K8 down-regulated MDA MB 468 clones (ShC1, C2 and C3) as compared to vector control clone (Vc) (Figure 5.2.6 D). Results of the real time PCR analysis for FGRL1 showed marginal increase in K8 over-expressed MDA MB 435 clones (non-significant) (Figure 5.2.6 E), while the K8 down-regulated MDA MB 468 clones did not show

consistent up-/down-regulation amongst the clones. MMP11 levels did not show consistent pattern in both MDAMB 435 and MDA MB 468 clones (Figure 5.2.6 F).

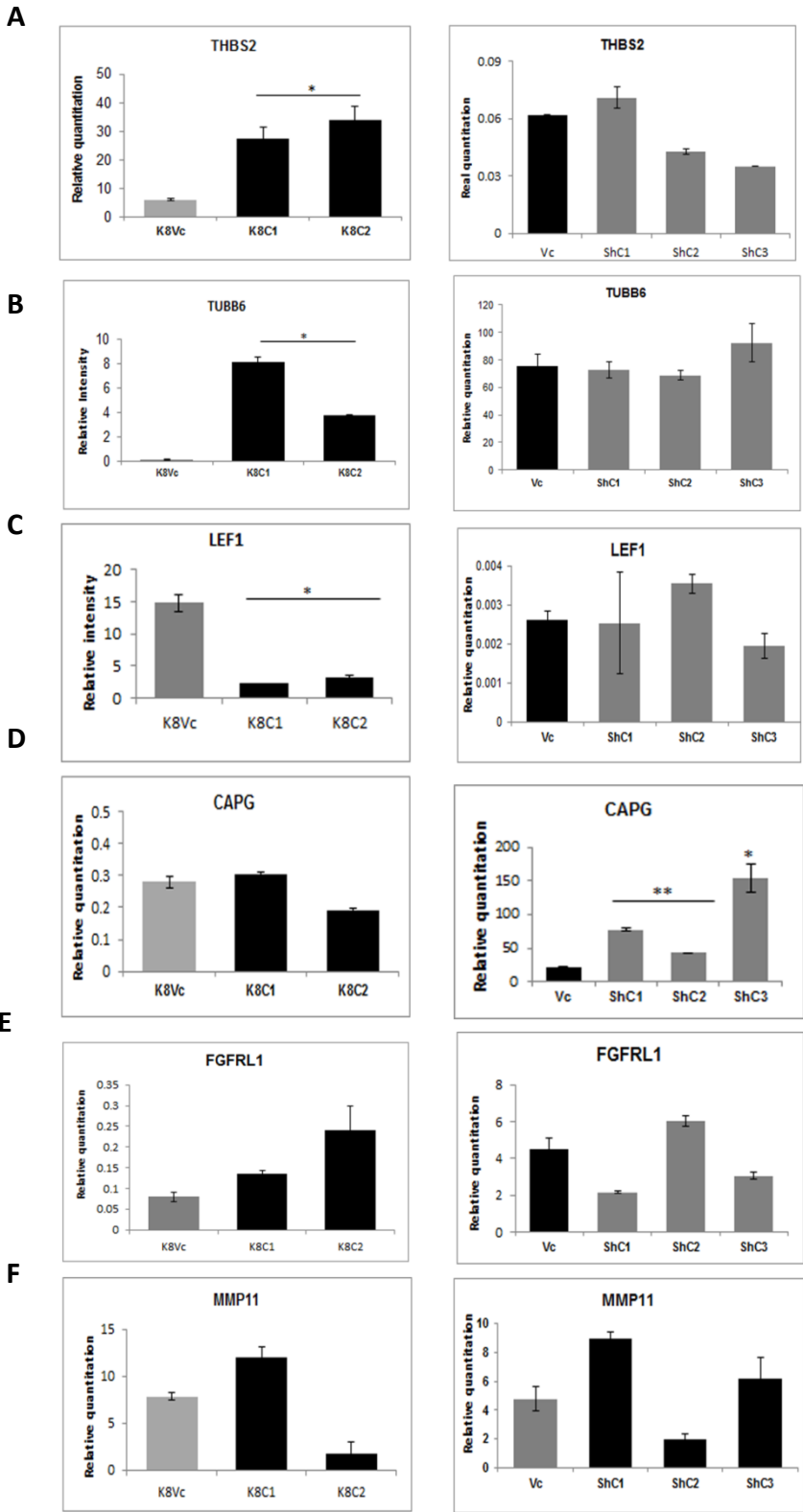


**Figure 5.6.2: Real time PCR analysis of K8 over-expressed MDA MB 435 and K8 down-regulated MDA MB 468 clones: Histogram showing changes in**

mRNA levels of MDA MB 435 and MDA MB 468 clones respectively in (A) THBS2 (B) TUBB6 (C) LEF1 (D) CAPG (E) FGFR1 and (F) MMP11 (\*p<0.05, \*\*p<0.01) **Note:** No commonalties in clones of MDAMB 435 and MDA MB 468.

### 5.6.3. Up-regulation of CAPG protein in K8 down-regulated MDA

**MB 468 clones:** Increased motility and lamellipodia formation was accompanied with change in CAPG, an actin binding protein. Microarray and further Real time RT PCR analysis showed that CAPG was significantly up-regulated in the K8 down-regulated clones (ShC1, C2 and C3) as compared to vector control clone (Vc). To understand whether this was reflected at the protein level, the levels of CAPG protein were analysed in MDA MB 468 and vector control clones. Western blot analysis showed up-regulation of CAPG in the K8 down-regulated clones (Figure 5.6.3).

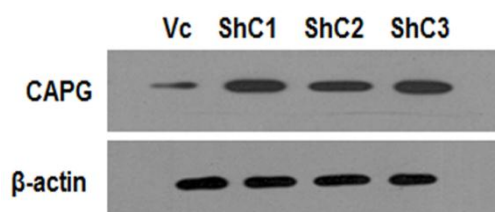


**Figure 5.6.3: Up-regulation of CAPG protein on K8 down-regulation in MDA MB 468:** Western blot analysis of CAPG in the K8 down-regulated clones of (ShC1, C2 and C3) as compared to vector control clone (Vc). **Note:** Up-regulation of CAPG in K8 down-regulated clones.

*Thus changes at molecular level corroborated with the change in transformed phenotype observed in MDA MB 435 and MDA MB 468 cells on K8 modulation. However a deeper analysis at the protein level will answer how these changes are brought about and highlight the potential of these molecules in breast cancer progression.*



# *Discussion*

## 6) Discussion:

---

Keratins are widely used as diagnostic markers. Their expression is known to change during or after malignant transformation [23,132] and therefore keratins have been proposed to be used in prognostication of different malignancies [27,64]. The available literature suggests that change in the expression of keratins during malignant transformation is an active event which may be governed by regulation/modulation of signalling pathways in response to alterations in keratin expression [11,29,81].

Previous reports from both our laboratory and others have shown that an increase in K8/K18 expression in squamous cell carcinomas as well as adenocarcinomas is associated with the metastatic phenotype [29,30,104]. In breast tissues, K8/18 pair is normally expressed in the luminal cells (cells that constitute the differentiation compartment) [3,20,42,133]. Whether changes in the keratin pair of K8/18 have any role to play in breast tumor progression is unclear and the literature available is not conclusive. Previous studies on breast tumor tissues have led to varying conclusions where its presence was either positively or negatively associated with progression of breast cancer and poor clinical outcome [30,34,35,37,48,103]. In an *in-vitro* study related to role of K8/18 in malignant transformation/progression of breast epithelia, Buhler *et. al.* have shown that re-expression of K18 caused partial re-differentiation of the tumor cells and regression of malignant phenotype in a highly invasive breast cancer derived cell line MDA MB 231 [20]. In a recent report, Mackinder *et. al.* have reported that the less invasive cell lines showed the presence of K8, 18, K19 and absence of vimentin while the highly invasive cell lines expressed lower levels of K8, 18 and no K19 and higher levels of vimentin. They have further shown that the

inhibition of tumor growth by Tissue Factor (TF) shRNA resulted in re-expression of K8 in the xenograft obtained by injecting the invasive MDA MB 436 cells [134], underscoring the importance of K8 in tumor prevention.

In the present study we have systematically attempted to understand the role of K8/18 in malignant transformation/ progression of breast epithelia. We have used three cell lines with different invasive and transformation potentials and modulated K8 expression to understand the exact role of K8/18 in breast cancer progression.

Initially we assessed changes in differentiation status of three cell lines in response to modulation of K8 expression using lipid droplet staining. Our results show that modulation of K8 expression did not alter lipid droplet levels (Figure 5.2.4, 5.3.3 & 5.4.3) thus indicating that K8 did not induce re-differentiation as observed by Buhler *et. al.* on transfecting K18 in MDA MB 231 cells. Buhler *et. al.* have not analysed the levels of lipid droplets but have used changes in expression of cell adhesion molecules like E-cadherin as marker of cell differentiation (Figure 5.2.12, 5.3.10 & 5.4.9) [20]. We have not observed changes in E-cadherin levels in response to modulation of K8 expression. Thus it is possible that changes in cell differentiation observed by Buhler *et. al.* could be cell line specific effect.

We then analysed changes in cell proliferation/ transformation in response to modulation of K8 expression in all the three cell lines. The decrease in proliferation, motility, tumor size, invasion *in-vitro* and less or no metastasis in lungs of the animals injected with K8 over-expressed MDA MB 435 clones (Figure 5.2.6-5.2.10) suggest that the presence of K8 may inhibit metastatic progression in an invasive cell line. In another set of experiments inhibition of K8 in a transformed less invasive cell line (MDA MB 468) resulted in cell growth at high density, increase in soft agar

colony number and volume, increased motility and invasion in-vitro. Previously, increase in motility has also been reported in pancreatic and gastric cancer cells in response to depletion of K8 or K18 [135,136].

Next, it was important to study changes in expression of other keratins and vimentin in response to K8 modulation, so as to understand the mechanism underlying the observed phenotypic changes. Alterations in cell transformation potential, motility, invasion etc. have been reported in response to changes in keratin expression [20,29,104,136,137]. We observed up-regulation in K18 expression in response to K8 over-expression in MDA MB 435 cells (Figure 5.2.1.1). These results are in agreement with those obtained by Buhler et.al where over-expression of K18 resulted in up-regulation of its binding partner K8 [20]. This may be the result of stabilization of K18 protein, as we did not observe any significant change in K18 mRNA levels on K8 over-expression (Figure 5.2.1.2C). It is possible that the K8/18 filaments formed after K8 over-expression may have led to increased rigidity and hence become less invasive [20]. A transient over-expression of K18 (type I) in MDA MB 435 cells (having no K8 expression) did not induce K8 (type II) (Figure 5.2.2) expression as previously reported [20]. Instead, K18 protein formed non-filamentous aggregates. Similar observations were reported by Giudice *et. al.* in fibroblast [138]. Here, transfection of K6 (type II keratin) triggered endogenous K14 (type I keratin) expression which formed filaments, whereas expression of K14 did not induce K6 expression. Together, these observations suggest that type I keratin expression may be dependent on accumulation of un-polymerized type II keratins. This observation also highlights the fact that expression of keratin pair in 1:1 stoichiometric ratio is essential for proper filament formation.

The down-regulation of K8 in MDA MB 468 did not show concomitant decrease in K18 expression and K18 filaments were still observed (Figure 5.3.1). The filament formation of K18 indicated possible compensatory pairing of K18 with some other type II keratin like K7 [80,139]. This possibility was explored by analysing the total keratin profile of the cells, which showed presence of K7, K18 and K19 in MDA MB 468 clones (Appendix Table 5.3.2). Keratin pair of K5/14 is often associated with poor prognosis in breast cancer [140], although K5 or K14 were not detected in MDA MB 468 clones even after K8 down-regulation. Western blot analysis showed up-regulation of K7 in the K8 down-regulated clones (Figure 5.3.2.1 B). Keratin 7 is one of the type II keratins that is expressed in breast epithelium but the expression is generally low and variable. It has been shown previously that K7 replaces K8 in its absence [80,139]. It is possible that K18 is forming filaments with K7 in the absence of K8, although these filaments may not have the same function as that of K8/18 filaments. The invasion data suggest that loss of K8 in these cells was sufficient to increase invasion (Figure 5.3.8). No change in K18 filament formation suggests that in addition to the rigidity imparted by keratin filaments other functions of K8 might be important in preventing neoplastic transformation in breast tissue.

We did not detect K7 in MDA MB 435 and MCF10A clones and we observe the concomitant up-/down-regulation of K18 in response to K8 up-/down-regulation (Figure 5.2.3.1 & 5.4.2.1), indicating that there was no compensation by K7 in these cells. In summary, these findings together underline the importance of K8/18 filaments in maintaining the non-transformed phenotype in breast cancer derived cell lines and also suggests that keratin 8 is required for the maintenance of epithelial integrity during migration.

Previous reports have shown the role of vimentin in breast cancer progression [2,20,31,33,35,37]. Although vimentin is widely studied in breast cancer, present study shows that change in motility or invasion were independent of vimentin expression (Figure 5.2.3B, 5.3.2 C-D & 5.4.2B,C) Results from our previous work on human oral tumor derived cell line have also indicated that the changes seen on modulation of K8 were independent of changes in vimentin expression, whose levels remained unchanged [29]. This indicates that K8/18 and vimentin may regulate invasion and motility via independent pathways in different cell types.

Another interesting finding of our study was change in localization of E-cadherin in K8 down-regulated clones of MDA MB 468 (Figure 5.3.10). Invasion being a multistep process and requires co-ordinated loss of cell adhesion molecules which would assist in loosening the cellular architecture and hence imparting invasiveness to the cells by helping the cells detach more easily [141]. We show here that the down-regulation of K8 in MDA MB 468 cells led to change in localization of E-cadherin from membrane to cytoplasm, without any change in protein levels. The direct link between keratins and E-cadherin is not known. Keratins form the cellular meshwork via anchoring to the desmosomal plaque. Plakoglobin (PG) is one of the desmosomal complex proteins which also forms part of adherens junction [142]. Recruitment of Plakophilin 3 by E-cadherin and PG is essential for desmosome formation [143]. Thus loss of keratin 8 in these cells may have resulted in the loss of membranous E-cadherin due to indirect effect of altered interaction of keratins with desmosomal proteins. E-cadherin being a cell adhesion molecule, its loss at the membrane might promote tumor cell dissemination. The increase in motility and invasion in these cells could be result of K8 loss leading to the loss of membranous E-cadherin. This could also indicate that in addition to loss of K8 further loss of E-

cadherin is required for acquisition of more motile phenotype in MDA MB 468 cells. The clinical significance of the cytoplasmic expression of E-cadherin has been shown in gastric cancer where it correlated with poor prognosis [40]. Thus, the cytoplasmic localization of E-cadherin in K8 down-regulated MDA MB 468 cells may be the downstream effect of the series of alterations that may influence invasion.

On the other hand, MDA MB 435 cells did not express E-cadherin and K8 over-expression in these cells did not induce its expression (Figure 5.2.12). The decreased invasion in the MDA MB 435 derived K8 over-expressing clones seems to be independent of E-cadherin expression. This observation also highlights the fact that K8 might modulate invasion by diverse pathways in different breast cancer derived cell lines. Taken together these results indicate that modulation of K8 expression and its effect on K8/18 filament formation does not induce or repress the levels of E-cadherin but results in re-localization of this protein. Re-localization could be the result of altered interaction of E-cadherin with other junctional complex proteins.

Previous work from our laboratory has shown that the keratin pair of K8/18 plays a role in promoting tumor progression in an oral SCC derived cell line. This change is brought about by  $\beta 4$  integrin mediated signalling and alterations in  $\beta 4$  integrin levels explain most of the phenotypes observed upon K8 knockdown, including decrease in invasion, migration and tumorigenicity [29]. There are no alterations in the levels of  $\beta 4$  integrin on K8 up-/down- regulation in the cell lines used in this study.  $\beta 4$  integrin was undetected in MDA MB 435 clones whereas no change in its expression was seen in K8 down-regulated clones of MDA MB 468 as compared to the vector control clone. The role of  $\alpha 6 \beta 4$  integrin in tumor progression is still obscure. Several reports have indicated that over-expression of this pair is seen in SCC of lung, skin, oral cavity and cervix. While its expression is down-regulated in adenocarcinomas of

breast and prostate [119]. The present study indicates that the changes in motility or invasion in these breast cancer derived cell lines may not be regulated by  $\beta 4$  integrin mediated pathway (Figure 5.2.13 & 5.3.11).

The role of other integrins in breast cancer has been reported in literature. Integrins  $\beta 1$  and  $\beta 3$  are the most common type of integrins that have been shown to mediate tumor progression in breast cancer [144]. K8/18 have been shown to mediate  $\beta 1$  integrin mediated cell adhesion in hepatomas [120]. Most of the previous studies show role of  $\alpha 3\beta 1$  integrin in promoting tumor progression and metastasis in breast cancer. While its over-expression in skin carcinoma is shown to decrease the rate of carcinoma formation [144]. In several malignancies up-regulation of  $\alpha \nu \beta 3$  integrin correlated with tumor progression e.g. in melanoma, glioma, ovarian cancer and breast cancer [118]. It will be interesting to see if the change in invasive property of the cell lines used in our study is brought about by any of these integrin pairs or by some other signalling pathways.

Although keratins show high tissue specificity in their expression, alterations in their expression profile have been reported in various malignancies. Previous reports from our laboratory and others have shown aberrant expression of K8/18 in precancerous lesions and SCC of oral mucosa [23,25,145]. We further showed that this keratin pair contributes in acquisition of transformed and metastatic phenotype of oral squamous epithelium derived cell line [104]. In breast epithelium K8/18 are normally expressed in the luminal/differentiation compartment and this study shows that loss of same keratin pair in breast cancer derived cell lines resulted in an invasive phenotype. Our results of K8 down-regulation in MCF10A suggest that K8 may not be involved in changing the motility or invasive potential of a non-transformed cell line (Figure 5.4.6-5.4.7). These findings suggest the possibility that the same keratin pair may



have dissimilar role in neoplastic progression of different epithelia. Hence it is tempting to speculate that K8 loss in breast cancer might be an important event in metastatic progression.

The exact mechanism by which these changes are brought about is still not understood. To understand the underlying mechanism, further detailed analysis of changes at the molecular and proteomic level in response to modulation of K8/18 level is required. As a first step in this direction microarray analysis was undertaken on the K8 over-expressed MDA MB 435 and MDA MB 468 K8 knock down clones in comparison to their respective vector controls to understand the molecular changes caused due to modulation of K8 in these cell lines.

Some of the important changes associated with the decrease in the transformation and invasive potential in MDA MB 435 cell line on over-expression of K8 were up-regulation in TUBB6 and THBS2 and down-regulation in LEF1. TUBB6 is known to be largely reduced in most tumors [146]. THBS2, an inhibitor of tumor growth and might be contributing to the decreased tumor formation and less or no metastasis seen in these cells (Figure 5.6.2A) [147,148] . We found down regulation of LEF1 in K8 overexpressed MDA MB 435 clones (Figure 5.6.2C). LEF1, transcription factor is the nuclear mediator of Wnt signaling pathway [149]. Since we did not find significant alterations in other mediators of Wnt signaling pathway it is not possible for us to comment whether Wnt signaling pathway is altered based on our microarray data. On down-regulation of K8 in MDA MB 468 cell line there was increase in transformation potential, motility and invasion. One of the major molecular changes observed in these clones, which correlated with the increased motility, lamellipodia formation (Figure 5.3.7) and invasion, seen in these cells was up regulation of CAPG (Figure 5.6.2 D). CAPG is actin-binding protein from Gelsolin family. It is expressed

at higher levels in breast cancer. Previous data have shown that this protein is responsible for increased motility and invasion in breast cancer [150].

We did not see commonalities in gene expression profiles in K8 up/down-regulated clones. It is possible that the changes observed are cell line specific and downstream effectors in case of K8 up/down-regulated clones may not be similar. The other possibility is that the alterations might have occurred at protein level and proteomic analysis may throw light on this aspect. In addition possible alterations like some PTMs which have already been reported in literature might have led to the change transformation potential of the cells [30,108,134]. Thus these molecular changes as result of K8 modulation need to be further substantiated with proteomic analysis.

To understand the clinical significance of K8/18 expression in breast cancer progression, it will be important to analyze primary breast tumors for expression of K8/18 and correlate the results with recurrence. Previously, aberrant over-expression of K8/18 has been shown to correlate with poor prognosis in SCC of oral cavity [27], while data from breast tumors is inconclusive. e.g. Chu *et. al.* have shown association of expression of K8/18 along with vimentin with increased drug resistance, invasion and metastasis in breast cell carcinomas and melanomas [34,103]. Contrary to this, Fuchs *et. al.* have shown association of loss of keratin 8 and expression of vimentin with early metastasis and a poor prognosis in breast cancer patients [38]. In another study they have shown that elevated Keratin 18 protein expression in patients of breast cancer correlated with favorable prognosis and indicated K18 to be an independent and significant predictor for overall survival (8 years) [35]. Our *in-vitro* data are in agreement with the results obtained by Schaller *et. al.* and others showing role of K8 in inhibition of metastatic progression. Thus to determine the relevance of K8/18 and vimentin expression in breast derived

tumors in Indian patients, we conducted a preliminary retrospective study. We analyzed 51 non-recurrent and 43 recurrent tumors for the expression of K8, 18 and vimentin and correlated them with recurrence or no-recurrence. The trends seen in our retrospective study correlated with our *in-vitro* data (Figure 5.5). The number of tumors showing strong presence of K8 and /or K18 proteins was more in the non-recurrent tumors while the number of tumors showing loss of K8 and/ or K18 protein was higher in the case of recurrent tumors. On the other hand no such correlation could be obtained for vimentin expression. This data needs to be expanded with larger sample size as we could not deduce statistical significance due to small sample size. It will be also important to correlate K8/18 expression with other clinical parameters. Such a study will prove useful in establishing prognostic value of K8/18 expression for human breast cancer.

## 6.1. K8/18 role in oral cancer and breast cancer

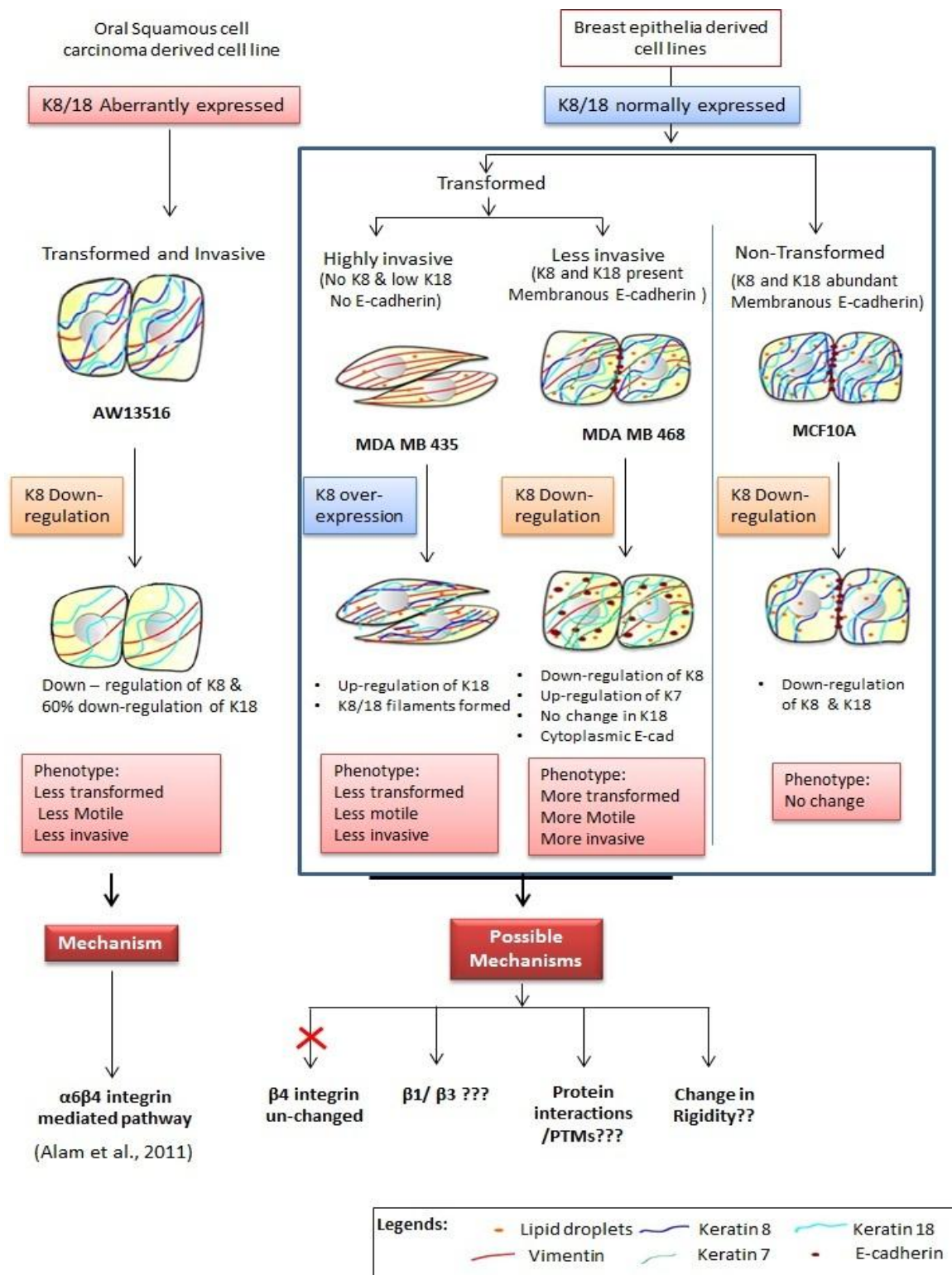


**Figure 6.1: Schematic representation of K8/18 role in oral cancer and breast cancer:** K8/18 aberrant expression in oral cancer derived cell line result in increase in transformation and invasion via  $\alpha 6 \beta 4$  integrin mediated pathway. K8/18 inhibits motility and invasion in breast cancer derived cell lines with no effect on non-transformed cell line.

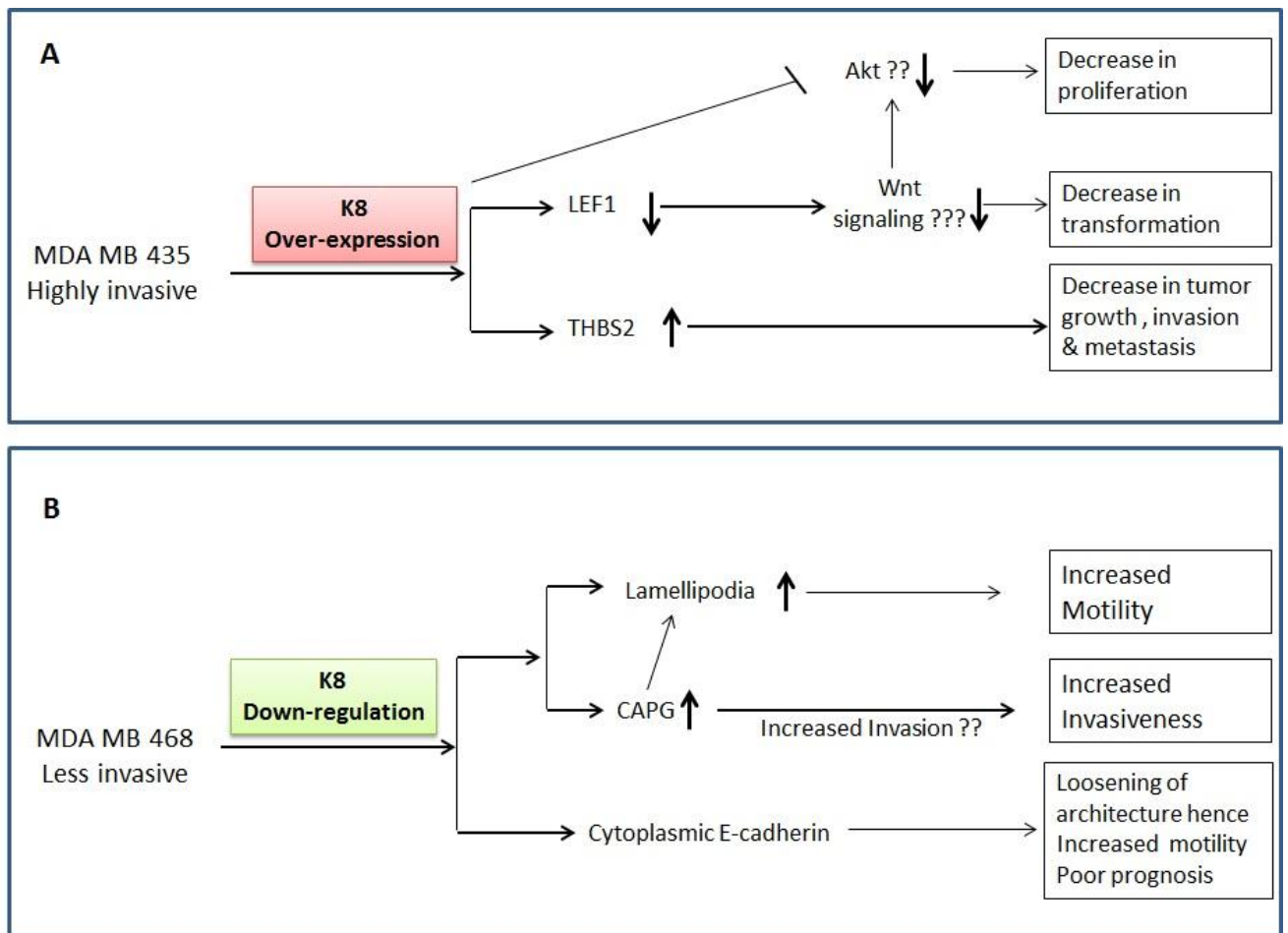


**Figure 6.2: Schematic representation:** Hypothetical mechanism for the role of K8/18 in (A) MDA MB 435 and (B) MDA MB 468 breast cancer derived cell lines.

# *Summary & Conclusion*

## 7) Summary & Conclusion:

---

Over-expression of K8 in MDA MB 435 resulted in a less invasive phenotype, while the knockdown of the K8 in MDA MB 468 led to an increase in neoplastic potential and increased invasion *in-vitro*. The down-regulation of K8 in MCF10A did not result in any phenotypic alterations. These results are indicative of the role of K8/18 in modulating motility and invasion in the breast cancer, the presence indicating less invasive phenotype while absence indicates highly invasive dedifferentiated phenotype. Our microarray data has given us some leads regarding molecular changes occurring as a result of K8 up/down-regulation. Further validation at protein level may help us understand the down-stream effectors and interacting proteins.

K8/18 aberrant over-expression has been shown to correlate with poor prognosis in SCC of oral cavity and loss of same keratin pair in breast cancer derived cell lines resulted in an invasive phenotype. These findings suggest the possibility that the same keratin pair may have dissimilar role in neoplastic progression of cancers derived from different epithelia. This information could prove useful in developing therapeutic targets for treatment of breast carcinomas in future. It will be also important to study K8/18 expression in larger cohort of breast cancer patients and correlate the same with their clinical parameters so as to understand its significance in prognostication of breast cancer.

# *References*



## 8) References:

---

1. Jemal A, Bray F, Center MM, Ferlay J, Ward E, et al. (2011) Global cancer statistics. *CA Cancer J Clin* 61: 69-90.
2. Taylor-Papadimitriou J, Stampfer M, Bartek J, Lewis A, Boshell M, et al. (1989) Keratin expression in human mammary epithelial cells cultured from normal and malignant tissue: relation to in vivo phenotypes and influence of medium. *J Cell Sci* 94 ( Pt 3): 403-413.
3. Moll R, Franke WW, Schiller DL, Geiger B, Krepler R (1982) The catalog of human cytokeratins: patterns of expression in normal epithelia, tumors and cultured cells. *Cell* 31: 11-24.
4. Moll R, Divo M, Langbein L (2008) The human keratins: biology and pathology. *Histochem Cell Biol* 129: 705-733.
5. Schweizer J, Bowden PE, Coulombe PA, Langbein L, Lane EB, et al. (2006) New consensus nomenclature for mammalian keratins. *J Cell Biol* 174: 169-174.
6. Fuchs E, Cleveland DW (1998) A structural scaffolding of intermediate filaments in health and disease. *Science* 279: 514-519.
7. Bornslaeger EA, Corcoran CM, Stappenbeck TS, Green KJ (1996) Breaking the connection: displacement of the desmosomal plaque protein desmoplakin from cell-cell interfaces disrupts anchorage of intermediate filament bundles and alters intercellular junction assembly. *J Cell Biol* 134: 985-1001.
8. Litjens SH, de Pereda JM, Sonnenberg A (2006) Current insights into the formation and breakdown of hemidesmosomes. *Trends Cell Biol* 16: 376-383.
9. Coulombe PA, Omary MB (2002) 'Hard' and 'soft' principles defining the structure, function and regulation of keratin intermediate filaments. *Curr Opin Cell Biol* 14: 110-122.
10. Oshima RG (2002) Apoptosis and keratin intermediate filaments. *Cell Death Differ* 9: 486-492.
11. Paramio JM, Jorcano JL (2002) Beyond structure: do intermediate filaments modulate cell signalling? *Bioessays* 24: 836-844.
12. Owens DW, Lane EB (2003) The quest for the function of simple epithelial keratins. *Bioessays* 25: 748-758.

13. Clausen H VP, Moe BD, Dablesteen E, Sun TT, Dale B (1986) Differentiation dependent expression of keratins in human oral epithelia. *J Invest Dermatol* 86: 249–254.
14. O'Guin WM, Galvin S, Schermer A, Sun TT (1987) Patterns of keratin expression define distinct pathways of epithelial development and differentiation. *Curr Top Dev Biol* 22: 97-125.
15. Galvin S, Loomis C, Manabe M, Dhouailly D, Sun TT (1989) The major pathways of keratinocyte differentiation as defined by keratin expression: an overview. *Adv Dermatol* 4: 277-299; discussion 300.
16. Moll R, Schiller DL, Franke WW (1990) Identification of protein IT of the intestinal cytoskeleton as a novel type I cytokeratin with unusual properties and expression patterns. *J Cell Biol* 111: 567-580.
17. Franke WW, Schiller DL, Moll R, Winter S, Schmid E, et al. (1981) Diversity of cytokeratins. Differentiation specific expression of cytokeratin polypeptides in epithelial cells and tissues. *J Mol Biol* 153: 933-959.
18. Ouhayoun JP, Gosselin F, Forest N, Winter S, Franke WW (1985) Cytokeratin patterns of human oral epithelia: differences in cytokeratin synthesis in gingival epithelium and the adjacent alveolar mucosa. *Differentiation* 30: 123-129.
19. Sawaf MH, Ouhayoun JP, Forest N (1991) Cytokeratin profiles in oral epithelial: a review and a new classification. *J Biol Buccale* 19: 187-198.
20. Buhler H, Schaller G (2005) Transfection of keratin 18 gene in human breast cancer cells causes induction of adhesion proteins and dramatic regression of malignancy in vitro and in vivo. *Mol Cancer Res* 3: 365-371.
21. Blobel GA, Moll, R., Franke, W. W. and Vogt-Moykopf, (1984) Cytokeratins in normal lung and lung carcinomas. I. Adenocarcinomas, squamous cell carcinomas and cultured cell lines. *Virchows Arch Cell Pathol Annu*: 407-429.
22. Oshima RG, Baribault H, Caulin C (1996) Oncogenic regulation and function of keratins 8 and 18. *Cancer Metastasis Rev* 15: 445-471.
23. Vaidya MM, Borges AM, Pradhan SA, Rajpal RM, Bhisey AN (1989) Altered keratin expression in buccal mucosal squamous cell carcinoma. *J Oral Pathol Med* 18: 282-286.
24. van der Velden LA, Schaafsma HE, Manni JJ, Ramaekers FC, Kuijpers W (1993) Cytokeratin expression in normal and (pre)malignant head and neck epithelia: an overview. *Head Neck* 15: 133-146.

25. Vaidya MM, Borges AM, Pradhan SA, Bhisey AN (1996) Cytokeratin expression in squamous cell carcinomas of the tongue and alveolar mucosa. *Eur J Cancer B Oral Oncol* 32B: 333-336.
26. Vaidya MM, Sawant SS, Borges AM, Ogale SB, Bhisey AN (1998) Cytokeratin expression in precancerous lesions of the human oral cavity. *Oral Oncol* 34: 261-264.
27. Fillies T, Werkmeister R, Packeisen J, Brandt B, Morin P, et al. (2006) Cytokeratin 8/18 expression indicates a poor prognosis in squamous cell carcinomas of the oral cavity. *BMC Cancer* 6: 10.
28. Ranganathan K, Kavitha R, Sawant SS, Vaidya MM (2006) Cytokeratin expression in oral submucous fibrosis--an immunohistochemical study. *J Oral Pathol Med* 35: 25-32.
29. Alam H, Kundu ST, Dalal SN, Vaidya MM (2011) Loss of keratins 8 and 18 leads to alterations in alpha6beta4-integrin-mediated signalling and decreased neoplastic progression in an oral-tumour-derived cell line. *J Cell Sci* 124: 2096-2106.
30. Khapare N, Kundu ST, Sehgal L, Sawant M, Priya R, et al. (2012) Plakophilin3 Loss Leads to an Increase in PRL3 Levels Promoting K8 Dephosphorylation, Which Is Required for Transformation and Metastasis. *PLoS One* 7: e38561.
31. Hendrix MJ, Seftor EA, Chu YW, Seftor RE, Nagle RB, et al. (1992) Coexpression of vimentin and keratins by human melanoma tumor cells: correlation with invasive and metastatic potential. *J Natl Cancer Inst* 84: 165-174.
32. Bauman PA, Dalton WS, Anderson JM, Cress AE (1994) Expression of cytokeratin confers multiple drug resistance. *Proc Natl Acad Sci U S A* 91: 5311-5314.
33. Hendrix MJ, Seftor EA, Chu YW, Trevor KT, Seftor RE (1996) Role of intermediate filaments in migration, invasion and metastasis. *Cancer Metastasis Rev* 15: 507-525.
34. Thomas PA, Kirschmann DA, Cerhan JR, Folberg R, Seftor EA, et al. (1999) Association between keratin and vimentin expression, malignant phenotype, and survival in postmenopausal breast cancer patients. *Clin Cancer Res* 5: 2698-2703.
35. Schaller G, Fuchs I, Pritze W, Ebert A, Herbst H, et al. (1996) Elevated keratin 18 protein expression indicates a favorable prognosis in patients with breast cancer. *Clin Cancer Res* 2: 1879-1885.
36. Schaller G, Fuchs I, Ebert A, Gstettenbauer M, Herbst H, et al. (1999) [The clinical importance of keratin 18 in breast cancer]. *Zentralbl Gynakol* 121: 126-130.

37. Woelfle U, Sauter G, Santjer S, Brakenhoff R, Pantel K (2004) Down-regulated expression of cytokeratin 18 promotes progression of human breast cancer. *Clin Cancer Res* 10: 2670-2674.
38. Fuchs IB, Lichtenegger W, Buehler H, Henrich W, Stein H, et al. (2002) The prognostic significance of epithelial-mesenchymal transition in breast cancer. *Anticancer Res* 22: 3415-3419.
39. Auersperg N, Pan J, Grove BD, Peterson T, Fisher J, et al. (1999) E-cadherin induces mesenchymal-to-epithelial transition in human ovarian surface epithelium. *Proc Natl Acad Sci U S A* 96: 6249-6254.
40. Ramesh S, Nash J, McCulloch PG (1999) Reduction in membranous expression of beta-catenin and increased cytoplasmic E-cadherin expression predict poor survival in gastric cancer. *Br J Cancer* 81: 1392-1397.
41. Reis-Filho JS, Pusztai L (2011) Gene expression profiling in breast cancer: classification, prognostication, and prediction. *Lancet* 378: 1812-1823.
42. Mohammadizadeh F, Naimi A, Rajabi P, Ghasemibasir H, Eftekhari A (2009) Expression of basal and luminal cytokeratins in breast cancer and their correlation with clinicopathological prognostic variables. *Indian J Med Sci* 63: 152-162.
43. Ishikawa H, Bischoff R, Holtzer H (1968) Mitosis and intermediate-sized filaments in developing skeletal muscle. *The Journal of cell biology* 38: 538-555.
44. Hesse M, Magin T, Weber K (2001) Genes for intermediate filament proteins and the draft sequence of the human genome: novel keratin genes and a surprisingly high number of pseudogenes related to keratin genes 8 and 18. *Journal of cell science* 114: 2569-2575.
45. Kreplak L, Aebi U, Herrmann H (2004) Molecular mechanisms underlying the assembly of intermediate filaments. *Experimental cell research* 301: 77-83.
46. Herrmann H, Aebi U (2004) Intermediate filaments: molecular structure, assembly mechanism, and integration into functionally distinct intracellular Scaffolds. *Annual review of biochemistry* 73: 749-789.
47. Sokolova A, Kreplak L, Wedig T, Mücke N, Svergun D, et al. (2006) Monitoring intermediate filament assembly by small-angle x-ray scattering reveals the molecular architecture of assembly intermediates. *Proceedings of the National Academy of Sciences of the United States of America* 103: 16206-16211.
48. Kim S, Kellner J, Lee CH, Coulombe PA (2007) Interaction between the keratin cytoskeleton and eEF1Bgamma affects protein synthesis in epithelial cells. *Nat Struct Mol Biol* 14: 982-983.

49. Hesse M, Zimek A, Weber K, Magin TM (2004) Comprehensive analysis of keratin gene clusters in humans and rodents. *Eur J Cell Biol* 83: 19-26.
50. Moll R, Moll I, Wiest W (1982) Changes in the pattern of cytokeratin polypeptides in epidermis and hair follicles during skin development in human fetuses. *Differentiation* 23: 170-178.
51. Winter H, Langbein L, Praetzel S, Jacobs M, Rogers MA, et al. (1998) A novel human type II cytokeratin, K6hf, specifically expressed in the companion layer of the hair follicle. *J Invest Dermatol* 111: 955-962.
52. Bragulla HH, Homberger DG (2009) Structure and functions of keratin proteins in simple, stratified, keratinized and cornified epithelia. *J Anat* 214: 516-559.
53. Jackson BW, Grund C, Schmid E, Burki K, Franke WW, et al. (1980) Formation of cytoskeletal elements during mouse embryogenesis. Intermediate filaments of the cytokeratin type and desmosomes in preimplantation embryos. *Differentiation* 17: 161-179.
54. Waseem A, Alexander CM, Steel JB, Lane EB (1990) Embryonic simple epithelial keratins 8 and 18: chromosomal location emphasizes difference from other keratin pairs. *New Biol* 2: 464-478.
55. Moll R, Achtstatter T, Becht E, Balcarova-Stander J, Ittensohn M, et al. (1988) Cytokeratins in normal and malignant transitional epithelium. Maintenance of expression of urothelial differentiation features in transitional cell carcinomas and bladder carcinoma cell culture lines. *Am J Pathol* 132: 123-144.
56. Dale BA, Salonen J, Jones AH (1990) New approaches and concepts in the study of differentiation of oral epithelia. *Crit Rev Oral Biol Med* 1: 167-190.
57. Presland RB, Dale BA (2000) Epithelial structural proteins of the skin and oral cavity: function in health and disease. *Crit Rev Oral Biol Med* 11: 383-408.
58. Paladini RD, Takahashi K, Bravo NS, Coulombe PA (1996) Onset of re-epithelialization after skin injury correlates with a reorganization of keratin filaments in wound edge keratinocytes: defining a potential role for keratin 16. *J Cell Biol* 132: 381-397.
59. Omary MB, Ku NO, Liao J, Price D (1998) Keratin modifications and solubility properties in epithelial cells and in vitro. *Subcell Biochem* 31: 105-140.
60. Srikanth B, Vaidya MM, Kalraiya RD (2010) O-GlcNAcylation determines the solubility, filament organization, and stability of keratins 8 and 18. *J Biol Chem* 285: 34062-34071.

61. Ku NO, Toivola DM, Strnad P, Omary MB (2010) Cytoskeletal keratin glycosylation protects epithelial tissue from injury. *Nat Cell Biol* 12: 876-885.
62. Ku NO, Omary MB (2006) A disease- and phosphorylation-related nonmechanical function for keratin 8. *J Cell Biol* 174: 115-125.
63. Snider NT, Weerasinghe SV, Iniguez-Lluhi JA, Herrmann H, Omary MB (2011) Keratin hypersumoylation alters filament dynamics and is a marker for human liver disease and keratin mutation. *J Biol Chem* 286: 2273-2284.
64. Sawant SS, Zingde SM, Vaidya MM (2008) Cytokeratin fragments in the serum: their utility for the management of oral cancer. *Oral Oncol* 44: 722-732.
65. Snider NT, Leonard JM, Kwan R, Griggs NW, Rui L, et al. (2013) Glucose and SIRT2 reciprocally mediate the regulation of keratin 8 by lysine acetylation. *J Cell Biol* 200: 241-247.
66. Magin TM, Vijayaraj P, Leube RE (2007) Structural and regulatory functions of keratins. *Exp Cell Res* 313: 2021-2032.
67. Magin TM, Kaiser HW, Leitgeb S, Grund C, Leigh IM, et al. (2000) Supplementation of a mutant keratin by stable expression of desmin in cultured human EBS keratinocytes. *J Cell Sci* 113 Pt 23: 4231-4239.
68. Ku NO, Wright TL, Terrault NA, Gish R, Omary MB (1997) Mutation of human keratin 18 in association with cryptogenic cirrhosis. *J Clin Invest* 99: 19-23.
69. Ku NO, Gish R, Wright TL, Omary MB (2001) Keratin 8 mutations in patients with cryptogenic liver disease. *N Engl J Med* 344: 1580-1587.
70. Toivola DM, Ku NO, Resurreccion EZ, Nelson DR, Wright TL, et al. (2004) Keratin 8 and 18 hyperphosphorylation is a marker of progression of human liver disease. *Hepatology* 40: 459-466.
71. Irvine AD, Corden LD, Swensson O, Swensson B, Moore JE, et al. (1997) Mutations in cornea-specific keratin K3 or K12 genes cause Meesmann's corneal dystrophy. *Nat Genet* 16: 184-187.
72. Peters B, Kirfel J, Bussow H, Vidal M, Magin TM (2001) Complete cytolysis and neonatal lethality in keratin 5 knockout mice reveal its fundamental role in skin integrity and in epidermolysis bullosa simplex. *Mol Biol Cell* 12: 1775-1789.
73. Kao WW, Liu CY, Converse RL, Shiraishi A, Kao CW, et al. (1996) Keratin 12-deficient mice have fragile corneal epithelia. *Invest Ophthalmol Vis Sci* 37: 2572-2584.

74. Baribault H, Price J, Miyai K, Oshima RG (1993) Mid-gestational lethality in mice lacking keratin 8. *Genes Dev* 7: 1191-1202.
75. Loranger A, Duclos S, Grenier A, Price J, Wilson-Heiner M, et al. (1997) Simple epithelium keratins are required for maintenance of hepatocyte integrity. *Am J Pathol* 151: 1673-1683.
76. Magin TM (1998) Lessons from keratin transgenic and knockout mice. *Subcell Biochem* 31: 141-172.
77. Ku NO, Michie S, Oshima RG, Omary MB (1995) Chronic hepatitis, hepatocyte fragility, and increased soluble phosphoglycokeratins in transgenic mice expressing a keratin 18 conserved arginine mutant. *J Cell Biol* 131: 1303-1314.
78. Ku NO, Zhou X, Toivola DM, Omary MB (1999) The cytoskeleton of digestive epithelia in health and disease. *Am J Physiol* 277: G1108-1137.
79. Ku NO, Darling JM, Krams SM, Esquivel CO, Keeffe EB, et al. (2003) Keratin 8 and 18 mutations are risk factors for developing liver disease of multiple etiologies. *Proc Natl Acad Sci U S A* 100: 6063-6068.
80. Magin TM, Schroder R, Leitgeb S, Wanninger F, Zatloukal K, et al. (1998) Lessons from keratin 18 knockout mice: formation of novel keratin filaments, secondary loss of keratin 7 and accumulation of liver-specific keratin 8-positive aggregates. *J Cell Biol* 140: 1441-1451.
81. Vaidya MM, Kanojia D (2007) Keratins: markers of cell differentiation or regulators of cell differentiation? *J Biosci* 32: 629-634.
82. Ku NO, Fu H, Omary MB (2004) Raf-1 activation disrupts its binding to keratins during cell stress. *J Cell Biol* 166: 479-485.
83. Ku NO, Azhar S, Omary MB (2002) Keratin 8 phosphorylation by p38 kinase regulates cellular keratin filament reorganization: modulation by a keratin 1-like disease causing mutation. *J Biol Chem* 277: 10775-10782.
84. Tao GZ, Toivola DM, Zhou Q, Strnad P, Xu B, et al. (2006) Protein phosphatase-2A associates with and dephosphorylates keratin 8 after hyposmotic stress in a site- and cell-specific manner. *J Cell Sci* 119: 1425-1432.
85. Planko L, Bohse K, Hohfeld J, Betz RC, Hanneken S, et al. (2007) Identification of a keratin-associated protein with a putative role in vesicle transport. *Eur J Cell Biol* 86: 827-839.

86. Toivola DM, Krishnan S, Binder HJ, Singh SK, Omary MB (2004) Keratins modulate colonocyte electrolyte transport via protein mistargeting. *J Cell Biol* 164: 911-921.
87. Gilbert S, Loranger A, Daigle N, Marceau N (2001) Simple epithelium keratins 8 and 18 provide resistance to Fas-mediated apoptosis. The protection occurs through a receptor-targeting modulation. *J Cell Biol* 154: 763-773.
88. Marceau N, Gilbert S, Loranger A (2004) Uncovering the roles of intermediate filaments in apoptosis. *Methods Cell Biol* 78: 95-129.
89. Gilbert S, Ruel A, Loranger A, Marceau N (2008) Switch in Fas-activated death signaling pathway as result of keratin 8/18-intermediate filament loss. *Apoptosis* 13: 1479-1493.
90. Caulin C, Ware CF, Magin TM, Oshima RG (2000) Keratin-dependent, epithelial resistance to tumor necrosis factor-induced apoptosis. *J Cell Biol* 149: 17-22.
91. Inada H, Izawa I, Nishizawa M, Fujita E, Kiyono T, et al. (2001) Keratin attenuates tumor necrosis factor-induced cytotoxicity through association with TRADD. *J Cell Biol* 155: 415-426.
92. Kim S, Wong P, Coulombe PA (2006) A keratin cytoskeletal protein regulates protein synthesis and epithelial cell growth. *Nature* 441: 362-365.
93. Vijayaraj P, Kroger C, Reuter U, Windoffer R, Leube RE, et al. (2009) Keratins regulate protein biosynthesis through localization of GLUT1 and -3 upstream of AMP kinase and Raptor. *J Cell Biol* 187: 175-184.
94. Galarneau L, Loranger A, Gilbert S, Marceau N (2007) Keratins modulate hepatic cell adhesion, size and G1/S transition. *Exp Cell Res* 313: 179-194.
95. Paramio JM, Casanova ML, Segrelles C, Mitnacht S, Lane EB, et al. (1999) Modulation of cell proliferation by cytokeratins K10 and K16. *Mol Cell Biol* 19: 3086-3094.
96. Habtezion A, Toivola DM, Butcher EC, Omary MB (2005) Keratin-8-deficient mice develop chronic spontaneous Th2 colitis amenable to antibiotic treatment. *J Cell Sci* 118: 1971-1980.
97. Roth W, Kumar V, Beer HD, Richter M, Wohlenberg C, et al. (2012) Keratin 1 maintains skin integrity and participates in an inflammatory network in skin through interleukin-18. *J Cell Sci* 125: 5269-5279.



98. Depianto D, Kerns ML, Dlugosz AA, Coulombe PA (2010) Keratin 17 promotes epithelial proliferation and tumor growth by polarizing the immune response in skin. *Nat Genet* 42: 910-914.
99. Haines RL, Lane EB (2012) Keratins and disease at a glance. *J Cell Sci* 125: 3923-3928.
100. Santos M, Paramio JM, Bravo A, Ramirez A, Jorcano JL (2002) The expression of keratin k10 in the basal layer of the epidermis inhibits cell proliferation and prevents skin tumorigenesis. *J Biol Chem* 277: 19122-19130.
101. Chen J, Cheng X, Merched-Sauvage M, Caulin C, Roop DR, et al. (2006) An unexpected role for keratin 10 end domains in susceptibility to skin cancer. *J Cell Sci* 119: 5067-5076.
102. Weidauer H, Nagle RB, Moll R, Franke WW (1986) [Cytokeratin expression in normal and malignant tongue epithelium]. *Laryngol Rhinol Otol (Stuttg)* 65: 164-168.
103. Chu YW, Seftor EA, Romer LH, Hendrix MJ (1996) Experimental coexpression of vimentin and keratin intermediate filaments in human melanoma cells augments motility. *Am J Pathol* 148: 63-69.
104. Raul U, Sawant S, Dange P, Kalraiya R, Ingle A, et al. (2004) Implications of cytokeratin 8/18 filament formation in stratified epithelial cells: induction of transformed phenotype. *Int J Cancer* 111: 662-668.
105. Casanova ML, Bravo A, Martinez-Palacio J, Fernandez-Acenero MJ, Villanueva C, et al. (2004) Epidermal abnormalities and increased malignancy of skin tumors in human epidermal keratin 8-expressing transgenic mice. *FASEB J* 18: 1556-1558.
106. Lau AT, Chiu JF (2007) The possible role of cytokeratin 8 in cadmium-induced adaptation and carcinogenesis. *Cancer Res* 67: 2107-2113.
107. Mizuuchi E, Semba S, Kodama Y, Yokozaki H (2009) Down-modulation of keratin 8 phosphorylation levels by PRL-3 contributes to colorectal carcinoma progression. *Int J Cancer* 124: 1802-1810.
108. Alam H, Gangadaran P, Bhate AV, Chaukar DA, Sawant SS, et al. (2011) Loss of keratin 8 phosphorylation leads to increased tumor progression and correlates with clinico-pathological parameters of OSCC patients. *PLoS One* 6: e27767.
109. Nielsen TO, Hsu FD, Jensen K, Cheang M, Karaca G, et al. (2004) Immunohistochemical and clinical characterization of the basal-like subtype of invasive breast carcinoma. *Clin Cancer Res* 10: 5367-5374.

110. Livasy CA, Karaca G, Nanda R, Tretiakova MS, Olopade OI, et al. (2006) Phenotypic evaluation of the basal-like subtype of invasive breast carcinoma. *Mod Pathol* 19: 264-271.
111. Livasy CA, Perou CM, Karaca G, Cowan DW, Maia D, et al. (2007) Identification of a basal-like subtype of breast ductal carcinoma in situ. *Hum Pathol* 38: 197-204.
112. Hedenfalk I, Duggan D, Chen Y, Radmacher M, Bittner M, et al. (2001) Gene-expression profiles in hereditary breast cancer. *N Engl J Med* 344: 539-548.
113. Zajchowski DA, Bartholdi MF, Gong Y, Webster L, Liu HL, et al. (2001) Identification of gene expression profiles that predict the aggressive behavior of breast cancer cells. *Cancer Res* 61: 5168-5178.
114. Pantel K, Woelfle U (2004) Micrometastasis in breast cancer and other solid tumors. *J Biol Regul Homeost Agents* 18: 120-125.
115. Fuchs E, Yang Y (1999) Crossroads on cytoskeletal highways. *Cell* 98: 547-550.
116. Green KJ, Simpson CL (2007) Desmosomes: new perspectives on a classic. *J Invest Dermatol* 127: 2499-2515.
117. Jones JC, Asmuth J, Baker SE, Langhofer M, Roth SI, et al. (1994) Hemidesmosomes: extracellular matrix/intermediate filament connectors. *Exp Cell Res* 213: 1-11.
118. Desgrosellier JS, Cheresch DA (2010) Integrins in cancer: biological implications and therapeutic opportunities. *Nat Rev Cancer* 10: 9-22.
119. E Tagliabue CG, P Squicciarini, et al. (1998) Prognostic value of alpha 6 beta 4 integrin expression in breast carcinomas is affected by laminin production from tumor cells. *Clinical cancer Research* 4: 407-410.
120. Bordeleau F, Galarneau L, Gilbert S, Loranger A, Marceau N (2010) Keratin 8/18 modulation of protein kinase C-mediated integrin-dependent adhesion and migration of liver epithelial cells. *Mol Biol Cell* 21: 1698-1713.
121. Windoffer R, Beil M, Magin TM, Leube RE (2011) Cytoskeleton in motion: the dynamics of keratin intermediate filaments in epithelia. *J Cell Biol* 194: 669-678.
122. Hartsock A, Nelson WJ (2008) Adherens and tight junctions: structure, function and connections to the actin cytoskeleton. *Biochim Biophys Acta* 1778: 660-669.

123. Tsukita S, Nagafuchi A, Yonemura S (1992) Molecular linkage between cadherins and actin filaments in cell-cell adherens junctions. *Curr Opin Cell Biol* 4: 834-839.
124. Onder TT, Gupta PB, Mani SA, Yang J, Lander ES, et al. (2008) Loss of E-cadherin promotes metastasis via multiple downstream transcriptional pathways. *Cancer Res* 68: 3645-3654.
125. Wu Y, Zhou BP (2008) New insights of epithelial-mesenchymal transition in cancer metastasis. *Acta Biochim Biophys Sin (Shanghai)* 40: 643-650.
126. Cailleau R, Olive M, Cruciger QV (1978) Long-term human breast carcinoma cell lines of metastatic origin: preliminary characterization. *In Vitro* 14: 911-915.
127. Soule HD, Maloney TM, Wolman SR, Peterson WD, Jr., Brenz R, et al. (1990) Isolation and characterization of a spontaneously immortalized human breast epithelial cell line, MCF-10. *Cancer Res* 50: 6075-6086.
128. Achstatter T, Moll R, Anderson A, Kuhn C, Pitz S, et al. (1986) Expression of glial filament protein (GFP) in nerve sheaths and non-neural cells re-examined using monoclonal antibodies, with special emphasis on the co-expression of GFP and cytokeratins in epithelial cells of human salivary gland and pleomorphic adenomas. *Differentiation* 31: 206-227.
129. Peterson GL (1977) A simplification of the protein assay method of Lowry et al. which is more generally applicable. *Anal Biochem* 83: 346-356.
130. Mosmann T (1983) Rapid colorimetric assay for cellular growth and survival: application to proliferation and cytotoxicity assays. *J Immunol Methods* 65: 55-63.
131. Xiang R, Davalos AR, Hensel CH, Zhou XJ, Tse C, et al. (2002) Semaphorin 3F gene from human 3p21.3 suppresses tumor formation in nude mice. *Cancer Res* 62: 2637-2643.
132. Moll R (1987) Diversity of cytokeratins in carcinomas. *Acta Histochem Suppl* 34: 37-44.
133. Dairkee SH, Puett L, Hackett AJ (1988) Expression of basal and luminal epithelium-specific keratins in normal, benign, and malignant breast tissue. *J Natl Cancer Inst* 80: 691-695.
134. Mackinder MA, Evans CA, Chowdry J, Staton CA, Corfe BM (2012) Alteration in composition of keratin intermediate filaments in a model of breast cancer progression and the potential to reverse hallmarks of metastasis. *Cancer Biomark* 12: 49-64.

135. Long HA, Boczonadi V, McInroy L, Goldberg M, Maatta A (2006) Periplakin-dependent re-organisation of keratin cytoskeleton and loss of collective migration in keratin-8-downregulated epithelial sheets. *J Cell Sci* 119: 5147-5159.
136. Busch T, Armacki M, Eiseler T, Joodi G, Temme C, et al. (2012) Keratin 8 phosphorylation regulates keratin reorganization and migration of epithelial tumor cells. *J Cell Sci* 125: 2148-2159.
137. Uchiumi A, Yamashita M, Katagata Y (2012) Downregulation of keratins 8, 18 and 19 influences invasiveness of human cultured squamous cell carcinoma and adenocarcinoma cells. *Exp Ther Med* 3: 443-448.
138. Giudice GJ, Fuchs E (1987) The transfection of epidermal keratin genes into fibroblasts and simple epithelial cells: evidence for inducing a type I keratin by a type II gene. *Cell* 48: 453-463.
139. Tao GZ, Toivola DM, Zhong B, Michie SA, Resurreccion EZ, et al. (2003) Keratin-8 null mice have different gallbladder and liver susceptibility to lithogenic diet-induced injury. *J Cell Sci* 116: 4629-4638.
140. Malzahn K, Mitze M, Thoenes M, Moll R (1998) Biological and prognostic significance of stratified epithelial cytokeratins in infiltrating ductal breast carcinomas. *Virchows Arch* 433: 119-129.
141. Mareel M, Leroy A (2003) Clinical, cellular, and molecular aspects of cancer invasion. *Physiol Rev* 83: 337-376.
142. Green KJ, Getsios S, Troyanovsky S, Godsel LM (2010) Intercellular junction assembly, dynamics, and homeostasis. *Cold Spring Harb Perspect Biol* 2: a000125.
143. Gosavi P, Kundu ST, Khapare N, Sehgal L, Karkhanis MS, et al. (2011) E-cadherin and plakoglobin recruit plakophilin3 to the cell border to initiate desmosome assembly. *Cell Mol Life Sci* 68: 1439-1454.
144. Guo W, Giancotti FG (2004) Integrin signalling during tumour progression. *Nat Rev Mol Cell Biol* 5: 816-826.
145. Heyden A HH, Koppang HS, Thrane PS, Bryne M, Brandtzaeg P. (1992 January) Cytokeratins as epithelial differentiation markers in premalignant and malignant oral lesions. *Journal of Oral Pathology & Medicine* 21: 7-11.
146. Leandro-Garcia LJ, Leskela S, Landa I, Montero-Conde C, Lopez-Jimenez E, et al. (2010) Tumoral and tissue-specific expression of the major human beta-tubulin isoforms. *Cytoskeleton (Hoboken)* 67: 214-223.

147. Streit M, Riccardi L, Velasco P, Brown LF, Hawighorst T, et al. (1999) Thrombospondin-2: a potent endogenous inhibitor of tumor growth and angiogenesis. *Proc Natl Acad Sci U S A* 96: 14888-14893.
148. Tokunaga T, Nakamura M, Oshika Y, Abe Y, Ozeki Y, et al. (1999) Thrombospondin 2 expression is correlated with inhibition of angiogenesis and metastasis of colon cancer. *Br J Cancer* 79: 354-359.
149. Behrens J, von Kries JP, Kuhl M, Bruhn L, Wedlich D, et al. (1996) Functional interaction of beta-catenin with the transcription factor LEF-1. *Nature* 382: 638-642.
150. Van den Abbeele A, De Corte V, Van Impe K, Bruyneel E, Boucherie C, et al. (2007) Downregulation of gelsolin family proteins counteracts cancer cell invasion in vitro. *Cancer Lett* 255: 57-70.

## Appendix

**Table 5.3.2:** Mass spectrometry analysis showing details of the bands with keratin identity.

Gel Piece No.	Protein Name	Protein Id	Accession No.	PMF						
				Total score	Mass (Da)	pI	IC (%)	SC (%)	Total peaks	Matches
Lane 1: MDA MB 468 VECTOR (Vc)										
Vc1	Keratin, type II cytoskeletal 7	K2C7_HUMAN	<a href="#">P08729</a>	79	51411	5.40	77.8	24.5	30	9
Vc2	Keratin, type II cytoskeletal 7	K2C7_HUMAN	<a href="#">P08729</a>	97	51411	5.40	79.3	28.6	38	11
	Keratin, type II cytoskeletal 8	<a href="#">K2C8_HUMAN</a>	<a href="#">P05787</a>	85	53671	5.52	69.3	28	38	11
Vc3	Keratin, type I cytoskeletal 18	<a href="#">K1C18_HUMAN</a>	<a href="#">P05783</a>	194	48029	5.34	50	46.7	68	22
V5	Keratin, type I cytoskeletal 19	K1C19_HUMAN	<a href="#">P08727</a>	211	44079	5.04	88.5	45	29	17
Lane 2: MDA MB 468 K8 knock-down clone shC1										
shC1-1	Keratin, type II cytoskeletal 7	K2C7_HUMAN	<a href="#">P08729</a>	40	51411	5.40	62.9	10	25	5
Shc1-2	Keratin, type II cytoskeletal 7	K2C7_HUMAN	<a href="#">P08729</a>	126	51411	5.40	80.7	32.6	31	12
ShC1-3	Keratin, type I cytoskeletal 18	<a href="#">K1C18_HUMAN</a>	<a href="#">P05783</a>	75	48029	5.34	37.5	33.5	24	7
ShC1-5	Keratin, type I cytoskeletal 19	K1C19_HUMAN	<a href="#">P08727</a>	168	44079	5.04	72.8	41.5	34	15
Lane 3: MDA MB 468 K8 knock-down clone shC2										
shC2-1	Keratin, type II cytoskeletal 7	K2C7_HUMAN	<a href="#">P08729</a>	158	51411	5.40	88.8	32.6	26	13
ShC2-2	Keratin, type II cytoskeletal 7	K2C7_HUMAN	<a href="#">P08729</a>	55	51411	5.40	51.6	17.7	20	6
ShC2-3	Keratin, type I cytoskeletal 18	<a href="#">K1C18_HUMAN</a>	<a href="#">P05783</a>	85	48029	5.34	49.5	28.8	26	9
shC2-5	Keratin, type I cytoskeletal 19	K1C19_HUMAN	<a href="#">P08727</a>	147	44079	5.04	75.1	32.8	27	13

Abbreviations: SC-Sequence coverage, IC –Intensity Coverage, PMF- Peptide Mass Fingerprinting, pI- Isoelectric point